Paclitaxel Release System

A Major Qualifying Project
Submitted to the faculty of
WORCESTER POLYTECHNIC INSTITUTE

In partial fulfillment of the requirements for the
Degree of Bachelor of Science
In Chemical Engineering

By:
Michaela Johnson
Jason Rivers
Summer Thurlow

Date: 18 May 2020
Report Submitted to:

Professor Susan Roberts, Advisor

Professor Jeannine Coburn, Co-Advisor

Abstract

Taxus plant suspension cultures can be used to produce paclitaxel (PTX), an anticancer compound. Currently PTX is administered systemically, which can have severe adverse side effects. To minimize these effects, this project investigates the use of a plant cell culture (PCC) delivery system for PTX using the cells that produce PTX in bioprocesses. Using cells that are used in the bioprocess not only had advantages in regards to delivery, but enables the inclusion of potentially synergistic compounds that may enhance the therapeutic effect of PTX. Research focused on exploring the retention of PTX and other specialized metabolites through processing of PCC, optimization of drug delivery through natural and synthetic polymer hydrogels, predicted release in an *in vitro* breast cancer model, and consideration of the pharmacokinetics of the optimized system.

When washing 10 mL of PCC prior to lyophilization, an average of 68.3% PTX, 75% flavonoids, and 40% phenolics were retained through wash processing. Although polyvinyl alcohol hydrogel microbeads were unable to maintain integrity for extended periods of time, alginate hydrogel microbeads consisting of 5% sodium alginate released PTX over 24 hr without degrading. Nile Red dye was used to mimic PTX and showed 81.1% release over 24 hr. To reduce viability of breast cancer cells, the desired release concentration of 8.5×10^{-4} mg/mL was confirmed through cytotoxic assays, which showed approximately 75% cell death. A mapping of the pharmacokinetics of the optimized drug delivery system for PTX from *Taxus* PCC demonstrates a feasible option for PTX administration.

Acknowledgements

Our team would like to extend our gratitude to several people for their guidance and constructive criticism that has contributed to the overall success of this project.

We would like to thank and acknowledge our advisors, Professor Susan Roberts and Professor Jeannine Coburn, for allowing us to continue their research towards creating a drug delivery system for paclitaxel through plant cell culture. Over the course of this year, Professor Roberts and Professor Coburn dedicated their time attending weekly meetings, suggesting further research avenues, and editing revisions.

We would also like to thank our PhD student mentor, Michelle McKee, for her patience with guiding us through the duration of this project. In addition to attending weekly meetings, Michelle exposed us to new lab techniques, collaborated with the process of developing experimental protocols, and edited countless revisions.

We further extend our gratitude to other members within Professor Roberts' and Professor Coburn's labs for allowing us to conduct our research alongside them, and Worcester Polytechnic Institute for providing us with the opportunity to complete such a project as a part of our curriculum.

Table of Contents

Table of Figures

Table of Tables

Chapter 1: Introduction

According to the World Health Organization, cancer is the leading cause of death worldwide, and second in the United States [1, 2]. An estimated 1.8 million new cases of cancer will be diagnosed in the United States in 2020, resulting in a predicted 606,520 deaths [2]. Therefore, the need to progress research of the disease and treatment options to decrease mortality rates remains. Congress recently passed an appropriations bill that provides the National Cancer Institute with $297 million for the 2020 fiscal year to advance oncology tools, diagnostics, treatments, and prevention strategies [3]. Current treatment options for cancer include chemotherapy, a form of cancer therapy that requires the use of drugs to destroy fast-dividing cells [4]. Common chemotherapy agents, such as Doxorubicin, Vinorelbine, and Capecitabine, are administered at high doses, which have dose limiting side effects that can cause severe health issues if not monitored closely [4, 5]. Because systemic drug delivery systems release the therapeutic agents via the digestive or circulatory systems, the administered drug can affect healthy cells and organs; thus, resulting in severe adverse side effects [4]. Such side effects include the damage of healthy cells in bone marrow, digestive tract, and reproductive systems, nerve damage, kidney malfunction, and infection [6]. Chemotherapy agents, such as paclitaxel (PTX), are continuously being investigated to shift from systemic to local administration to decrease the harmful effects that are associated with current chemotherapy options.

The U.S. Food and Drug Administration first approved PTX as a treatment for ovarian cancer in 1992, and has since approved it for the treatment of breast cancer, non-small cell lung cancer, and AIDS-related Kaposi sarcoma under the trademark of Taxol ® [7]. PTX is currently administered intravenously once every two to three weeks. Depending on the patient's treatment plan, treatments may require 175 mg/m² over the course of 3 hr or 135 mg/m² over the course of 24 hr per treatment, both followed with cisplatin [8].

PTX is naturally produced in the bark of Pacific yew trees (*Taxus spp.)*, which is one of five common potential methods in which natural products can be synthesized: heterologous expression systems, chemical synthesis, semi-synthesis, extraction from yew trees, and plant cell cultures [9]. Although PTX was first discovered through isolating the compound from the bark, it has since been determined that this method of crude extraction is not a sustainable option [10]. Furthermore, alternative methods of PTX production including heterologous expression systems are limited by the underdeveloped biosynthetic pathway of PTX, and chemical synthesis and semi-synthesis are limited by the low yields and depleting sources of PTX precursors (baccatin III and 10-deacetylbaccatin III) [9, 11]. Therefore, *Taxus* suspension cultures, a method of producing PTX through differentiating cells from yew tree needles, bark, and stems, are used as a more sustainable method of producing PTX for treatment [10].

The therapeutic performance of drugs may be further enhanced when produced in suspension cultures because of the synergistic interactions that may occur between the drug compound and other specialized metabolites, naturally produced plant compounds that often contain medicinal properties [12]. Although no studies have proven to increase efficacy of PTX due to synergistic interactions, researchers hypothesize that other specialized metabolites enhance the drug's cytotoxic properties

when produced in *Taxus* suspension cultures [13]. The differentiated cells from plant cell suspension cultures (PCC), containing these compounds, can be processed and loaded into a delivery vehicle to control the release rate of the therapeutic agents [14]. The local administration of PTX through the use of delivery vehicles can target the delivery of the drug; thus, minimizing the adverse side effects that are associated with current cancer therapies, including the current delivery methods for PTX [15].

In a previous Major Qualifying Project (MQP), students from Worcester Polytechnic Institute investigated the use of PCC to create a local delivery system for PTX. For the purposes of the project, students sought to increase cell-associated PTX accumulation, remove DNA from the cells for biocompatibility, and compare the release kinetics of free PTX to calcium alginate encapsulated PTX [16]. This MQP expands beyond this initial research to further provide insight on the delivery of PTX through PCC through the following aims:

Aim 1: Develop a wash process that retains PTX, flavonoid, and phenolic compounds, and prepare PCC material for encapsulation.
Aim 2: Optimize delivery of PTX, flavonoid, and phenolic compounds by encapsulating PCC material in a biomaterial suitable for desired delivery.
Aim 3: Establish an *in vitro* model to optimize drug delivery design for maximum breast cancer cell culture cytotoxicity, and predict release studies for PCC delivery.
Aim 4: Understand pharmacokinetics for components of the optimized drug delivery system to determine feasibility and administration parameters.

Chapter 2: Background

2.1 Drug Delivery Systems for Chemotherapy

Chemotherapy drug delivery systems (DDSs) deliver anticancer drug compounds to cancer cells [17]. The administration of anticancer drugs generally falls into two categories: systemic and local [15]. Systemic DDSs, such as intravenous or oral dosage forms, release the drugs via the circulatory or digestive systems and affect the entire body, including healthy cells and organs [4]. Common anticancer drugs used in the treatment of drug cancer such as Doxorubicin, capecitabine, and paclitaxel (PTX), are often administered intravenously [6]. However, because these drugs are administered systemically, patients can experience severe adverse side effects such as internal bleeding, blood clots, arrhythmia, and pericardial effusion [18, 19]. To minimize the side effects associated with systemic administration, targeted delivery systems for anticancer drugs have been in development over the past decade [20]. In these systems, physicochemical or surface interactions attach the anticancer drugs to the surface of nanoparticles [20]. A targeting molecule, such as an antibody or ligand, is also attached to the surface of the drug-nanoparticle conjugate [20]. Once administered systemically, the targeting molecule directs the nanoparticle towards complementary receptors on the surface of tumor cells; thus, resulting in more local accumulation of the anticancer drug on the tumor [20]. For instance, PTX-loaded poly(D,L-lactide-co-glycolide) (PLGA) nanoparticles are covalently conjugated to antibodies target perlecan, a cell surface protein overexpressed in triple-negative breast cancer that promotes tumor growth [21]. In one study, researchers grafted triple-negative breast cancer tumors into mice, and administered six doses (20 mg/kg equivalent dose of PTX) of the PTX-loaded PLGA nanoparticle conjugates or Isotope IgG nanoparticles via tail vein injection once every 96 hr, and utilized untreated mice as a control [21]. Isotope IgG nanoparticles contain antibodies that lack specificity in targeting [21]. In this study, researchers found that Isotope IgG nanoparticles increased tumor growth inhibition by 18%, whereas the PTX-loaded PLGA nanoparticle conjugates increased tumor growth inhibition by 44% [21]. Despite targeted delivery systems increasing local accumulation of systemically administered anticancer drugs, physiological barriers, such as tumor penetration, tumor heterogeneity, relative hypoxia, and endosomal escape, limit the drug efficacy in these systems [22].

To minimize the side effects experienced with systemic administration and bypass the physiological barriers associated with targeted delivery systems, local DDSs, such as topical dosage forms, are administered to directly apply the anticancer compounds to the tumor [22, 23]. For instance, carmustine, an anticancer compound used to treat high grade malignant gliomas, is loaded into wafers and applied directly to the tumor site [14, 24]. This method of administration bypasses the challenges often associated with delivering chemotherapy drugs systemically across the blood-brain barrier, such as insufficient intratumoral concentrations of the anticancer compound [14, 24]. Furthermore, local DDSs meet the three criteria that characterize successful DDSs for chemotherapy: controlled release rate, desired drug concentration, and reduction of adverse side effects [25]. By meeting these criteria, the anticancer drug can effectively treat the tumor while

minimizing lethal side effects associated with chemotherapy [22]. One study found 8.1% of patients receiving chemotherapy for lymphoma, myeloma, and leukaemia die within the first 30 days [26]. Of those deaths, 7.5% are related to chemotherapy side effects such as neutropenic sepsis, multiorgan failure, and chemotherapy toxicity from impaired renal failure [26]. Therefore, it is crucial that chemotherapy treatments shift from systemic to local administration to minimize these adverse side effects.

2.1.1 Local Drug Delivery Systems

Local DDSs deliver compounds via direct contact to the target area, as opposed to systemic DDSs which deliver the therapeutic agents throughout the entire body [15]. Local administration is often the preferred method of drug delivery because it can deliver high drug concentrations to the target area with minimal side effects [15]. Examples of regularly utilized local DDSs include topical dosage forms. For instance, sulfacetamide sodium eye drops (Bleph®-10) are a topical treatment for bacterial conjunctivitis [27]. Additionally, topical dosage forms are used in chemotherapy, such as fluorouracil cream (Tolak®) for patients with superficial basal cell carcinoma, a type of skin cancer [28].

Although some local DDSs can be applied externally, other treatment plans may require a vehicle to deliver the drug to the target site inside the body. Drug-eluting films, gels, wafers, rods, and particles can be implanted into the treatment site to control the release rate of the therapeutic agents [14]. Furthermore, drug, polymer, and geometry-related factors of these vehicles can affect the release rate of therapeutic agents from the local DDSs [29].

Drug-Related Factors Affect Release Kinetics

Drug-related factors such as drug solubility and molecular size can affect drug release from delivery vehicles [29]. A drug's chemical structure, including its functional groups and stereo-chemical configuration, can affect its solubility properties [29]. These properties affect a drug's ability to diffuse across the chemical gradient of the medium [29]. Drugs with high solubilities are readily available to pass through the gradient, resulting in a faster release [29]. However, drugs with lower solubilities not only have slower release rates, but complete release from the delivery vehicle may not be feasible [29]. Additionally, diffusion is dependent on the size of the drug molecule. As the diameter of the molecule increases, the drug's physical ability to pass through the matrix hinders diffusion [29].

Polymer-Related Factors Affect Release Kinetics

Once a drug's physicochemical properties are understood, the drug is loaded into a biomaterial suited to promote the desired release kinetics. Polymer properties such as polymer type, viscosity grade, and particle size affect drug release kinetics [29].

The biomaterials used to encapsulate drugs are split into two broad categories based on their polymer composition: natural and synthetic [14]. Natural polymers include polysaccharides (alginate, hyaluronic acid, dextran, and chitosan), proteins, and peptides (collagen, albumin, elastin, and gelatin) [14, 30, 31]. These polymers form hydrogels easily within itself via self-assembly or cross-linking [14, 31, 32]. Therefore, natural polymer delivery vehicles can be readily injected into the body and gelation can be induced by a change in temperature, pH, and/or ionic composition [14]. Some natural polymers require cross-linking to form hydrogels and are surgically implanted into the tumor site. Regardless of administration, natural polymers create minimal immune response in the body and are biodegradable; thus, circumventing the need for further implant removal surgeries [14, 33]. However, to ensure successful drug delivery through natural polymer hydrogels, one must consider that these materials must be in high purity to be biocompatible [14, 31].

An example of a successful local DDS that utilizes a natural polymer delivery vehicle includes the administration of PTX to brain glioma-bearing mice through a biodegradable phospholipid-based gel (PG) system [34]. For this study, researchers injected the tumors with PTX loaded PG or unbound PTX, and utilized saline as a control [34]. Results showed little difference between the control group and the unbound PTX group, with the mice dying in a similar time frame (15 to 18 day survival time) [34]. However, the group treated with PTX loaded PG remained alive until the end of the study (>40 days) [34]. In another study, chitosan thermogel solutions loaded with PTX (6.4% w/v) were locally administered to mice with subcutaneous EMT-6 mammary carcinoma tumors [14]. Researchers compared tumor growth inhibition when they administered PTX to the tumors via intratumoral injections or intravenous administration and utilized saline as a control [14]. This study showed the thermogel injections were just as effective at inhibiting tumor growth when compared to intravenous administration (38-40% growth inhibition over 17 days) [14]. However, the mice administered with PTX systemically experienced side effects such as weight loss, while the mice administered with PTX locally did not [14].

Comparatively, synthetic polymers include polyesters, polyanhydrides, polyamides, polycarbonates, polyorthoesters, and phosphate-based polymers [14, 30, 31]. The hydrophobic nature of synthetic polymers allows for long-term delivery of drugs and stabilizes water-insoluble drugs [14]. However, these polymers often present higher risks of immune response due to acidic degradation products that accumulate in the body [35]. An example of a successful synthetic drug delivery vehicle includes the administration of PTX through Paclimer (polyphosphoester) microspheres [14]. In one study, researchers injected mice with two non-small cell lung cancer lines (A549 and H1229) and administered Paclimer microspheres loaded with 10% wt/wt PTX via intratumoral injection or unbound PTX via intraperitoneal injection [14]. The microspheres were able to successfully deliver the drug directly to the tumor site at a rate of approximately 1-2% per day continuously over 90 days; thus, decreasing the A549 tumor doubling times 6-fold, and the H1229 tumor doubling times 3-fold when compared to the results from intraperitoneal injection [14]. In another study, researchers used OncoGel to locally control the release of PTX in rats with intracranial 9L gliosarcoma [36]. OncoGel is a DDS designed to slowly release PTX from a gel, ReGel. ReGel is a tri-block copolymer consisting of PLGA and polyethylene glycol [36]. For this

study, researchers loaded the gel with 6.3 mg/mL PTX and compared efficacy to the following controls: ReGel only, radiation therapy only, and OncoGel with 6.3 mg/mL PTX [36]. Once injected with the tumor, subjects died within 17 days when treated with ReGel only, 26 days when treated with radiation therapy only, and 31 days when treated with OncoGel only [36]. Therefore, using the OncoGel to directly deliver PTX to the tumor site, showed increased survival rates when compared to no drug delivery and systemic radiation therapy [36].

In addition to the aforementioned properties of natural and synthetic polymers, polymer viscosity grade and particle properties should be considered when choosing a polymer as a drug delivery vehicle [29]. Polymers with high viscosities are able to form a mechanically stable gel layer that provides a greater physical barrier for diffusion, thus extending release rates [29]. For instance, researchers studied the release rates of flurbiprofen (FB), a nonsteroidal anti-inflammatory drug used in the treatment of arthritis, from dialysis bags when loaded into low (0.32–0.44 dL/g) or high (0.7–1.1 dL/g) viscosity PLGA nanospheres, and utilized unbound FB as a control [37]. Unbound FB released completely from the bag within 6 hr [37]. Within this time frame, low viscosity PLGA nanospheres released approximately 80% FB, and high viscosity PLGA nanospheres released approximately 65% FB [37]. This study demonstrates that drug release rates increase as polymer viscosity increases [37]. Furthermore, the polymer particle size and distribution of the particles influences the rate that the drug penetrates through the gel layer [29]. In one study, researchers loaded theophylline, a bronchodilator, into polyethylene oxide tablets to analyze the effects of polymer particle size on drug release rate [38]. The tablets consisted of various polyethylene oxide particle size fractions (20–45, 45–90, 90–180 and 180–425 μm) [38]. Dissolution tests showed that tablets consisting of larger particle fractions released above 60% of theophylline within the first 30 min of the study [38]. Larger polymer fractions hydrate slowly and allow water to penetrate into the matrix; thus, causing a burst release of the drug [38]. Comparatively, smaller polymer particle fractions increase the polymer-water contact surface area. This allows the gel to crosslink faster and prolongs drug release [38]. This study supported this claim through water uptake tests [38]. Within 30 min, 180-450 μm polymer particles experienced $336 \pm 50\%$ increase in the weight, whereas 20–45 μm polymer particles experienced $275 \pm 49\%$ increase in weight [38].

Delivery Vehicle Geometries Affect Release Kinetics

Lastly, drug release from delivery vehicles are affected by vehicle geometries. Some types of vehicles previously used in cancer treatment technology include drug-eluting films, gels, wafers, rods, and particles [14]. The rate of diffusion of drugs from these vehicles is dependent on the effective surface area available for diffusion [29]. Increased surface area results in an increased drug release rate [39]. For instance, researchers loaded lamivudine, an HIV antiviral, into hydroxypropyl methylcellulose tablets and altered tablet shape to analyze the effects of tablet surface area on drug release rate [40]. As the researchers increased tablet thickness (3.96 mm to 5.3 mm) and held surface area/volume constant (approximately 0.873 mm^2/mm^3), the surface area decreased (327 mm^2 to 234 mm^2) [40]. The tablet with the larger surface area completely released the drug within 14 hr;

however, within the same time frame, the tablet with the smaller surface area released 90% of the drug [40].

2.2 Plant-Derived Chemotherapy Compounds and Natural Product Drugs

Naturally produced chemotherapy compounds can be encapsulated in delivery vehicles for local administration. Researchers have exploited chemical substances derived from plants for their therapeutic benefits since the 19th century with the development of morphine [41]. Morphine, derived from *Papaver somniferum*, contains analgesic compounds [41]. With 35,000 to 70,000 plant species screened for medical use, various natural compounds are used in medicine today, particularly within oncology [42]. Examples of naturally produced antitumor compounds are vincristine, derived from *Catharanthus roseus*, monocrotaline, derived from *Crotalaria sessiliflora*, and PTX, derived from *Taxus brevifolia* [41, 42]. However, due to production costs, processing times, and drug efficacy, many manufacturers have turned to synthetic pharmaceuticals to mimic the naturally produced therapeutic compounds found in plants [41]. For instance, Pfizer manufacturers irinotecan (Camptosar®), a chemical analog for a plant alkaloid found in *Camptotheca acuminata*, for the treatment of metastatic colorectal cancer [42]. Additionally, GlaxoSmithKline manufactures topotecan (Hycamtin®), another chemical analog for a plant alkaloid found in *Camptotheca acuminata*, for the treatment of ovarian and small cell lung cancer [42]. Despite the advantages of producing synthetic chemotherapy drugs, the safety levels and drug efficacy are questionable, leaving over 80% of the world dependent on natural counterparts [41].

2.2.1 Plant Cell Suspension Cultures for Drug Production

To produce plant-based pharmaceutical compounds, plant cell suspension cultures (PCC) are used as an alternative to other pharmaceutical production methods such as microbial fermentation and mammalian cell-based production [43]. Through this process, undifferentiated plant calli are suspended in liquid media and propagated *in vitro* under sterile and controlled environments, such as those in bioreactors [43]. PCC was initially designed for the production of specialized metabolites, such as PTX, digoxin, and ajmalicine; however, in recent years, this method has been approved as a viable option to produce pharmaceutical proteins [43]. For instance, Protalix manufactures glucocerebrosidase (Elelyso®) injections, derived from *Daucus carota* suspension cultures, as an enzyme replacement therapy for patients with Gaucher's disease [43]. Additionally, Greenovation Biotech GmbH manufactures humanized glycoproteins through *Physcomitrella patens* suspension cultures [43]. Although producing pharmaceuticals through suspension culture poses several limitations that are not a concern for alternative bioproduction methods, such as lower scalability, higher capital cost, and genetic instability, suspension cultures provide an environmentally conscious alternative with consistent yields that require less production time and simpler purification steps [43]. Researchers can produce and maintain PCCs from batch-to-batch within days or weeks as compared to the months or years it takes for other bioproduction methods [43].

Synergistic Interactions in Plant Cell Suspension Cultures

In addition to the aforementioned benefits of producing pharmaceuticals through PCCs, researchers hypothesize that the naturally produced metabolites and proteins synergistically interact to enhance therapeutic performance [12]. For example, one study produced artemisinin, an antimalarial compound, through *Artemisia annua* (*A. annua*) suspension cultures to study synergistic interactions for enhanced therapeutic performance [44]. In addition to artemisinin, these suspension cultures produce a variety of flavonoids (artemetin, casticin, chrysosplenetin, chrysosplenol-D, cirsilineol, and eupatorin) with antimalarial benefits [44]. To study the potential synergistic interactions between artemisinin and flavonoids, researchers administered artemisinin orally to malaria-bearing mice through either powdered dried leaves of whole plant *A. annua* (24 mg/kg) or comparable doses of pure artemisinin (24 mg/kg), and utilized a mouse chow placebo as a control [44]. The highest concentrations of artemisinin in the bloodstreams were reached after 30 min and over 60 min after administration, respectfully [44]. Whole plant *A. annua* demonstrated greater parasite killing activity when compared to the pure drug counterpart [44]. Researchers suspect that the flavonoids contained within the whole plant inhibited the intestinal and hepatic CYP enzymes; thus, increasing the bioavailability of artemisinin [44]. Furthermore, the artemisinin contained in the whole plant *A. annua* leaves decreased IC50 by 20-50%, thus demonstrating the potential synergistic interactions between the drug and additional naturally produced flavonoids [44]. Although the synergistic interaction mechanism is not fully understood, it is suspected that the flavonoids enhance the artemisinin-heme complex, which increases the release of free radicals [44]. As a result, the induced oxidative stress kills the parasites [45].

Researchers exploit flavonoids, as well as a variety of specialized metabolites, for their medicinal properties [12]. Plant specialized metabolites are generally characterized by three classifications: terpenoids, alkaloids, and phenolics [12]. These main types of classifications, as well as other metabolite classifications, are described below in terms of their location and pharmaceutical activity (Table 2.1).

Table 2.1: Classification of specialized metabolites (adopted from [12, 46, 47]).

Metabolite Classification	Description	Produced In	Pharmaceutical Activity
Polyketides and Fatty Acids	Linear combinations of acetate units	● Plant oils ● Animal fats	● Antiangiogenic ● Antidiabetic
Terpenoids	Polymeric isoprene derivatives synthesized from acetate via the mevalonic acid pathway	● Essential oils	● Antimicrobial ● Insecticidal ● Antiviral ● Antifungal
Phenolics	Present in hydroxylated aromatic rings One of the largest classes of specialized metabolites	● Plants	● Antioxidant ● Anti-Inflammatory ● Anti-Carcinogenic ● Bactericidal ● Antiseptic ● Anthelmintic ● Antiviral
Flavonoids	Water-soluble pigments	● Plants ● Fungi	● Anti-Allergenic ● Anticancer ● Antioxidant ● Anti-Inflammatory ● Antiviral
Alkaloids	Contains basic nitrogen atoms, carbone, hydrogen, and sometimes oxygen, sulfur, chlorine, bromine, or phosphorus	● Bacteria ● Fungi ● Animals ● Plants	● Anti-Inflammatory ● Antibacterial ● Antidiabetic ● Anticancer ● Antiarrhythmic ● Antineoplastic ● Anticholinergic
Saponins	Compounds whose active portions form colloidal solutions in water and precipitate cholesterol	● Plants	● Antimicrobial ● Hemolytic ● Antitumor ● Anti-Inflammatory

Researchers can use *Taxus spp.* cell cultures to produce PTX [10]. Within *Taxus* suspension cultures, various specialized metabolites, such as flavonoids and phenolics, are also synthesized [13]. Researchers hypothesize that these compounds synergistically interact with PTX to enhance the drug's cytotoxic properties [13]. Examples of specialized metabolites naturally produced in *Taxus* cultures include flavonoids, naringin and apigenin, and phenolics, curcumin and bithionol [48-51]. Studies have shown, naringin or apigenin, in combination with PTX, inhibits cell proliferation, and

induces apoptosis and cell arrest in the G1 phase [48, 49]. Similarly, when combined with PTX, bithionol enhances apoptosis by decreasing pro-survival factors and increasing the expression of pro-apoptotic factors in the treatment of ovarian cancer [50]. Additionally, when combined with PTX, curcumin suppresses nuclear factor kappa B, a protein complex that controls cell survival, in the treatment of metastatic breast cancer [51]. Current production of PTX cannot exploit the beneficial effects of synergistic interactions experienced in PCC. Additional downfalls of current PTX production methods include the adverse side effects caused by the harsh solvents used to extract and deliver the drug compound [10]. Therefore, the use of PCC to produce and deliver PTX will reduce the inefficiencies associated with current production methods that are also applicable to other plant-derived drugs.

2.3 Paclitaxel: A Natural Anticancer Agent

2.3.1 History of Paclitaxel

The United States Agriculture Department started an initiative in the 1960's to discover plants with anticancer agents [7]. In 1964, researchers extracted PTX, a compound that inhibits and prevents the development of tumors, from the bark of Pacific yew trees (*Taxus brevifolia)* [7]. PTX was originally tested through a series of assays against both leukemias and solid tumors, and it was discovered to be effective against the Walker tumor inhibition assay, as well as L1210 leukemia and 1534 (P4) leukemia [52]. PTX was originally mediocre against P-388 and L-1210 leukemia *in vivo*, which discouraged research on the drug [52]. The interest in PTX testing was revived when researchers confirmed PTX's antitumor activity through testing on the mouse melanoma B16 model [7, 52]. In this testing, PTX was administered to mice with B16 melanoma, where these mice decreased tumor size in a dose-dependent manner, resulting in up to 60% cure [53]. Researchers believe that this effectivity was due to PTX inducing bone marrow toxicity as well as induction of differential signal-transduction pathways which regulate the anti-apoptotic protein Bcl-2 [53]. As a result, PTX became a chemotherapeutic candidate for clinical development [7].

The U.S. Food and Drug Administration (FDA) first approved PTX as a treatment for ovarian cancer in 1992, and has since approved it for the treatment of breast cancer, non-small cell lung cancer, and AIDS-related Kaposi sarcoma under the trademark of Taxol® [7]. PTX is currently administered through intravenous therapy (IV) once every two to three weeks [8]. Depending on the patient's treatment plan, treatments may require 175 mg/m² over the course of 3 hr or 135 mg/m² over the course of 24 hr per treatment, both followed with cisplatin [8]. PTX binds to tubulin on the inner surface of microtubules, biopolymers involved in the splitting of cells during mitosis, to enhance the stability of the microtubules thus causing mitotic arrest [54]. By targeting these biopolymers, PTX is able to target fast-dividing cancer cells [54].

However, due to its systemic delivery, PTX is not selective and affects the entire body, particularly the fast-dividing hair and nail cells, which leads to the hair loss and weakening of nails often associated with chemotherapy [54]. Patients may also experience neutropenia, as well as severe

cardiac disturbances including sinus bradycardia, atrioventricular conduction, and bundle branch blocks [55]. Furthermore, PTX is dissolved in Cremophor El, a delivery vehicle used for poorly-water soluble drugs [55]. This solvent can cause patients to experience anaphylaxis and severe hypersensitivity [55]. Despite these side effects, PTX continues to be one of the most effective chemotherapy drugs. In efforts to utilize this drug for other forms of cancers, PTX is currently the subject of many clinical trials.

Although PTX is only approved by the FDA as treatment for the four aforementioned cancers, the drug is currently used in clinical trials for other solid-tumor cases including gastroesophageal, endometrial, cervical, prostate, and head and neck cancers, as well as sarcoma, lymphoma, and leukemia [54]. Some clinical trials involving PTX focus on the effects of PTX in conjunction with other cancer therapies. For instance, in one clinical trial, patients with advanced peritoneal cancer are treated with Letrozole, a hormone-based type of chemotherapy, with and without the presence of PTX carboplatin [56]. PTX carboplatin, a chemotherapy compound typically used in the treatment of small-cell lung cancers, is known for its minimal, delayed side effects [56]. The delayed side effects are due to the delayed interaction between the PTX carboplatin and nucleophilic sites of DNA [57, 58]. This delay in the interaction between PTX carboplatin and DNA nucleophilic sites results in less side effects on the nervous system, as well as reduced nausea, as compared to other treatments where these are usually significant side effects [57]. In another trial, researchers compare two types of therapies, proton and photon radiation therapy, in the treatment of esophageal cancer [59].

Additionally, researchers are exploring different forms of PTX to reduce the adverse side effects associated with PTX administration. For instance, researchers incorporated PTX with amphipathic hybrid peptides and lipids for targeted tumor treatment [60]. This study found that addition of biomimetic low-density lipoproteins successfully increases the biocompatibility of the DDS; thus reducing negative side effects that are typically associated with PTX treatment [60]. These lipoproteins carry hydrophobic compounds, such as PTX, by a hydrophobic core surrounded by more hydrophilic compounds, such as cholesterol [60]. This cholesterol layer surrounding the DDS is important, because it is known that to rapidly proliferate a tumor, a large amount of cholesterol is required, which this DDS helps to provide [60]. Similarly, researchers have investigated the effects of utilizing PTX albumin-stabilized nanoparticles to treat patients with breast, non-small cell, and pancreatic cancer [61]. Researchers believe this form of PTX has less negative side effects than pure PTX due to its delivery in the form of protein nanoparticles [61]. This nanoparticle delivery allows for solvent-free delivery of the PTX, allowing the system to bypass any associated side effects [62]. This nanoparticle formulation also reduces adverse side effects by directing the drug to the tumor site for increased local accumulation through endogenous albumin transport mechanisms [62].

Researchers use clinical trials as a means to expand and improve PTX's function as a chemotherapy drug; however, research is still need to improve upon its production. For instance, PTX production is inefficient in keeping up with its growing demand. Eight mature yew trees are needed to extract 2.5-3 g of PTX, the amount required for a typical treatment [9]. Yew trees

propagate sparsely and must mature for approximately 100 years before the bark is ready for harvesting [63]. As a result of the inefficiencies in producing PTX through yew tree extraction, PTX costs upward of $600,000/kg [9]. Therefore, due to the current limitations in PTX production, researchers are exploring more efficient ways to produce PTX.

2.3.2 Production of Paclitaxel

PTX is naturally produced in the bark of Pacific yew trees, which is one of the five common potential methods in which the drug can be synthesized: heterologous expression systems, chemical synthesis, semi-synthesis, extraction from yew trees, and plant cell cultures [9]. Heterologous expression systems involve introducing recombinant DNA or RNA that encode proteins to host cells to carry out chemical functions they would not otherwise [64]. However, producing metabolites through heterologous expression presents challenges in expressing full length proteins and producing substantial yields [65].

To understand other methods of PTX production, the biosynthetic pathway of PTX must be understood [11]. Researchers believe the biosynthetic pathway to produce PTX has putatively nineteen steps; however, not all enzymatic steps are understood or confirmed [11]. As a result, synthetic production of PTX is not a feasible production method [11]. As an alternative, semi-synthetic production has been considered [11]. Semi-synthetic production includes the use of the biosynthetic precursors harvested from yew needles [11]. PTX is a diterpenoid pseudoalkaloid with the chemical formula $C_{47}H_{51}NO_{14}$, and is a member of the taxane family [66]. The most notable structure of all taxanes, and an important precursor in the synthesis of PTX, is the taxadine three-ring core [67]. This core is the initial structure of all taxanes that exhibit anticancer activity [67]. The known pathway for PTX, including its precursors, is shown in Figure 2.1.

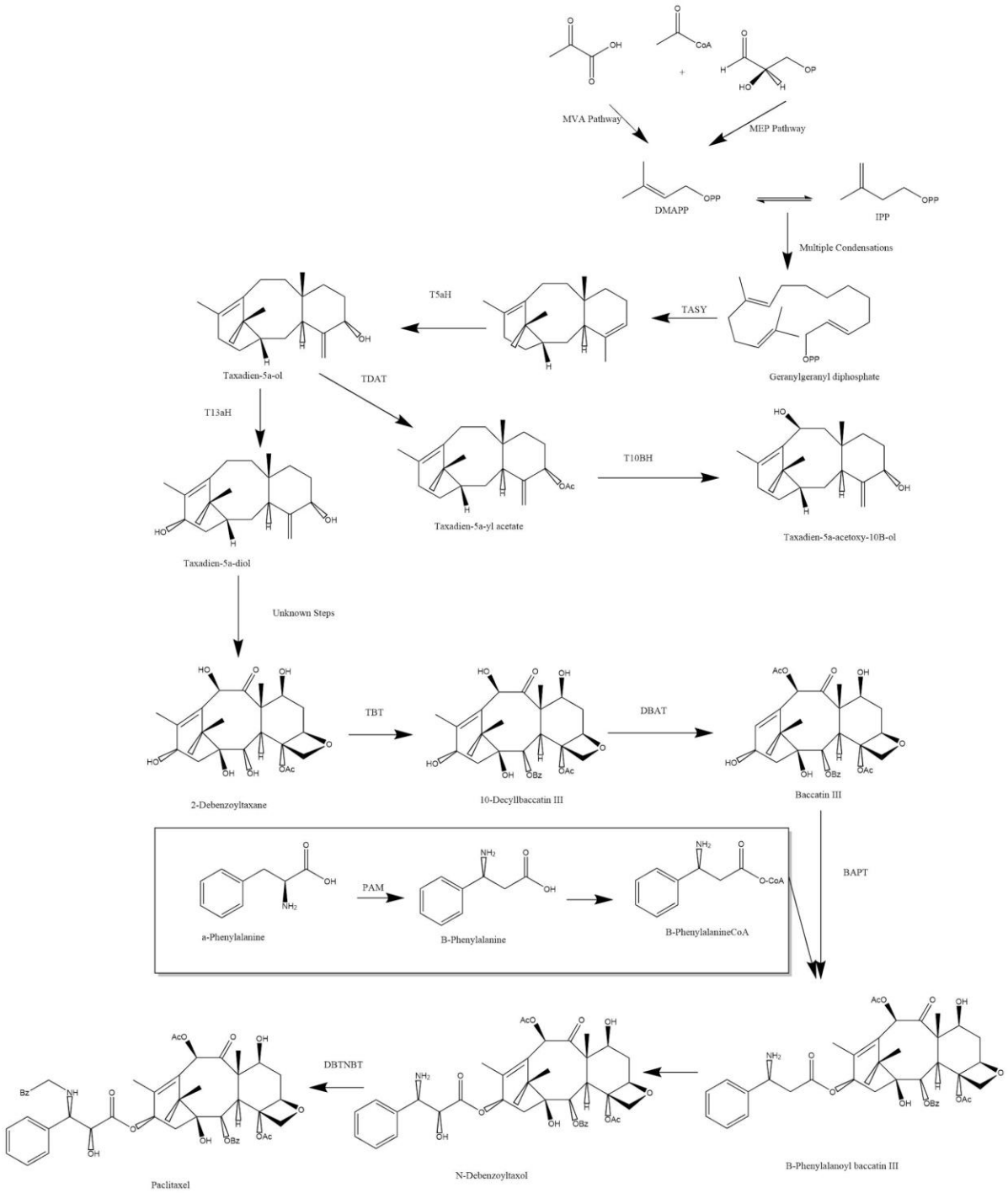

Figure 2.1: Biosynthetic pathway of PTX (adapted from [9]).

Baccatin III and 10-deacetylbaccatin III are important precursors in the synthesis of PTX (Figure 2.1) [11]. However, the supply of precursors used in the semi-synthetic pathways are depleting from their European and Himalayan plant sources due to the high demand [10]. Due to this depletion, more reliable sources of these precursors or an alternative form of PTX production is needed.

PTX is extracted from the bark of Pacific yew trees with aggressive solvents [10]. These solvents include chlorinated hydrocarbons, such as chloroform, which are dangerous to humans if exposed through inhalation [10]. In addition to the danger presented by the severity of the solvents, large amounts of the solvents are required to effectively extract PTX [10]. This presents issues regarding the raw material cost of the solvent, and the difficulty to then remove PTX from the large volume of solvent [10]. Furthermore, extraction methods produce low yields of PTX [10]. Twelve kg of dry bark produces only 500 mg of PTX (0.004% yield) [68]. Because the extensive extraction process produces low drug yields, the process is inefficient in keeping up with growing demand for PTX. The demand for PTX has increased from 50 kg a year to 500 kg per year [68]. This demand could diminish the yew tree supply within 5-10 years [68]. Therefore, researchers are investigating more efficient methods of PTX production to preserve these trees [10].

The crude extraction of PTX from yew tree bark is not a sustainable method in producing the drug; however, less invasive methods of PTX production include extracting the compound from the trees' leaves [10]. Extracting PTX from leaves does not kill the trees as bark extraction would and produces a greater percent yield than bark extraction (0.02%) [68]. However, this method is still limited by the number of Pacific yew trees in a harvest year, which is severely limited by the specific environment the trees grow in [10, 68]. Therefore, researchers have been exploring alternative methods of PTX production, such as PCC, to preserve yew tree forests and provide a sustainable supply of PTX.

2.3.3 *Taxus* Plant Cell Culture

While PTX is currently administered as a purified compound, the use of PCC to produce and deliver PTX would synthesize the drug in concert with other natural compounds. These compounds include precursors to PTX, and other specialized metabolites that may exhibit synergistic effects in treatment of cancer [51].

Researchers are interested in PTX precursors to supplement natural production and produce synthetic chemotherapy drugs. Two of the most desired precursors are baccatin III and 10-deacetylbaccatin-III [68]. In addition to naturally creating PTX, researchers can utilize these precursors to synthetically produce docetaxel, another taxane chemotherapy agent that is distributed under the trademark Taxotere® [68].

Although PTX is a known anticancer agent produced in *Taxus* PCCs, other naturally produced metabolites, such as phenolics and flavonoids, exhibit medicinal properties [69]. Phenolics are naturally produced in plant cells to protect the plants from ultraviolet radiation, or aggression by pathogens, parasites and predators [69]. Similarly, in humans, phenolics exhibit antioxidant properties and can be used for bactericides and antiseptics [12]. The antioxidant activity of phenolic compounds is associated with the structure of the molecule: conjugated double bonds and functional groups bound to the ring [70]. This structure allows phenolics to inhibit the formation of reactive oxygen species and interrupt free radical reactions by rapidly donating hydrogen atoms to radical groups [69, 70].

Additionally, phenolics exhibit anticancer properties [69]. For instance, researchers utilized phenolics isolated from strawberries, including anthocyanins and kaempferol, to inhibit the growth of human oral, breast, colon, and prostate cancer lines *in vitro* [69]. Researchers have also found that phenolics contained within bilberry, raspberry, tea extracts are effective anticancer agents for cancers such as leukemia, lymphoma, prostate, breast, lung, head, and neck cancers *in vitro* [69]. Researchers have found similar results with phenolics *in vivo.* For instance, researchers supplied rats with colon cancer anthocyanin-rich diets including bilberries, chokeberries, and grapes [69]. For those receiving the diet, tumor size improved after 14 days in comparison to the control group who did not receive this diet [69]. In another study, researchers supplied cyanidin-rich diets to mice [69]. Mice receiving the diet showed reduced number of skin tumors when treated twice per week as compared to mice who were not introduced to cyanidin [69].

One subclass of phenolics, flavonoids, also demonstrate medicinal properties, including anticancer properties. Flavonoids are a specific, hydroxylated class of phenolics, naturally produced in fruits and vegetables, that defend the plants from microbial infections and plaques [71, 72]. Similarly, flavonoids exhibit multiple beneficial effects in humans, such as anti-inflammatory and anticancer properties. Inflammation occurs naturally after tissue damage, infection, or chemical irritation [71]. The inflammation process produces reactive oxygen species, as well as reactive nitrogen species, including tyrosine and serine-threonine protein kinases, as the body heals itself [71]. Flavonoids specifically target these species by binding with ATP at the catalytic sites to inhibit the kinases; thus, reducing inflammation [71].

Furthermore, flavonoids have been a focal point of chemoprevention research, as epidemiological and clinical studies suggest that these compounds can prevent cancer through their interaction with various genes and enzymes [73]. For instance, researchers have shown that flavonoids naturally produced in apples, onions, and wine can lower the risk of prostate, lung, stomach, and breast cancers [71]. Researchers attribute the anticancer properties of flavonoids to their ability to inhibit various proteins that promote tumor growth [71]. For instance, flavonoids downregulate mutant p53 proteins, proteins that are unable to suppress tumor formation. In breast cancer cells specifically, researchers have demonstrated that flavonoids downregulate the p53 protein to nearly undetectable levels [71]. The inhibition of the expression of this protein can lead to the arrest of the cancer cells [71]. Additionally, researchers have shown that flavonoids inhibit heat shock proteins in breast cancer, leukemia, and colon cancer cell lines [71]. These heat shock proteins allow cancerous cells to survive various conditions in the body [71]. The inhibition of these proteins may lead to easier cancer cell death [71].

Therefore, in addition to producing PTX, PCCs have the ability to produce other metabolites that exhibit medicinal properties that may enhance the cytotoxic properties of the drug. By encapsulating the PCC material drug performance may be enhanced, costly downstream processing can be bypassed, PTX loss through separation processes can be prevented, and the need for the use of harsh solvents that are currently used in the production and delivery of PTX can be eliminated.

2.4 Research Plan: *Taxus* Cell Culture as a Drug Delivery System for Paclitaxel

Currently, PTX is an FDA approved treatment for four types of cancers: breast, ovarian, non-small cell lung, and AIDS-related Kaposi sarcoma [7]. However, current PTX production methods are ineffective, produce low yields of the drug, and require processing steps with harsh solvents. As a result, there is current research to address these challenges in producing PTX, including the use of PCC to manufacture the drug. Producing PTX through PCC has various benefits including the following: enhanced therapeutic agents through the natural synergistic interactions within the plant compounds, rapid processing and maintenance time compared to other culture methods, and less toxic delivery systems.

In a previous Major Qualifying Project (MQP), students from Worcester Polytechnic Institute investigated the possibility of using PCC to create a local delivery system for PTX. For the purposes of the project, students sought to increase cell-associated PTX accumulation, remove DNA from the cells for biocompatibility, and compare the release kinetics of free PTX to calcium alginate encapsulated PTX [16]. This MQP expands beyond this initial research to further provide insight on the delivery of PTX through a targeted PCC drug delivery system through the following aims:

Aim 1: Develop a wash process that retains PTX, flavonoid, and phenolic compounds, and prepare PCC material for encapsulation.
Aim 2: Optimize delivery of PTX, flavonoid, and phenolic compounds by encapsulating PCC material in a biomaterial suitable for desired delivery.
Aim 3: Establish an *in vitro* model to optimize drug delivery design for maximum breast cancer cell culture cytotoxicity, and predict release studies for PCC delivery.
Aim 4: Understand pharmacokinetics for components of the optimized drug delivery system to determine feasibility and administration parameters.

Chapter 3: Retention of Paclitaxel, Flavonoids, and Phenolics Through Wash Processing

3.1 Background

3.1.1 Production of Paclitaxel

Paclitaxel (PTX) is naturally produced throughout all parts of yew trees, but is most concentrated in the bark [10]. Extraction of PTX from the bark requires large amounts of energy. However, even the most productive species of yew produce small concentrations of PTX (0.004% wt/wt dry) making large scale manufacturing of the drug difficult [74]. Given these small concentrations, it takes upwards of eight 60-year-old yew trees to treat the average patient [75]. Alternative methods of PTX production, such as synthetic synthesis, requires a comprehensive understanding of PTX's complex biosynthetic pathway, which is currently not fully understood [9]. With a high demand for the drug and low concentrations of PTX naturally produced, there is a need to uncover alternative methods for PTX production, such as *Taxus* plant cell cultures (PCC) [75].

Although the natural supply of PTX is limited through all production avenues, PCC technology has emerged as a viable and renewable option for commercial supply [76]. Several companies worldwide, such as Python Biotech and Corean Samyang Genex, have begun exploring PCC for PTX production because of its improved drug yield (0.02% wt/wt dry) and noninvasive methods [76]. Optimizing production of PTX and other taxanes via PCC can be achieved through manipulating culture conditions, selecting high-producing cell lines, and adding elicitors or precursors [76]. In fact, current supply of PTX in the United States is through PCC.

In *Taxus* PCCs, exogenously adding purified PTX to existing *Taxus* cultures aids in carefully controlling the concentration of PTX in a culture [77]. However, this method requires a constant supply of purified PTX, which is expensive [77]. Alternatively, researchers can add elicitors, chemicals that enhance synthesis of specialized metabolites in plants to ensure survival persistence and competitiveness, to increase PTX production in *Taxus* PCCs [77, 78]. The addition of abiotic elicitors, including metal ions and inorganic compounds such as silver complexes, copper sulphate, and cobalt complexes, have increased PTX production in *Taxus* cultures by improving the production of specialized metabolites in PCCs [77, 78]. In one study, researchers added silver nitrate to *Taxus* PCCs to increase PTX production [79]. Elicitation with silver nitrate minimized the negative effects of the plant hormone ethylene, a hormone that typically inhibits plant cell growth and specialized metabolite production [79]. Furthermore, researchers have discovered abiotic chemicals, such as methyl jasmonate (MeJA), to be successful elicitation agents for PTX in *Taxus* cultures [78, 80, 81]. MeJA, a natural plant hormone, elicits a stress signal in *Taxus* cells, which causes the cells to produce a variety of specialized metabolites, including PTX [81]. Additionally, MeJA plays an active role in regulating defense genes in *Taxus* cells, which leads to the release of

PTX [81]. Studies have indicated that the introduction of 100 μM MeJA in *Taxus* cultures can increase the production of PTX by more than 50% [80].

The production of complex metabolites, such as PTX, through elicited PCCs presents challenges, as the level and pattern of production is often unstable and unpredictable between batches [74]. Currently small-scale PCC produces between 1-5 mg/mL PTX [82, 83]. However, considering projected demands of tens to hundreds of kg of PTX are needed per year, it is imperative that PTX production is improved to increase consistent PTX concentrations [83]. In one study, researchers used a 500 L bioreactor to produce PTX in concentrations of up to 3 mg/L after 27 days in a balloon-type bubble reactor [84]. Even though these results are promising, scaling up PTX production via PCC would require more research in reactor type and conditions to maintain continuous productivity [85]. With these challenges, improvement in PTX production through PCC is needed to enable higher yields in current processes.

After PTX is produced via PCC, the drug is extracted from the PCC media and material; however, there is a potential to use the cell culture material containing PTX for treatment [10, 86, 87]. To separate and purify PTX from PCC media and material, several steps including isolation, crude purification, and final purification are required [86]. Isolation of PTX from PCCs commonly involves liquid-liquid extraction, in which solvents can be used to separate the drug from the encapsulating cell culture [88]. Although isolating PTX from cell culture for therapeutic applications is an effective way to use the drug, using the cell culture material for treatment circumvents the costly and time intensive processing steps involved in drug separating and purification [12]. Additionally, treatment involving the PCC material takes advantage of the potential synergistic interactions that occur between PTX and other specialized metabolites and proteins that could enhance the drug's cytotoxic properties [12]. When considering treatment involving PCC material, PTX and those additional metabolites must be retained when preparing the material for administration.

3.1.2 Retention and Detection of Paclitaxel

Although using PCC material does not require crude purification, it does require additional processing to remove the cell-based material from the media. In processing PCCs to obtain PTX, retention of PTX through washing and processing steps is crucial, as it is necessary for media components and water-soluble impurity removal to isolate the PTX and other specialized metabolites used in drug delivery. However, through these wash steps, PTX is lost. Because of this, optimization of the wash steps is necessary to minimize this PTX loss to the media and maximize the PTX concentration in the cells. In a previous MQP, students from Worcester Polytechnic Institute washed cell culture samples after lyophilizing them [16]. Washing after lyophilization led to the 85% loss in metabolites, such as PTX, after processing [16].

To increase PTX retention in the plant cell material throughout processing, washing before lyophilizing the material through high-speed centrifugation is a promising alternative [89]. Through centrifugation, the cell-associated metabolites and cellular material are separated from media and

water-soluble compounds and localized into a pellet, allowing for an easy removal of the media-rich supernatant [89]. Researchers can repeat the process by replenishing the conical tube with water; thus, effectively washing the sample [89]. To detect PTX concentrations after processing, researchers can use ultra high performance liquid chromatography (UPLC) to determine the concentrations of PTX produced in the elicited *Taxus* cultures and retained through processing [90].

In addition to PTX, the *Taxus* species produces various specialized metabolites [76]. Among these are flavonoids and phenolics, which provide therapeutic benefits [12]. Researchers hypothesize that the presence of flavonoids and phenolics could create synergistic interactions with drugs, such as PTX, that may enhance the therapeutic properties due to previous evidence of these metabolites working synergistically with other antibodies [12]. For example, phenolics residing in *Taxus cuspidata*, such as hydroxycaffeic acid and protocatechuic acid, demonstrated anticancer activities and enhanced the cytotoxic properties of PTX by inducing cancer cell apoptosis [91]. Due to these interactions, the retention of flavonoids and phenolics throughout the wash process is important and should be maximized. To test the retention of these metabolites, flavonoid and phenolic assays may be performed to analyze metabolite concentrations before and after samples are processed [92].

3.2 Methods

3.2.1 Plant Cell Culture Maintenance

Taxus cuspidata cell lines 48.82A.11 were grown and maintained in 50 mL liquid suspension cultures and transferred every 14 days to new media. Media, prepped in 4 L batches, consisted of 0.67 L nanopure water/L media, 20 g/L sucrose (Caisson Laboratories, Smithfield, UT), 3.21 g/L Gamborg-B5 (PhytoTechnology Laboratories, Lenexa, KS), 0.1 µM benzyl adenine (Sigma-Aldrich, St. Louis MO), and 2.7 µM 1-naphthaleneacetic acid (Sigma-Aldrich, St. Louis, MO). Erlenmeyer flasks (125 mL) were filled with 40 mL of media and closed with Bellco foam caps before being autoclaved on the liquid cycle (121 °C) for 20 min. In a sterile environment, 10 mL of 14-day-old cell culture were subcultured into fresh media with 2.5 mL of filter-sterilized antioxidant solution containing 2.5 mg/mL ascorbic acid (Fisher Scientific, Hampton, NH), 2.5 mg/mL citric acid (PhytoTechnology Laboratories, Lenexa, KS), and 14.6 mg/mL L-glutamine (Caisson Laboratories, Smithfield, UT). All cultures were incubated in a gyratory shaker (New Brunswick Scientific Co. Inc, Edison, NJ, Model 44) at 125 rpm, 23 °C, and in the dark.

3.2.2 Eliciting Cells with Methyl Jasmonate

Seven-day-old cultures were elicited with 100 µM MeJA to promote the production of PTX within the cells. The following reagents were added successively to create the MeJA solution: 50 µL MeJA (Sigma-Aldrich, St Louis, MO, 392707), 450 µL ethanol, and 500 µL nanopure water. These reagents were filter-sterilized through a 0.22 µM polyvinylidene difluoride (PVDF) filter and 1 mL syringe (PrecisionGlide®, Becton Dickinson, Franklin Lakes, NJ) into a 1.5 mL microcentrifuge

tube. Each flask containing approximately 50 mL of 7-day-old culture with media and antioxidants was elicited with 21.8 µL of MeJA solution. Each elicited flask was covered with a Bellco cap and aluminum foil to prevent volatilization of MeJA.

3.2.3 Wash Processing

This study was performed in two phases. The first phase investigated whether the initial volume of PCC used in wash processing affects PTX retention. This part of the study was completed by comparing PTX retention in 10 mL and 25 mL washed PCC samples, as described in further detail in Phase 1. The second phase sought to identify whether lyophilization degrades specialized metabolites and PTX after being washed, as further described in Phase 2.

Phase 1

Within six identical 50 mL conical tubes (Eppendorf, Hamburg, Germany), 25 mL of PCC were added to half of the tubes, and 10 mL of PCC were added to the others using an electric pipettor. All tubes were filled to the 40 mL line with deionized (DI) water, and weighed to be within 0.5 g of each other to ensure proper balance within the centrifuge. The tubes were spun in a fixed-angle rotor (FA-45-6-30, Eppendorf, Hamburg, Germany) centrifuge (5808F, Eppendorf, Hamburg, Germany) at 9,000 g and 4 °C for 30 min.

After centrifugation was complete, 25 mL of supernatant were removed from the tubes initially filled with 25 mL culture, and 30 mL were removed from the tubes initially filled with 10 mL culture with an adjustable volume pipette. The removed supernatants were transferred to individual flasks, and six 1 mL samples were taken from each flask. The tubes were refilled to the 40 mL line with DI water and reweighed. The pellet was resuspended by manually shaking the tubes. The tubes were centrifuged again under the same conditions for a total of three wash steps.

At the end of the third wash step, the tubes were refilled to the 10 mL and 25 mL lines respectfully with DI water, and the pellets were resuspended by shaking. Four 1 mL samples were taken from each final culture. This wash processing procedure is presented below (Figure 3.1).

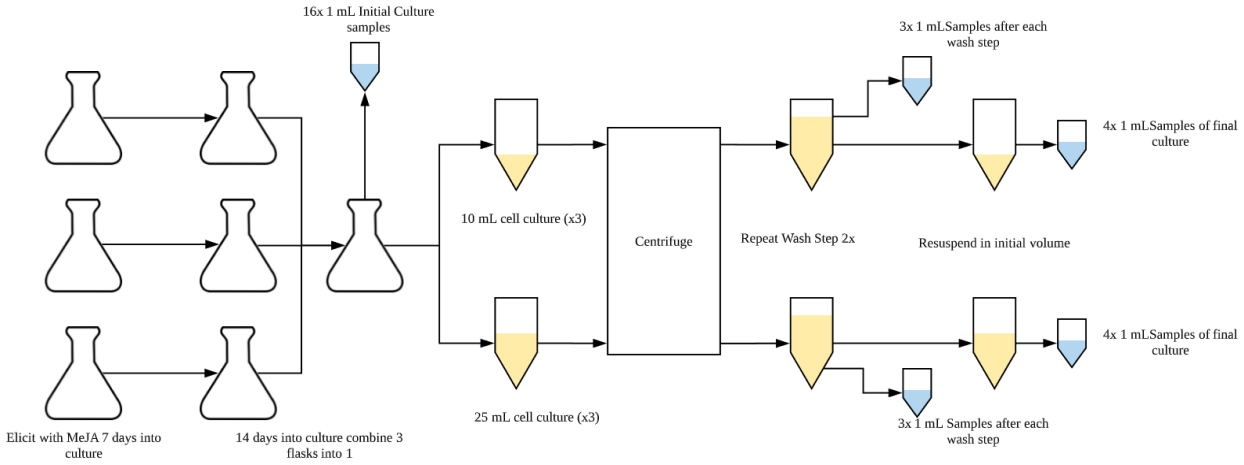

Figure 3.1. Flow chart of the wash processing procedure for Phase 1.

All 1 mL samples were placed in an evaporative centrifuge (Vacufuge plus, Eppendorf, Hamburg, Germany) overnight (approximately 15 hr) under aqueous conditions (1,400 rpm, suction capacity: 1.8 m^3/hr). Dried samples were stored at -80 °C (SU80XLE, Global Cooling Inc., Athens, OH) until further processing for PTX concentration retention (Section 3.2.4).

Phase 2

Twenty-six 1 mL samples were taken from the initial PCC. Six 50 mL conical tubes were filled with 10 mL of PCC with an electric pipettor. All tubes were filled to the 40 mL line with DI water. The tubes were spun in a fixed-angle rotor centrifuge at 9,000 g and 4 °C for 30 min.

After centrifugation was complete, 30 mL of supernatant were removed from each tube with an adjustable volume pipette. The tubes were refilled to the 40 mL line with DI water and reweighed. The pellet was resuspended by manually shaking the tubes. The tubes were centrifuged again under the same conditions for a total of three wash steps.

At the end of the third wash step, the tubes were refilled to the 10 mL line with DI water, and resuspended. After resuspension, six 1 mL samples were taken from each final culture. This wash processing procedure is presented below (Figure 3.2).

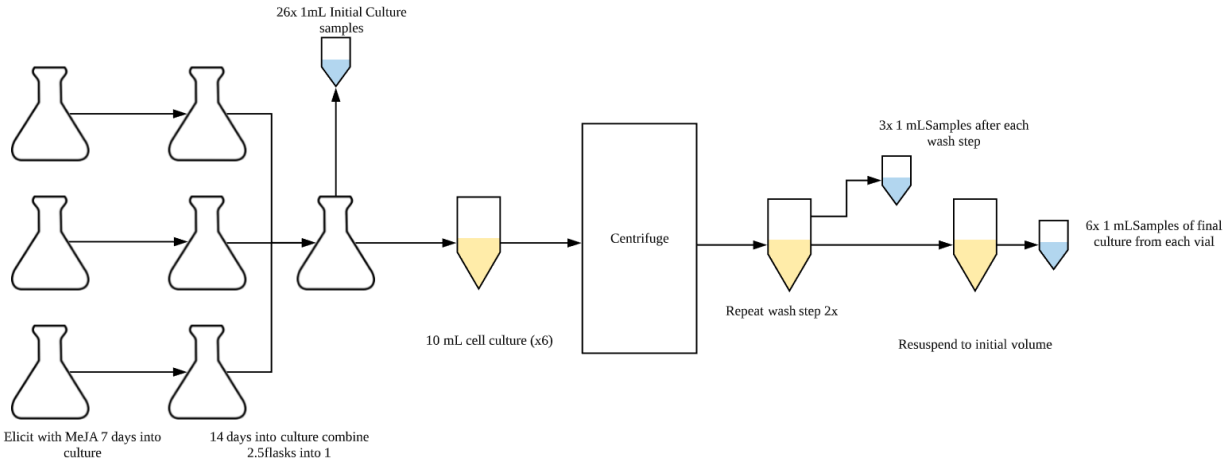

Figure 3.2. Flow chart of the wash processing procedure for Phase 2

Six of the 1 mL final culture samples from each tube were lyophilized (VirTis BenchTop Pro with Omnitronics, SP Scientific, Stone Ridge, NY) for 24 hr to compare the effects of lyophilization on the retention of flavonoids, phenolics, and PTX.

All samples were placed in an evaporative centrifuge overnight under aqueous conditions and stored at -80 °C until further processing for PTX (Section 3.2.4), flavonoid, and phenolic concentration retention (Section 3.2.5).

3.2.4 UPLC Preparation

Sample Preparation

The dried 1 mL samples were resuspended in 1 mL acidified methanol (0.01% acetic acid). Samples were vortexed (Scientific Mini Vortexer, VWR, Radnor, PA) and sonicated (Aquasonic 75HT, VWR, Radnor, PA) for 20 min on ice. The samples were manually broken up with a spatula, vortexed, and sonicated for another 20 min. Samples were transferred into a microcentrifuge tube rack and placed on a shaker (New Brunswick Scientific Co. Inc, Edison NJ, Model 44) for 30 min, revortexed, and centrifuged (5424, Eppendorf, Hamburg Germany) for 20 min at 16,000 rpm. From each supernatant, 800 µL were transferred to new microcentrifuge tubes. Samples were placed in an evaporative centrifuge for 2.5 hr under alcohol conditions (1400 rpm, suction capacity: 1.8 m^3/hr), and stored at -80°C until further processing.

UPLC Processing

To prepare the chromatography vials for UPLC processing, the samples were resuspended in the following order: 25 µL methanol, 35 µL acetonitrile, and 40 µL nanopure water. In between adding each reagent to the samples, the samples were vortexed, sonicated, and vortexed again for a 10 sec each to dissolve the samples completely. Once the samples were dissolved, the samples were filtered through a 0.22 µm PVDF and 1 mL syringe into a 2 mL UPLC vial (VWR, Radnor, PA)

with a low-volume (0.15 mL) insert (VWR, Radnor, PA). In between filtering each sample, the syringe was flushed with 1 mL acidified methanol to prevent cross-contamination between samples. The samples were analyzed through UPLC (Waters, Milford, MA, Acquity UPLC H-Class) consisting of a 10 µL injection and a 6-min separation time in which molecules are separated in a 70:30 (v:v) water-acetonitrile solvent in a C 18 2.1x50 mm, 1.7 µm column. The samples were read at a wavelength of 228 nm and compared to PTX standards (0 mg/L, 12.5 mg/L, 25 mg/L, 50 mg/L, and 100 mg/L) (Alfa aesar, Ward Hill, MA). The concentration of PTX in each sample was found by measuring the area under the curve.

3.2.5 Phenolics and Flavonoids Assays

Sample Preparation

To prepare the samples for flavonoid and phenolic assays, 1 mL samples were resuspended in 500 µL of acidified methanol. Samples were vortexed and broken up mechanically with a spatula to ensure the release of the plant compounds from the pellet. To further release the plant compounds, the samples were spun in a microcentrifuge for 5 min at 16,000 rpm.

Flavonoids Assay

The following reagents were placed directly into a 96-well plate and incubated for 30 sec: 6.25 µL resuspended sample, 18.75 µL acidified methanol, 50 µL nanopure water, and 75 µL sodium nitrite (Acros, NJ, 42435-5000) (6 g/L). Note that the resuspended sample was further diluted in acidified methanol to ¼ to ensure concentrations fell within the standard range. Once incubated, 75 µL aluminum chloride (Sigma-Aldrich, St Louis, MO, 7784-13-6) (22 g/L $AlCl_3 \cdot 6H_2O$) was added to each well, followed by another 2 min incubation period. Lastly, 75 µL of 0.8 M sodium hydroxide (Sigma-Aldrich, St Louis, MO, 1310-73-2) were added to each well. The colorimetric absorbance of the plate was read on a Multiskan^{TM} GO Microplate Spectrophotometer (Accuskan GO, Fisher Scientific, Hampton, NH) at 490 nm. These absorbance values were compared to catechin standards (0.0 mg/mL, 0.1 mg/mL, 0.2 mg/mL, 0.4 mg/mL, 0.6 mg/mL, 0.8 mg/mL, and 1.0 mg/mL) (Cayman Chemical, Ann Arbor, MI, 70940) which were prepared and analyzed with the same protocols as the samples.

Phenolics Assay

The following reagents were placed directly into 1.5 mL microcentrifuge tubes: 5 µL resuspended sample, 15 µL acidified methanol, 40 µL 0.2 M Folin-Ciocalteau reagent, and 160 µL 700 mM sodium carbonate (Fisher Scientific, Hampton, NH, S263-500). Note that the resuspended sample was further diluted in acidified methanol to ¼ to ensure concentrations fell within the standard range. The reagents incubated for 10 min. Then the samples were spun in a microcentrifuge

for 1 min at 16,000 rpm. From each sample, 200 µL of supernatant were transferred to a 96-well plate. The colorimetric absorbance of the plate was read on a Multiskan^{TM} GO Microplate Spectrophotometer at 750 nm. These absorbance values were compared to gallic acid standards (0.0 mg/mL, 0.025 mg/mL, 0.05 mg/mL, 0.075 mg/mL, 0.10 mg/mL, and 0.20 mg/mL) (Acros Organics, Hampton, NH) which were prepared and analyzed with the same protocols as the samples.

3.3 Results and Discussion

3.3.1 Media and Cell Association of Flavonoids, Phenolics, and Paclitaxel

Metabolite association to cells, rather than to media, is necessary to prevent loss of metabolites through wash processing; thus, producing product containing sufficient levels of metabolites for a drug delivery system (DDS). Therefore, metabolite concentrations in cells and media were analyzed prior to processing.

Prior to washing the cell culture, 6 initial culture samples were used to determine whether the PTX was cell- or media-associated. To test this association, samples were spun in a microcentrifuge for 5 min at 16,000 rpm. The media-rich supernatant was extracted from the cell pellet with a low-volume adjustable volume pipette and placed into new 1.5 mL microcentrifuge tubes. Specialized metabolite assays and UPLC analyses were used to determine the cell and media association of flavonoids, phenolics, and PTX (Figure 3.3).

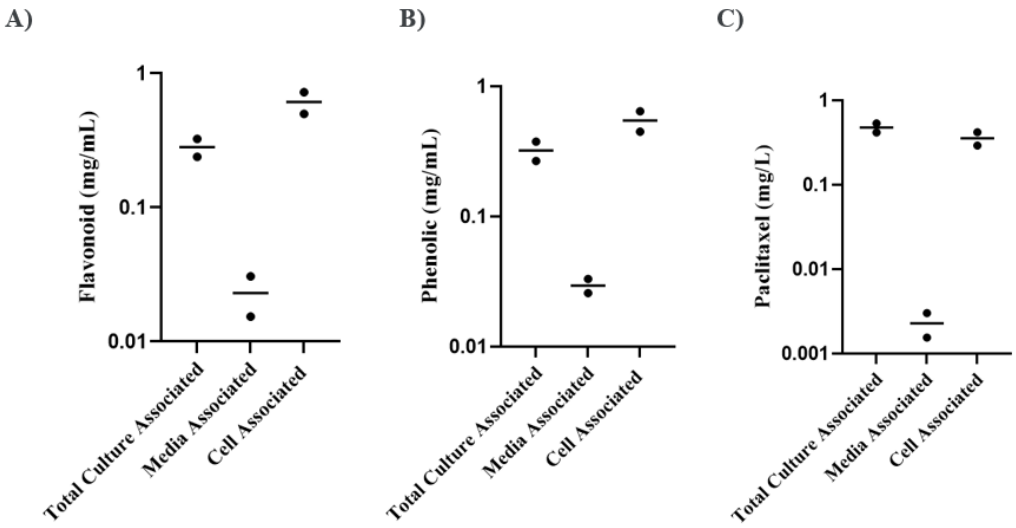

Figure 3.3: Concentration of A) flavonoids, B) phenolics, and C) PTX in initial culture samples for an elicited culture both in total and split into media and cell components. The data show values for two biological replicates (dots) with the average indicated by a line.

The flavonoids, phenolics, and PTX were primarily cell associated. Approximately 0.6 mg of flavonoids per 1 mL of cell culture, 0.5 mg of phenolics per 1 mL of cell culture, and 0.5 mg of PTX per 1 mL of cell culture were associated to the cells (Figure 3.3). On the contrary, only 0.03 mg of

flavonoids per 1 mL of cell culture, 0.03 mg of phenolics per 1 mL of cell culture, and 0.002 mg of PTX per 1 mL of cell culture were associated to the media (Figure 3.3). Because of the metabolic association to cells, and the lack of media association, the PCC could feasibly undergo the wash process and retain the therapeutic components.

3.3.2 Comparing Paclitaxel Retention in 10 mL and 25 mL Volumes of Plant Cell Culture

Once it was determined that the therapeutic agents within the PCC were cell associated, the cells were washed from the media. The effects of initial cell culture volume on PTX retention were first analyzed. To determine the effects, 10 mL and 25 mL of initial PCC underwent the same wash processing procedure (Figure 3.1). The initial PTX concentrations were compared to final concentrations through the use of UPLC analysis.

To obtain PTX concentrations, UPLC analysis was performed on six initial PCC samples, one supernatant sample from each tube for all three wash steps, and one final PCC sample from each tube after being resuspended to the respective initial volume (Figure 3.4).

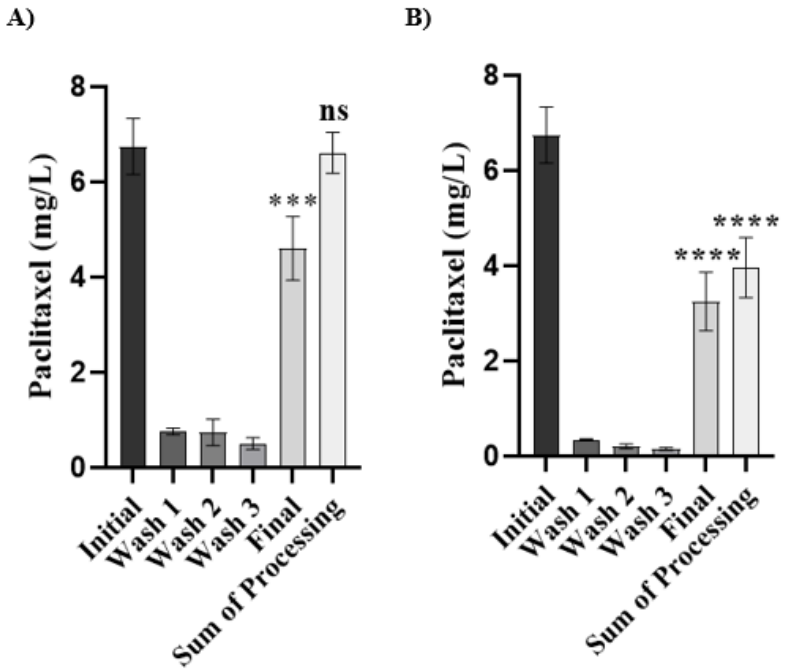

Figure 3.4. Concentration of PTX in A) 10 mL and B) 25 mL initial culture volumes at each stage of the wash process for an elicited culture. Sum of processing values are the summation of PTX in wash step samples and final culture samples. The error bars represent standard deviation amongst three biological replicates. A two-way ANOVA statistical analysis compares column means to the initial culture samples: ***=p≤0.001, ****=p≤0.0001, ns=p>0.05.

Although final PTX concentrations for the 10 mL and 25 mL samples were statistically different from the initial PTX concentrations, the 10 mL initial culture retained more PTX through the wash processing when compared to the PTX retention of the 25 mL initial culture (Figure 3.4). When washing 10 mL of PCC, an average of 68.3% of PTX was retained from the initial culture samples

through three wash steps to the final culture samples (Figure 3.4). However, when washing 25 mL of PCC, an average of 48.2% of PTX was retained from the initial culture samples through three wash steps to the final culture samples (Figure 3.4).

To further compare the final PTX concentrations from each PCC volume to the initial PTX concentrations, a statistical comparison of PTX concentrations was analyzed between initial culture samples and final culture samples of both volumes (Figure 3.5).

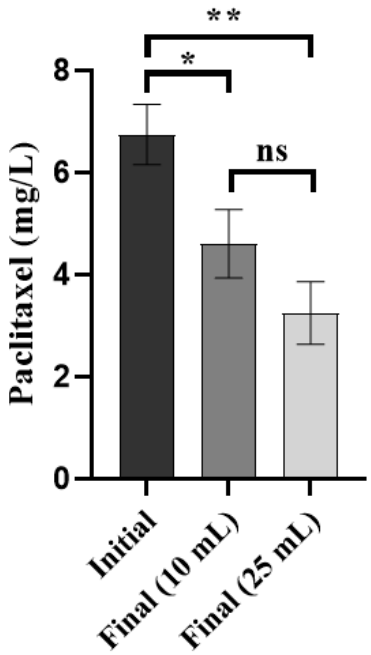

Figure 3.5. Concentration of PTX in initial culture samples compared to final culture samples from 10 mL and 25 mL initial volume cultures for an elicited culture. The error bars represent standard deviation amongst three biological replicates. A two-way ANOVA statistical analysis compares each column mean to each other: *=p≤0.05, **=p≤0.01, ns=p>0.05.

Although the final cultures were not statistically different from each other, washing 10 mL of PCC showed a smaller statistical difference in PTX concentrations after being processed (Figure 3.5). The difference in PTX retention may be due to the difference in density of the centrifuged cells. The 10 mL samples formed denser pellets when centrifuged compared to the 25 mL. It is hypothesized that more PTX is lost in the supernatant in less dense pellets. Therefore, further experimentation (Phase 2) proceeded with washing 10 mL of PCC to retain high PTX concentrations through the wash processing steps.

3.3.3 Effects of Lyophilization on Final Flavonoid, Phenolic, and PTX Concentrations

The PCC material must be lyophilized to prepare the material for encapsulation. Therefore, experiments were conducted to determine if lyophilization compromises the integrity of specialized metabolites, including flavonoids, phenolics, and PTX after the cell culture undergoes wash

processing. To determine these effects, 10 mL of initial PCC were washed (Figure 3.2), and final culture samples, both non-lyophilized and lyophilized, were compared for metabolite and PTX concentrations.

Analyzing the Impact of Lyophilization on Flavonoid and Phenolic Retention

Once washed, retention of flavonoids and phenolics with the PCC material through the wash processing and lyophilization was investigated. Retention of these metabolites is important because of the potential synergistic interactions the compounds have with PTX, which could enhance the therapeutic benefits of the drug. The retention of flavonoids through the wash process is shown in Figure 3.6.

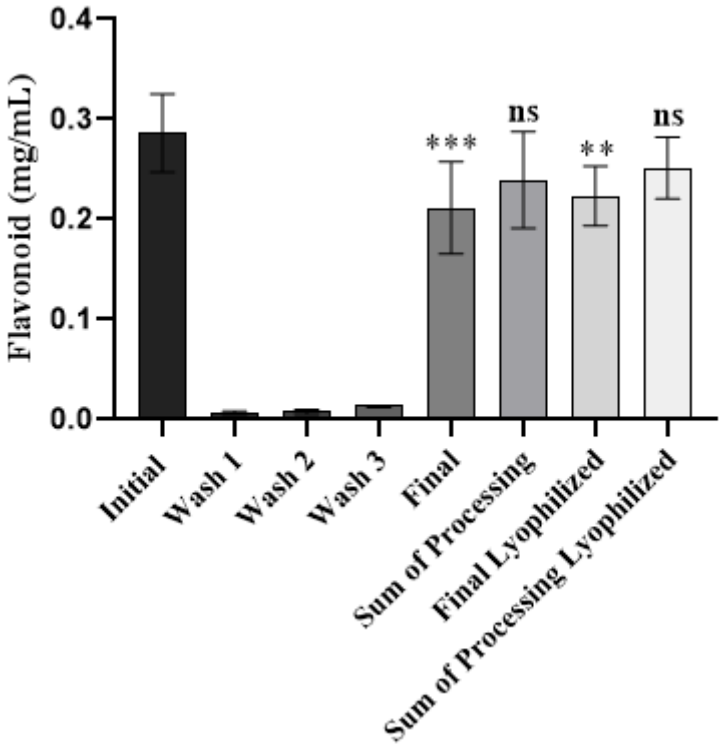

Figure 3.6. Concentration of flavonoids at each stage of the wash process for an elicited culture including after lyophilization of final culture samples. Sum of processing values are the summation of flavonoids in wash step samples and respective final culture samples. The error bars represent standard deviation amongst six biological replicates. A two-way ANOVA statistical analysis compares column means to the initial culture samples: **=$p \leq 0.01$, ***=$p \leq 0.001$, ns=$p > 0.05$.

From the initial culture, 75% of the flavonoids were retained through the wash process to the final culture (Figure 3.6). Although showing a statistical difference from the initial culture flavonoid concentration, these data show that washing cells prior to lyophilization can retain a majority of flavonoids.

To determine whether lyophilization affected flavonoid retention, the statistical comparison of flavonoid concentrations was analyzed between final culture samples of both non-lyophilized and lyophilized samples (Figure 3.7).

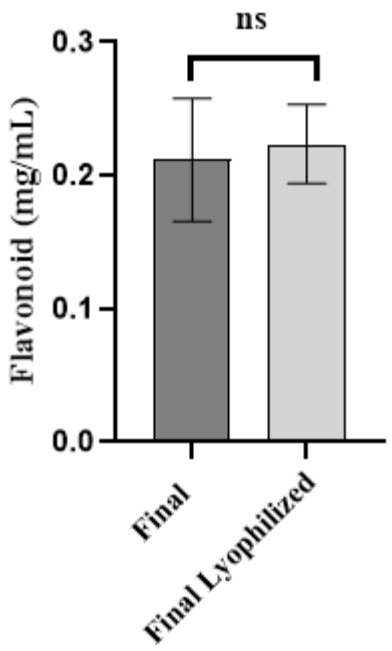

Figure 3.7. Concentration of flavonoids in the non-lyophilized and lyophilized final culture samples for an elicited culture. The error bars represent standard deviation amongst six biological replicates. A two-way ANOVA statistical analysis compares each column mean to each other: ns=p>0.05.

The difference between the flavonoid concentration in the final non-lyophilized culture samples and the final lyophilized culture samples was statistically insignificant; thus, signifying that lyophilization after wash processing had little effect on flavonoid retention with the PCC material (Figure 3.7).

In addition to flavonoid retention, phenolic retention through the wash processing study was analyzed (Figure 3.8).

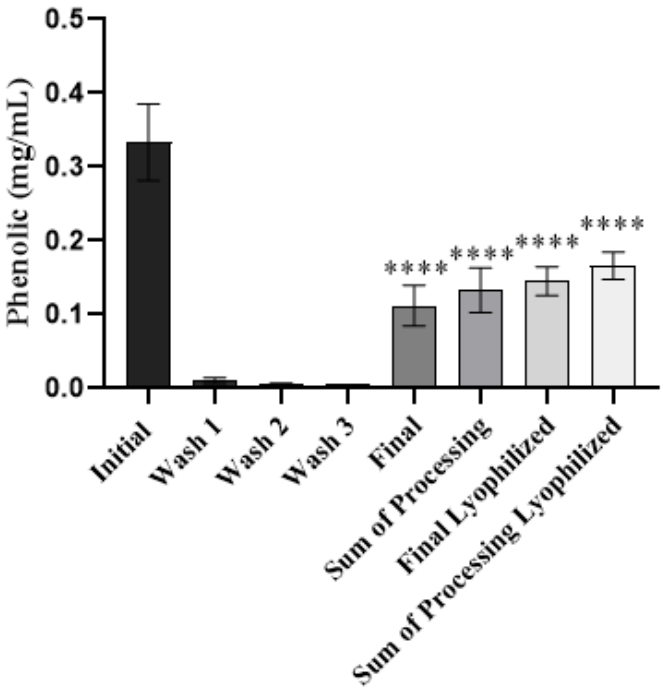

Figure 3.8. Concentration of phenolics at each stage of the wash process for an elicited culture including after lyophilization of final culture samples. Sum of processing values are the summation of phenolics in wash step samples and respective final culture samples. The error bars represent standard deviation amongst six biological replicates. A two-way ANOVA statistical analysis compares column means to the initial culture samples: ****=p≤0.0001.

Phenolics showed a greater loss through the wash steps when compared to flavonoids (Figure 3.8). From the initial culture, 40% of phenolics were retained through the wash process to the final step (Figure 3.8). Phenolics showed less retention than the flavonoids potentially due to their volatility [93]. Therefore, these compounds could have evaporated throughout the wash processing or assay preparation procedures.

To determine whether lyophilization affected phenolic retention, a statistical comparison of phenolic concentrations was analyzed between final culture samples of both non-lyophilized and lyophilized samples (Figure 3.9).

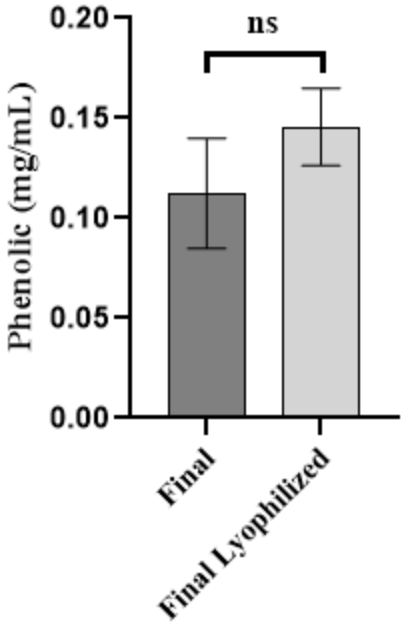

Figure 3.9. Concentration of phenolics in the non-lyophilized and lyophilized final culture samples for an elicited culture. The error bars represent standard deviation amongst six biological replicates. A two-way ANOVA statistical analysis compares each column mean to each other: ns=p>0.05.

The difference between the phenolic concentration in the final non-lyophilized culture samples and the final lyophilized culture samples was statistically insignificant; thus, signifying that lyophilization after wash processing had little effect on phenolic retention (Figure 3.9).

Analyzing the Impact of Lyophilization on Paclitaxel Retention

To determine the effects of lyophilization on PTX retention, a statistical comparison of PTX concentrations was analyzed between final culture samples of both non-lyophilized and lyophilized samples (Figure 3.10).

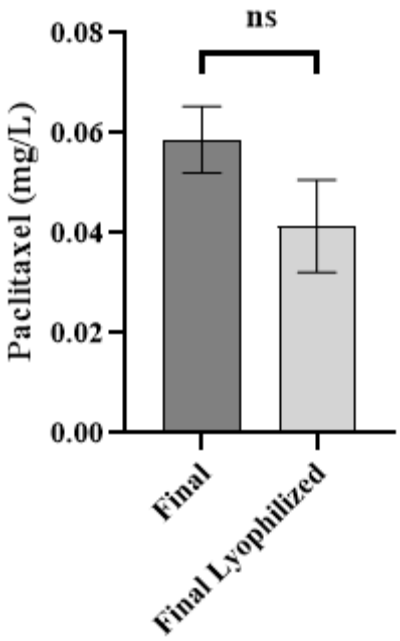

Figure 3.10: Concentration of PTX in the non-lyophilized and lyophilized final culture samples for an elicited culture. The error bars represent standard deviation amongst six biological replicates. A two-way ANOVA statistical analysis compares each column mean to each other: ns=p>0.05.

Samples from the second experiment (Phase 2), there was a much lower retention of PTX (12.8 ± 0.05%) when compared to the results from the first experiment (Phase 1) (68.5 ± 0.05%) (Figure 3.10). The low PTX retention could be attributed to the quality of the initial cell culture. The cells used in this experiment were relatively less dense than those used in prior experiments; thus, causing the cells to not form a completely packed pellet when centrifuged. Therefore, more PTX could have been lost in the removal of the supernatant due to dispersal of the pellet. Given the loosely packed pellet of PCC material, it was likely that some cells were still suspended in the supernatant and were removed during the wash process. When the supernatant was removed, these cells were likely removed with it, and thus PTX was removed. It is not likely that PTX would be suspended in the supernatant without being bonded to a cell due to the fact that PTX is hydrophobic and DI water was used as the supernatant.

Despite the low retention of PTX through the wash processing, the difference between the PTX concentrations in the final non-lyophilized culture samples and the final lyophilized culture samples was statistically insignificant; thus, signifying that lyophilization after wash processing had little effect on PTX integrity (Figure 3.10).

3.4 Conclusions

The processing studies suggest that PTX and specialized metabolites are cell associated, which is optimal in creating a PCC DDS. The PCC had to be washed to remove media components and water-soluble impurities. In processing different volumes of initial PCC, 10 mL of initial PCC

retained higher PTX concentrations (68.3%) when compared to 25 mL of initial PCC (48.2%). As a result, further studies washed 10 mL of initial PCC to determine flavonoid and phenolic retention. Through wash processing, approximately 75% flavonoids and 40% phenolics were retained. In addition to analyzing metabolite retention, the effects of lyophilization on final culture PTX and specialized metabolite retention were evaluated. Lyophilization of PCC prepares the material for encapsulation. Post-lyophilization showed statistically no difference in these retention rates. Therefore, washing cells prior to lyophilization is an avenue for cell washing as compared to a previous MQP, in which up to 85% of flavonoids and phenolics were lost after washing lyophilized cell culture [16]. However, it was observed that, to obtain high retention rates, the initial cell culture must be dense with cell matter, and if there are not enough cells in the suspension, the culture should be left for an extra day before splitting or eliciting to minimize the amount of metabolites lost through the processing.

For further research in processing PCC material, it is recommended that the culture be washed prior to lyophilization. However, it is also recommended that alternative methods be explored to retain higher concentrations of PTX and specialized metabolites. Possible alternatives include centrifuging the cell culture at different speeds or at different initial volumes. Additionally, washing the PCC in polar protic solvents, solvents capable of hydrogen bonding through a hydrogen directly bonded to an electronegative atom, other than DI water, such as acetic acid, methanol, ethanol, or n-propanol could have an effect on retention rates [94]. The solvent must be polar protic due to minimize PTX loss because of the compound’s hydrophobic properties.

Chapter 4: Optimization of Delivery

4.1 Background

4.1.1 Drug Delivery Mechanisms

Paclitaxel (PTX) is systemically administered through intravenous therapy once every two to three weeks [8]. Depending on the patient's treatment plan, treatments may require 175 mg/m² over the course of 3 hr or 135 mg/m² over the course of 24 hr per treatment, both followed with cisplatin [8]. Because these compounds are systemically released into the circulatory system, the administered drug can affect healthy cells and organs; thus, resulting in severe adverse side effects, such as damage of healthy cells in bone marrow, digestive tract, and reproductive systems, nerve damage, kidney malfunction, and infection [4, 6]. Furthermore, harsh solvents, such as those containing ethanol or Cremophor El, a formulation vehicle used to improve solubility of various poorly-water soluble drugs, are needed to deliver the hydrophobic compound [95]. These solvents cause patients to experience further negative side effects such as anaphylactic hypersensitivity, labored breathing, rashes, swelling, hives, and low blood pressure [95, 96]. Therefore, researchers need to explore delivery systems that minimize or eliminate these adverse side effects [95, 96].

Local administration of PTX minimizes these side effects by directing the drug absorption to the cancerous tissues [14]. Localized drug delivery systems (DDSs) for hydrophobic drugs, such as PTX, require drug encapsulation in a polymer scaffold, which may consist of natural or synthetic materials [14]. However, several design challenges arise with local delivery systems including the natural removal and sequestration of nanomaterials by the reticuloendothelial system [14]. With this in mind, biocompatibility and minimal immune response is of utmost importance when choosing a material for local DDSs.

4.1.2 Natural and Synthetic Polymers in Local Drug Delivery

Researchers have explored various synthetic and natural polymers to encapsulate and deliver PTX, and similar plant-based drugs [14]. These polymers can be used in a variety of geometries including gels, nanoparticles, polymeric films, rods, and wafers [14, 97]. Hydrogels, gels consisting of a network of hydrophilic polymers, are promising for drug encapsulation and targeted delivery, as it has tunable physical properties and controllable degradability [98].

Researchers can form hydrogels from synthetic polymers, which have been used in drug delivery due to their strength, customizability, and hydrophobic properties [97]. For instance, polyvinyl alcohol (PVA) hydrogels are one example of a synthetic polymer DDS. When reacted with sodium tetraborate (Borax), PVA undergoes esterification to form a hydrogel [99]. Due to biocompatibility, drug compatibility, water-solubility, film forming, and good mechanical and swelling properties, researchers have studied PVA hydrogels for oral, transdermal, and intramuscular administration [99]. By altering gelling properties, solubility, and adding copolymers

to PVA, researchers can control the drug release from PVA hydrogels, and optimize the vehicles for different drugs [100]. One method that has been used to manipulate these properties is freezing and thawing the PVA matrix numerous times to increase physical crosslinking of the polymer, which, in turn, increases retention in the polymer for long-term biomedical applications [99]. Although the degradation, drug release, and mechanical properties of synthetic materials are easy to manipulate, these materials pose several limitations [97]. For example, many synthetic polymers form acidic degradation products that may accumulate and cause inflammation at the implant site [97]. Moreover, synthetic polymers are more toxic, expensive, environmentally harmful, and require a longer development time compared to natural counterparts [97].

Comparatively, natural polymers are also used in local drug delivery. Commonly used natural polymers include gums, chitosan, silk, and polypeptides including collagen, albumin, elastin, and gelatin [97, 101]. These materials are ideal because they are economical, readily available, non-toxic, and capable of chemical modifications [101]. Furthermore, natural polymers are often more biocompatible than synthetic polymers, thus lowering the risk of immune reaction [101]. Unlike synthetic polymers, many natural polymers are biodegradable which eliminates the need for further surgical removal [14]. An example of a natural polymer that is commonly used for drug delivery is alginate [102]. When crosslinked in an aqueous solution of divalent cations, such as Ca^{2+}, alginate forms into a hydrogel [102]. The ability to assemble alginate gels at neutral pH and mild temperatures makes the material a promising choice for the encapsulation and delivery of therapeutic drugs, such as those that exist in a cell culture [103]. Additionally, alginate hydrogels have demonstrated high stability in systems ranging from 0 to 100°C, which is important for preventing rapid degradation in a drug delivery environment [102]. Despite the advantages of utilizing natural polymers for drug delivery vehicles, there are several drawbacks. These materials must be in high purity to retain biocompatibility [14]. Additionally, there is limited opportunity for changing polymer compositions to alter drug release kinetics and degradation rates [14].

A driving mechanism of drug release from local drug delivery vehicles is the drug concentration gradient between the implanted biomaterial and the *in vivo* environment [104]. Drug concentration will begin to equilibrate through molecular diffusion, which, depending on the solubility and diffusivity of a biomaterial, governs the release kinetics [104]. An *in vivo* drug delivery vehicle containing a high concentration of drug relative to its surroundings will release the drug at a faster rate of diffusion compared to that of a vehicle containing a lower drug concentration [104].

To release any remaining drug from inside the delivery vehicle to the tumor site, researchers can chelate hydrogels to reverse the crosslinked structure and dissolve the material [97]. This process bypasses the need for further removal surgery [97]. For instance, in *in vitro* experiments, researchers utilize ethylenediaminetetraacetic acid (EDTA) and sodium citrate to chelate natural polymer hydrogels [105]. EDTA binds with metal ions and forms chelates with both transition-metal ions and main-group ions [105]. *In vivo*, natural chelation may occur through the release of divalent ions that crosslink the gel into the surrounding media due to exchange reactions with monovalent cations, such as sodium ions [106].

4.1.3 Optimizing Paclitaxel Release Kinetics Using Nile Red Dye Models

To investigate release kinetics of PTX DDSs, ultra high performance liquid chromatography (UPLC) analysis is a common method for measuring concentrations at various time points throughout the release. However, UPLC analysis is a long process that requires tedious and lengthy preparations, limiting the number and speed of experiments [16]. Additionally, PTX is expensive, and difficult to measure in small concentrations through UPLC [16]. To overcome these challenges, alternative methods can be used to model PTX release.

For colored compounds, UV-Vis spectroscopy is used to define the direct relationship between a compound's light absorbance and concentration [107]. UV-Vis spectroscopy is a faster and simpler analytical technique compared to UPLC, as it only takes seconds for the instrument to scan samples and report results. However, this method requires the samples to be colored and absorb a UV or visible light wavelength to calculate changes in concentration.

Nile Red dye (NR) is a colored compound that can be used to mimic PTX in release experiments. The chemical structure of NR to PTX is compared below (Figure 4.1).

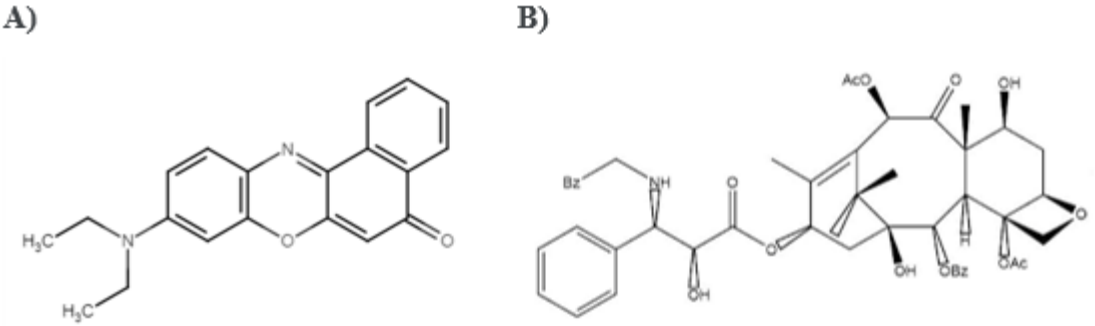

Figure 4.1: Chemical structures of A) Nile Red and B) paclitaxel (adopted from [Sigma-Aldrich, 2020] and [Howat, 2014]).

NR is similar to PTX in solubility, as both chemicals are poorly soluble in water (<0.1 mg/mL) but easily dissolve in polar aprotic solvents such as dimethylsulfoxide (DMSO) (>50 mg/mL) [7, 108]. When dissolved, NR has a visible red color, absorbing the peak value of visible light around 560 nm [108]. Therefore, the following experiments utilized NR and UV-Vis spectroscopy to model PTX release from both natural and synthetic polymers to optimize the PTX delivery vehicle.

4.2 Methods

4.2.1 Nile Red Dye Encapsulated in Polyvinyl Alcohol Hydrogel Release Profile

The integrity of the PVA was analyzed over an extended period of time to determine if the material would be a viable option for PTX delivery. A 1 mg/mL stock solution of NR (Sigma-Aldrich, St. Louis, MO) in DMSO (Fisher Scientific, Fair Lawn, NJ) was combined with 20% (w/v) PVA (363170 Sigma-Aldrich, St. Louis, MO) to produce beads with a 2.0 mm diameter in a 0.1 mg/mL concentration. The PVA solution loaded with NR was formed into a droplet using a 22-gauge needle (PrecisionGlide®, Becton Dickinson, Franklin Lakes, NJ) and a 1 mL syringe (PrecisionGlide®, Becton Dickinson). While the droplet was still on the tip of the needle, it was lowered and placed into a 24-well plate containing 1 mL of sodium tetraborate for 30 sec to crosslink. After 30 sec, the microbead was sheared off of the needle with a spatula into a well containing 1 mL of 4% (w:v) bovine serum albumin-phosphate buffered saline (BSA-PBS) (Sigma-Aldrich, St. Louis, MO) solution with a spatula. Duplicate sets of three beads and nine beads were created. The beads were placed on a shaker at room temperature (MaxQ 4000, Thermo Fisher Scientific, Waltham, MA) and observed over 30 min.

4.2.2 Nile Red Dye Encapsulated in Alginate Hydrogel Release Profile

Determining Alginate Concentration for Hydrogel Microbeads

To model and predict the release profile of PTX from alginate hydrogel microbeads, a series of experiments were performed with NR. The first experiment determined the threshold concentration of low viscosity sodium alginate to maintain consistent bead integrity over 24 hours. A 1 mg/mL stock solution of NR suspended in DMSO was combined with four different concentrations (1.5%, 2%, 3%, and 5% (w/v)) of low viscosity sodium alginate (Alfa Aesar, Haverhill, MA) to produce microbeads of a NR concentration of 0.1 mg/mL. The sodium alginate solution loaded with NR was slowly added dropwise with a 22-gauge needle and a 1 mL syringe into a 24-well plate containing 1 mL of 100 mM calcium chloride (C1016, Sigma-Aldrich, St. Louis, MO), creating beads with a diameter of 1.8-2.0 mm. Beads were measured using an in-picture ruler scale and size estimations were made with ImageJ. Three sets of three microbeads and three sets of nine microbeads were added to the calcium chloride for each alginate concentration. The microbeads in calcium chloride were placed on a shaker for 30 min to crosslink. The calcium chloride solution was pipetted from each well and replaced with 1 mL of 4% (w/v) BSA-PBS solution, a protein-buffer solution that mimics physiological fluids. The microbeads were incubated at 37 °C and observed over 24 hr. A schematic of how the microbeads were prepared is pictured below (Figure 4.2).

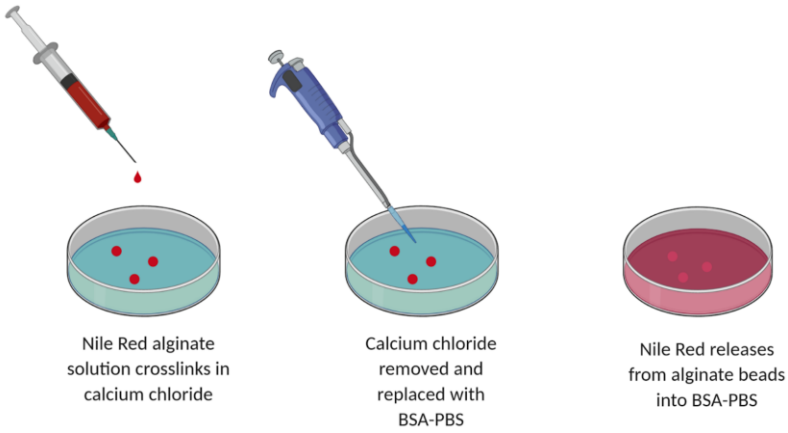

Figure 4.2: Alginate hydrogel microbeads loaded with Nile Red dye preparation schematic. Solution is dropped into calcium chloride to crosslink, and calcium chloride is then replaced with BSA-PBS solution for the release experiment.

Analyzing the Release Profile of Nile Red from Alginate Microbeads

To gain an understanding of the release profile of NR from alginate hydrogel microbeads, 1 mg/mL NR was combined with 3% and 5% (w/v) low viscosity sodium alginate to produce microbeads with 0.1 mg/mL NR. Preparation of the microbeads was consistent with protocols from the aforementioned experiment. From each release media, 200 µL samples were taken every 30 min, and centrifuged in a microcentrifuge (5424, Eppendorf, Hamburg Germany) for 5 min at 16,000 rpm. From each supernatant, 100 µL was pipetted into a 96-well plate and the colorimetric absorbance of the plate was read on a Multiskan^{TM} GO Microplate Spectrophotometer (Accuskan GO, Fisher Scientific) at 552 nm. After the first 90 min, samples were taken every hour for 12 hr, and then again at 23 hr. Once processed, the sample was resuspended into its original well.

Determining Final Nile Red Concentration in Microbeads After Release

To determine the percentage of NR released from the alginate hydrogel microbeads after 23 hr, the microbeads were chelated with EDTA disodium salt to determine the concentration of NR remaining in the microbeads. The BSA-PBS solution was removed from each well with a pipette, and the microbeads were washed with DI water 3 times. A 0.1 M stock solution of EDTA disodium salt (Fisher Scientific) was combined with BSA to create a 4% (w/v) BSA-EDTA solution. To each of the wells, 1 mL of the BSA-EDTA solution was added, and the microbeads were placed on a shaker for 1 hr. Once fully dissolved, 200 µL samples were taken from each well, and centrifuged in a microcentrifuge for 5 min at 16,000 rpm. From each supernatant, 100 µL was pipetted into a 96-well plate and the colorimetric absorbance of the plate was read at 552 nm.

4.2.3 Paclitaxel Encapsulated in Alginate Hydrogel Release Profile

Determining Paclitaxel Concentration for Desired Release

To gain an understanding of the release profile of PTX from alginate hydrogel microbeads, the loading concentration of PTX had to be determined. A 1 mg/mL stock solution of PTX suspended in methanol was combined with 5% (w/v) low viscosity sodium alginate to produce microbeads with 0.1, 0.05, 0.01, 0.005, 0.001 mg/mL concentrations. The sodium alginate solution loaded with PTX was added dropwise with a 22-gauge needle and a 1 mL syringe into a 24-well plate containing 2 mL of 100 mM calcium chloride. The beads for this study were approximately 3.0 to 3.1 mm in diameter. Beads were measured using an in-picture ruler scale and size estimations were made with ImageJ. Triplicate sets of nine microbeads were added to the 100 mM calcium chloride solution for each PTX concentration. One 24-well plate was designated for the release concentrations sampled after 12 hr, and the other plate was designated for the release concentrations sampled after 24 hr. The beads were placed on a shaker for 30 min to crosslink. Once crosslinked, the calcium chloride was removed, and replaced with 1 mL of 4% BSA-PBS solution and incubated at 37 °C. After 12 hr, the BSA-PBS solution was removed from each well of one 24-well plate and placed into microcentrifuge tubes. This process was repeated after 24 hr for the second plate. The samples were placed in an evaporative centrifuge overnight and stored at -80 °C until further processing for PTX concentrations with UPLC as detailed in Chapter 3.2.4.

4.3 Results and Discussion

4.3.1 Nile Red Dye Encapsulated in Polyvinyl Alcohol Hydrogel Release Profile

The integrity of the NR loaded PVA hydrogel microbeads in BSA-PBS solution were observed over 30 min (Figure 4.3).

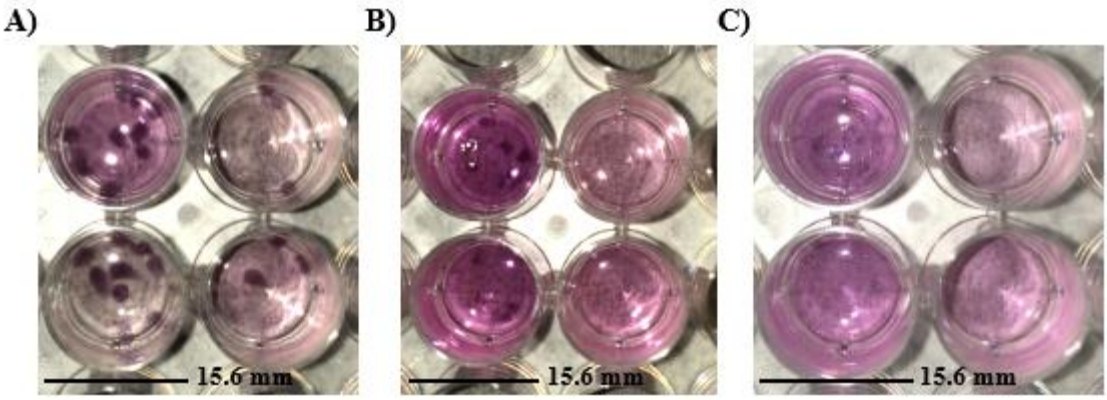

Figure 4.3: Visualization of PVA microbeads releasing NR into BSA-PBS solution at A) 5 min B) 20 min and C) 30 min. Nine beads/well are shown in the left columns and three beads/well in the right columns.

Within 30 min of submerging the PVA hydrogel microbeads into the BSA-PBS solution, the microbeads degraded and dissolved completely; thus, releasing the total concentration of NR into the system (Figure 4.3). The quick degradation of the hydrogels may have been due to the lack of crosslinks within the matrix. Oftentimes, successful PVA hydrogel delivery vehicles have undergone physical modifications such as the freeze-thaw method to induce greater amounts of crosslinks within the matrix or have been combined with other polymers to ensure hydrogel stability [99]. Therefore, pure PVA was not a viable option for encapsulating PTX because there was minimal control of the drug's release rate from the polymer, and no further studies were conducted with this material.

4.3.2 Nile Red Dye Encapsulated in Calcium Alginate Hydrogel Release Profile

Determining Alginate Concentration

The integrity of the NR loaded calcium alginate hydrogel microbeads in BSA-PBS solution was observed over 24 hr (Figure 4.4).

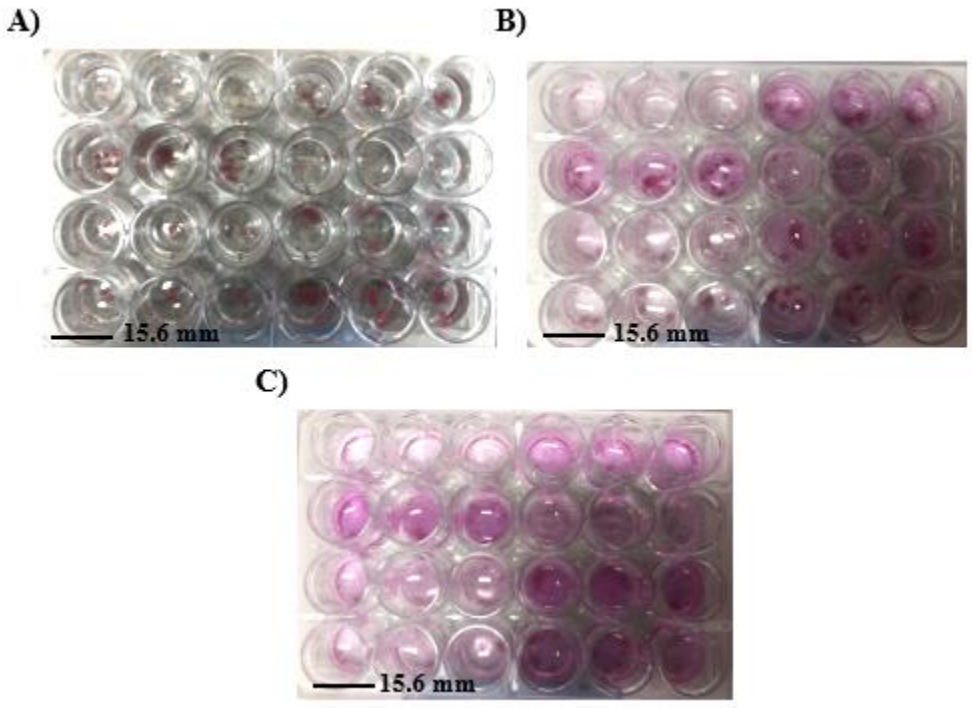

Figure 4.4: Visualization of alginate microbeads releasing NR into BSA-PBS solution at A) 0 hr B) 8.5 hr and C) 24 hr. From rows top to bottom, the low viscosity sodium alginate concentrations are: 1.5%, 2%, 3%, and 5%. Triplicates of three beads and nine beads were studied for each sodium alginate concentration.

Within 8.5 hr of submerging the calcium alginate hydrogel microbeads into the BSA-PBS solution, the hydrogels consisting of 1.5% or 2% sodium alginate began to degrade (Figure 4.4). For these

concentrations, the wells containing three microbeads had either nearly or completely dissolved, whereas the nine microbead counterparts maintained their integrity. However, the integrity of the microbeads consisting of 3% or 5% sodium alginate were visually unaffected at this time.

After 24 hr of release, all microbeads consisting of 1.5% or 2% sodium alginate had completely dissolved (Figure 4.4). The wells containing three microbeads of 3% or 5% sodium alginate began to degrade, and the nine microbead counterparts were visually unaffected. The integrity of hydrogels created from higher concentrations of low viscosity sodium alginate were not compromised over longer periods of time; thus, allowing for more control of a drug's release. Moving forward, experiments performed to understand the release kinetics of NR and PTX utilized 3% and 5% low viscosity sodium alginate.

Nile Red Release Profile

The release profiles of NR from calcium alginate hydrogel microbeads consisting of 3% and 5% sodium alginate were compared (Figure 4.5).

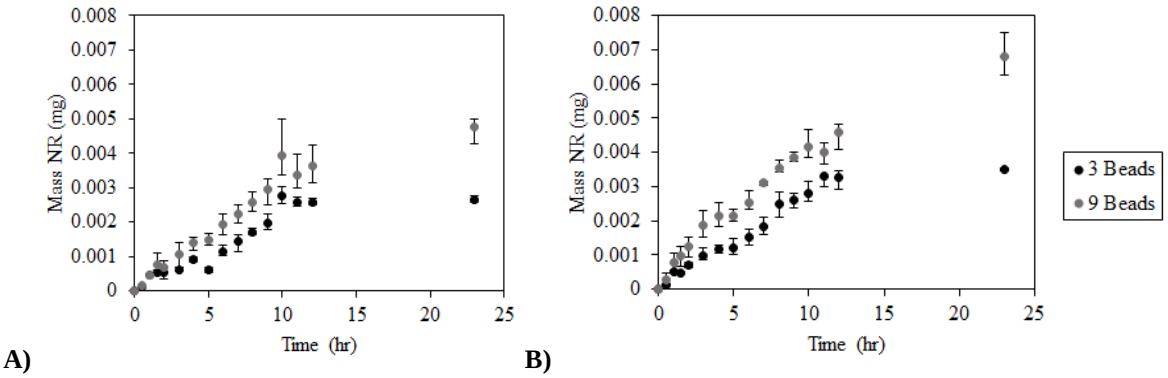

Figure 4.5: Accumulated mass of NR (mg) released over 23 hr by hydrogel beads consisting of A) 3% and B) 5% low viscosity sodium alginate suspended in a 4% BSA-PBS solution. The initial mass of NR in three beads is 0.0034 ± 0.0003 mg, and 0.0068 ± 0.002 mg in nine beads. Error bars represent average ± min/max of three samples.

Release media containing three microbeads, for both 3% and 5% sodium alginate, reached nearly complete release of the NR after 12 hr (Figure 4.5). However, release media containing nine microbeads, for both 3% and 5% sodium alginate continued to slowly release the NR over 23 hr (Figure 4.5). For release media containing nine microbeads with 3% sodium alginate nearly reached complete release of NR after 23 hr. The data suggests that for release media containing nine microbeads with 5% sodium alginate, the beads would continue to slowly release the drug over 23 hr until the concentration of NR in the beads and the release media were in equilibrium.

Once the alginate microbeads were chelated with EDTA, the mass percent release of NR over 23 hr could be determined (Figure 4.6).

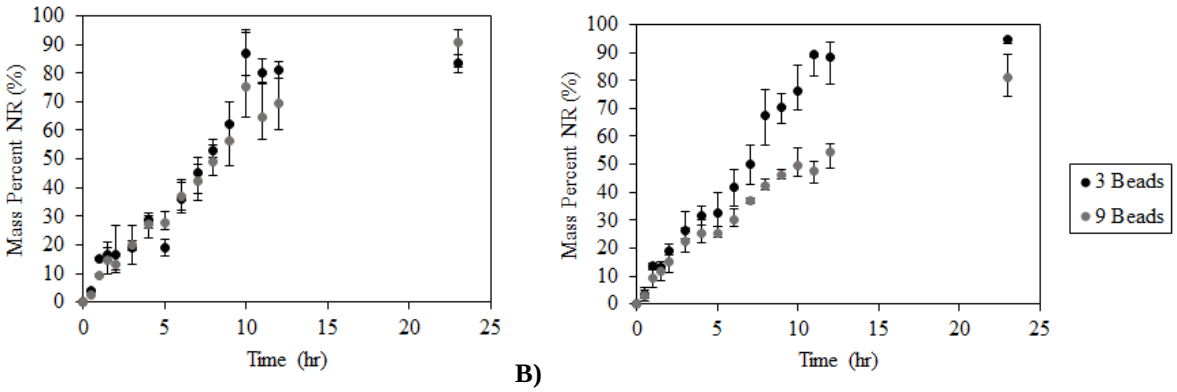

Figure 4.6: Mass percent of NR released over 23 hr by hydrogel beads consisting of A) 3% and B) 5% low viscosity sodium alginate suspended in a 4% BSA-PBS solution. Error bars represent average ± min/max of three samples.

Analyzing the mass percent release of NR from alginate hydrogels further supported that wells containing smaller initial volumes of NR resulted in a faster release of NR into the BSA-PBS solution when compared to wells containing higher initial volumes of NR (Figure 4.6). After 12 hr, three microbeads containing 3% sodium alginate released an average of 81.1% of the initial volume of NR, and nine microbeads with the same concentration released an average of 69.3% of the initial volume of NR. After 23 hr, the three microbeads released an average of 83.6% of the initial volume of NR, and the nine microbeads released an average of 90.7% of the initial volume of NR. After 12 hr, three microbeads containing 5% sodium alginate released an average of 88.2% of the initial volume of NR, and nine microbeads with the same concentration released an average of 54.5% of the initial volume of NR. After 23 hr, the three microbeads released an average of 94.7% of the initial volume of NR, and the nine microbeads released an average of 81.1% of the initial volume of NR.

The release rate for microbeads containing 3% sodium alginate were comparable regardless of the initial volume of NR in the system, whereas after 7 hr the release rates between three and nine microbeads began to differentiate for microbeads containing 5% sodium alginate. As alginate concentration increased, the solid volume fraction and density of crosslinks increased, thus resulting in greater stiffness of the gel [109]. Therefore, regardless of the initial volume of NR in the systems containing beads consisting of 3% sodium alginate, the dye did not have to overcome a greater physical barrier compared to the beads created from 5% sodium alginate. With a lower crosslinking density, the NR was able to release from the hydrogels to near completion. However, for the beads containing 5% sodium alginate, the dye had to overcome a greater physical barrier to reach higher mass release percentages. Moving forward, experiments to understand PTX release from calcium alginate hydrogels were conducted with nine beads containing 5% sodium alginate to have the most control over the drug's release rate.

4.3.3 Paclitaxel Encapsulated in Alginate Hydrogel Release Profile

Determining Paclitaxel Concentration Required for Desired Release

The release of PTX from calcium alginate hydrogel microbeads over 12 and 24 hr for initial loading concentrations of 0.1, 0.05, 0.01, 0.005, and 0.001 mg/mL were compared (Figure 4.7).

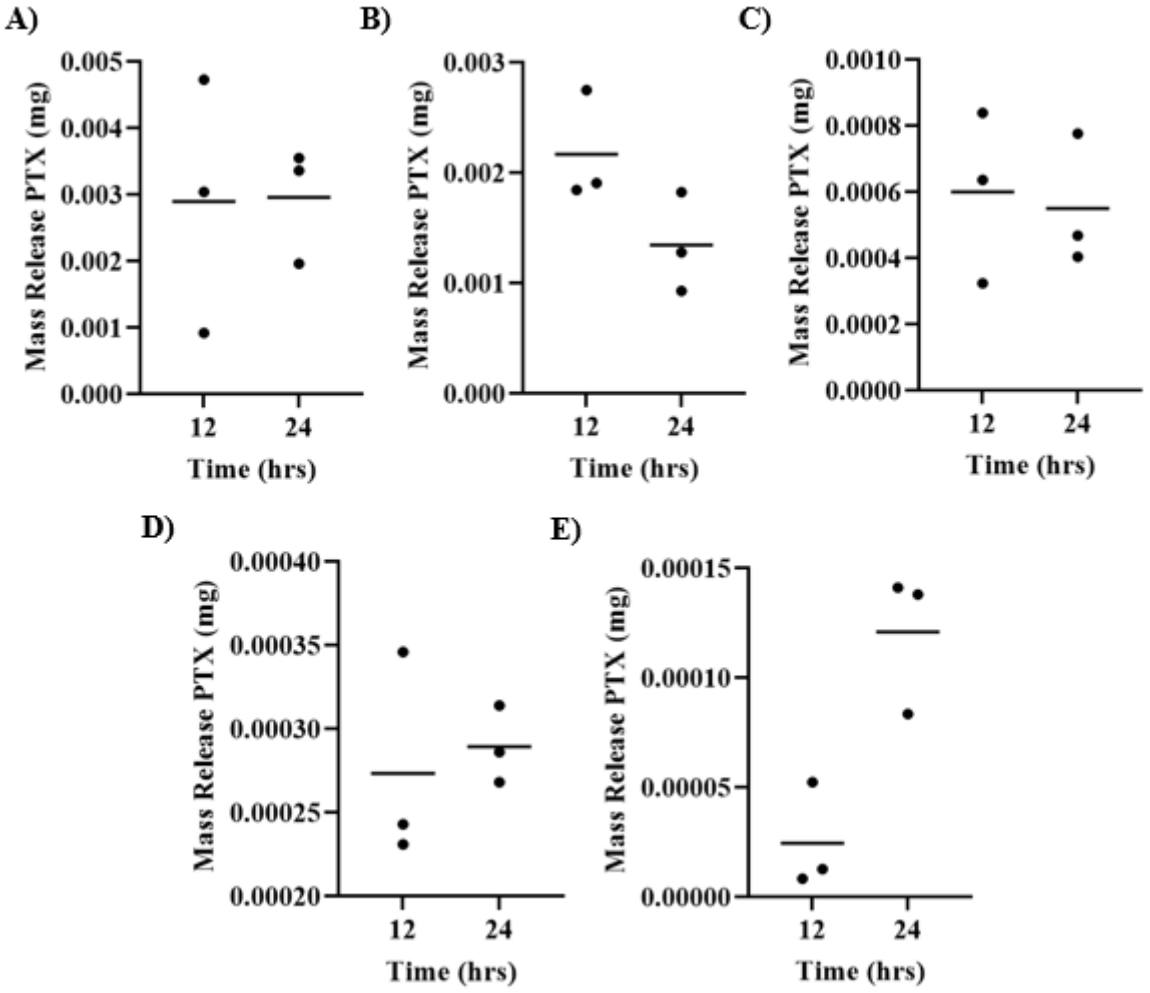

Figure 4.7: Mass of PTX (mg) released over 12 and 24 hr from alginate hydrogel beads loaded with the following initial concentrations (mg/mL) of PTX A) 0.1, B) 0.05, C) 0.01, D) 0.005, and E) 0.001. A horizontal line represents the mean of three samples.

From literature, the desired drug release concentration from the hydrogel beads after 24 hr is 8.5 x 10^{-4} mg/mL [7]. The data above was interpolated and it was determined that 0.025 mg/mL PTX is required to be loaded into the beads to achieve the desired release concentration after 24 hr (Figure 4.7). To achieve this initial bead and desired release concentrations, 0.0104 mg of 0.059 mg/L (Chapter 3.3) lyophilized PCC material must be added to 10 µL of sodium alginate. Theoretically, the release of PTX from the PCC material encapsulated in alginate hydrogels would behave similar to the release kinetics of the pure PTX studies.

In some cases, the mass of PTX released decreased between sample times (Figure 4.7). Incubating the beads at 37°C could have caused the PTX to degrade. Literature describes one study that showed PTX undergoes two types of degradation, hydrolysis and epimerization, when released into PBS media at 37°C over 6 hr [110]. Therefore, further experimentation to determine PTX integrity over 24 hr at 37°C is needed to confirm the use of a hydrogel DDS to deliver PTX within these environmental conditions for breast cancer cell cytotoxicity.

4.4 Conclusions

Through preliminary testing, it was established that PVA is not a suitable material for the DDS because the crosslinked PVA beads disintegrated within 30 min. This short time frame is not feasible for PTX delivery, as typical treatments are administered over the course of 3 to 24 hr [111]. PVA is most frequently used in conjunction with other materials, such as chitosan, or as a thin hydrogel, rather than in the form of microbeads [112].

Alginate in the form of hydrogel microbeads was established as a feasible option for PTX delivery. When testing microbeads consisting of 5% low viscosity alginate crosslinked in 100 mM calcium chloride, the integrity of the microbeads remained over 23 hr, indicating that the release rate of the drug can be better controlled. When administering PTX, increased control is ideal because PTX treatments are customized to each specific patient depending on their height, weight, and age. Therefore, 5% alginate was determined to be the ideal concentration of sodium alginate to act as an encapsulation polymer for the delivery of PTX through PCC material.

When encapsulated in 5% alginate, there was a difference in release rates in the three and nine microbead studies. The studies involving the three microbeads released an average of 94.7% of the initial NR concentration, whereas the studies with nine microbeads released an average of 81.1% of the initial NR concentration. A high concentration of NR in the microbeads and a low concentration of NR in the surrounding environment will result in large diffusion of the dye from the microbeads into the lowly concentrated BSA-PBS solution. In the study with the three microbeads, this concentration gradient drives a higher percentage of NR to release into the BSA-PBS solution. In the nine microbead study, there is more total NR, and after the initial burst of diffusion, the concentration gradient of NR between the microbeads and the BSA-PBS solution is no longer that large, which limits, slows, and controls further diffusion. Therefore, moving forward, nine beads were used in experiments due to its slower release rate and increased control of the compound release.

From the PTX release studies, the ideal starting microbead concentration of PTX was determined to be 0.025 mg/mL through interpolating the 24-hr mass release data. Results from the studies were inconsistent, as the total mass release of PTX decreased from 12 to 24 hr in the microbeads loaded with 0.05 and 0.01 mg/mL PTX. The decrease could be due to degradation of the PTX, as the tests occurred at 37°C, and the drug loses stability at temperatures higher than room temperature. Additionally, NR may not have accurately modelled PTX release. While the solubilities of these chemicals are similar, the sizes of these molecular compounds are different, with PTX

having a molecular weight of 853.9 g/mol and NR having a molecular weight of 318.4 g/mol. A size difference could impact diffusion properties, as molecule size is a determinant for molecular diffusion rate.

From the experiments and research described in the above chapter, it was concluded that alginate hydrogels are a promising polymer for administering PTX locally. The microbeads containing 5% sodium alginate delivered a sustained concentration of the drug for 24 hr. Therefore, future research should explore the potential alginate hydrogels have for drug delivery. However, researchers should identify different colored compounds to mimic PTX for release studies to decrease raw material cost and analyzing time. Conducting UV-Vis spectroscopy to model drug release is an efficient and convenient method for carrying out otherwise lengthy preliminary drug release studies. Other compounds, with similar solubility properties and molecular weight, such as water insoluble vat dyes, should be explored. Vat Yellow 33 is an example of a potential modeling compound, as its size and solubility properties are very similar to those of PTX [Vat Yellow 33, 2017].

Chapter 5: Establishing an *In Vitro* Breast Cancer Model to Optimize Drug Delivery Design

5.1 Background

Currently, the U.S. Food and Drug Administration has approved paclitaxel (PTX) for the treatment of four different cancers: AIDS-related Kaposi sarcoma, breast cancer, non-small cell lung cancer, and ovarian cancer [7]. Of these cancers, breast cancer is the most prevalent, as it was the second most common cancer worldwide with over 2 million new cases reported in 2018 [113].

Breast cancer patients treated with PTX on a weekly basis have an 89.7% chance of survival 5 years after diagnosis, whereas chemotherapy treatments that require administration on a bi-weekly or monthly basis have an 86.5% chance of survival [114]. Weekly administration of PTX requires half the standard dose; thus, decreasing the severity of chemotherapy side effects that patients experience [114]. Given the pervasiveness and severity of the disease, it is of utmost importance to develop effective treatment plans. Therefore, optimal drug treatment plans vary for each patient, depending on the severity of their cancer, as well as how their body reacts to treatment. Regardless, optimizing DDSs results in less severe side effects in patients, as well as improved effectiveness in killing cancer cells.

To test the efficacy of drugs on cancer cells, researchers can utilize mammalian cancer cell cultures [39]. Human cancer-derived cell lines are the most widely used models to study the biology of cancer and to test hypotheses to improve the efficacy of cancer treatment [39]. Particularly, mammalian cell cultures and cancer cell lines have been instrumental in testing drug delivery systems [115]. For example, researchers used HepG2 liver cancer cells in the development of a targeted drug delivery system for PTX [116]. These cells were treated with a range of concentrations within hydroxypropyl-β-cyclodextrin nanoparticles and as free PTX [116]. By testing the PTX delivery system on this cell culture, researchers determined that biotin and arginine modified hydroxypropyl-β-cyclodextrin nanoparticles are a successful delivery system for PTX [116]. Furthermore, this system was successful in delaying tumor growth and reducing tumor size [116]. Therefore, this chapter utilizes a cancer cell line to effectively model the effects of drug release, and drug efficacy against *in vitro* breast cancer cells.

5.2 Methods

5.2.1 Mammalian Cells

MDA-MB-231 breast cancer cells were maintained in a Dulbecco's Modified Eagle Medium (DMEM) supplemented with 10% (v/v) fetal bovine serum, 100 U/mL penicillin, 100 µg/mL streptomycin, and 2 mM l-glutamine (Fisher Scientific, Hampton, NH). The cells were subcultured 2 to 3 times per week. The media was aspirated from the cells, and 5 ml DPBS (-) (Cat # 21-031-CV, Corning) was added to rinse cells. The DPBS (-) was then aspirated, and 3ml 0.25% Trypsin

(Cat # 25-053-Cl, Corning) was added. The cells were incubated for 3 min at 37°C to detach the cells from the walls of the container. Then, 2 mL of the aforementioned media was added, and the cell suspension was transferred to a 15 mL conical tube. Next, 6 µl of cell suspension was removed and injected into a hemocytometer for cell counting. The cells were centrifuged at 200G for 5 min, and the media was aspirated carefully to not disturb the cell pellet. The cells were suspended in the amount of media that would result in a cell density of 1 x 10^6 cells/mL. The cells were re-plated on a sterile plate to achieve desired density, and media is added to obtain a total volume to 10 ml/plate.

5.2.2 Resazurin Assay

A resazurin assay was used to test the cytotoxicity of PTX at varying concentrations. This assay measured the metabolic activity in cells, which, in turn, determined the viability of cells after treatment. Live cells have the ability to reduce resazurin, which is not fluorescent, to resorufin, which is fluorescent, through mitochondrial reductase [117]. The fluorescence of the sample is proportional to the amount of viable cells [117]. In this assay, 5,000 MDA-MB-231 breast cancer cells per well were seeded into a 96-well plate, 24 hr prior to treatment. To treat the cells, a 1 M stock solution of PTX was diluted through a serial dilution to create 12 PTX concentrations ranging from 0.005 nM to 1000 nM (100 µL each). The media covering the cells was aspirated, and 100 µL of PTX containing media was added to the wells. Each PTX concentration was tested in 4 replicates. Six control wells were not treated with PTX. The cells were left in an incubator at 37° C for 72 hr.

The cells were then imaged with phase contrast microscopy under 10x magnification (Nikon Eclipse TS100, Tokyo, Japan) to visualize cell shape and quantify. In media, 140 µL of sterile resazurin stock (1.5 mg/mL) was diluted 10-fold. The PTX and media solution was aspirated, and 100 µL of the working resazurin solution was added to each well. The cells were left to incubate in the resazurin solution for 3 hr at 37° C. After this incubation period, the 100 µL was transferred to a black 96-well plate, and read with a fluorescence plate reader (Victor 3 – PerkinElmer 1420 Multilabel Counter).

5.3 Results and Discussion

The resazurin assay performed on the breast cancer cells determined the viability of breast cancer cells at varying PTX concentrations (Figure 5.1).

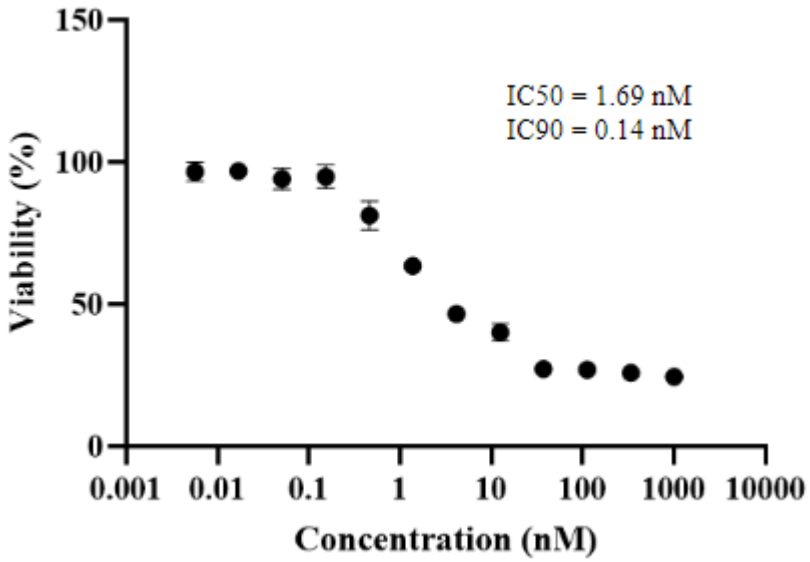

Figure 5.1: Results of resazurin assay depicting the viability of cells exposed varying concentrations of PTX ranging from 0.005 nM to 1000 nM.

Cell viability began to decrease when exposed to 0.45 nM PTX (Figure 5.1). The viability of the cells began to plateau to approximately 25% viability when exposed to 37 nM PTX (Figure 5.1). The viability of these cells may have plateaued at 25% because of natural resistance to the drug, or acquired resistance in response to previous treatments. This result is comparable to similar studies where cytotoxicity never reached 100%, and viability levels plateaued at similar concentrations [118, 119]. Researchers have attributed acquired resistance to PTX to the activation of the NF-κB protein, which controls DNA transcription, and the induction of the Pregnane X receptor, which senses foreign substances in the body [119].

Furthermore, the IC50 value for this cell line was 1.69 nM. This IC50 value is lower than those found in literature. For instance, in one study, researchers observed the effects of PTX (0 to 300 nM) on MDA-MB-231 breast cancer cells [120]. The IC50 value for this study was 8 nM [120]. Several factors could have contributed to the discrepancy in IC50 values such as different drug resistance rates and PTX concentration ranges. Therefore, it is recommended that researchers conduct this study several times on the same cell culture to confirm results for literature comparison.

In addition to cell viability, the cells were imaged to visually observe the cells after being treated with PTX. Control cells, cells not exposed to PTX, were used as the baseline for 100% cell viability (Figure 5.2).

Figure 5.2: Control cells not exposed to paclitaxel in resazurin assay. These cells were used as a baseline to compare viability of cells exposed to PTX.

A majority of the cells were characterized by the typical shape of a breast cancer cell, a large nuclear mass with two tendrils opposite each other (Figure 5.2). This shape gave the cells a stretched, elongated appearance. The cells treated with a range of PTX concentrations were compared to control cells (Figure 5.3).

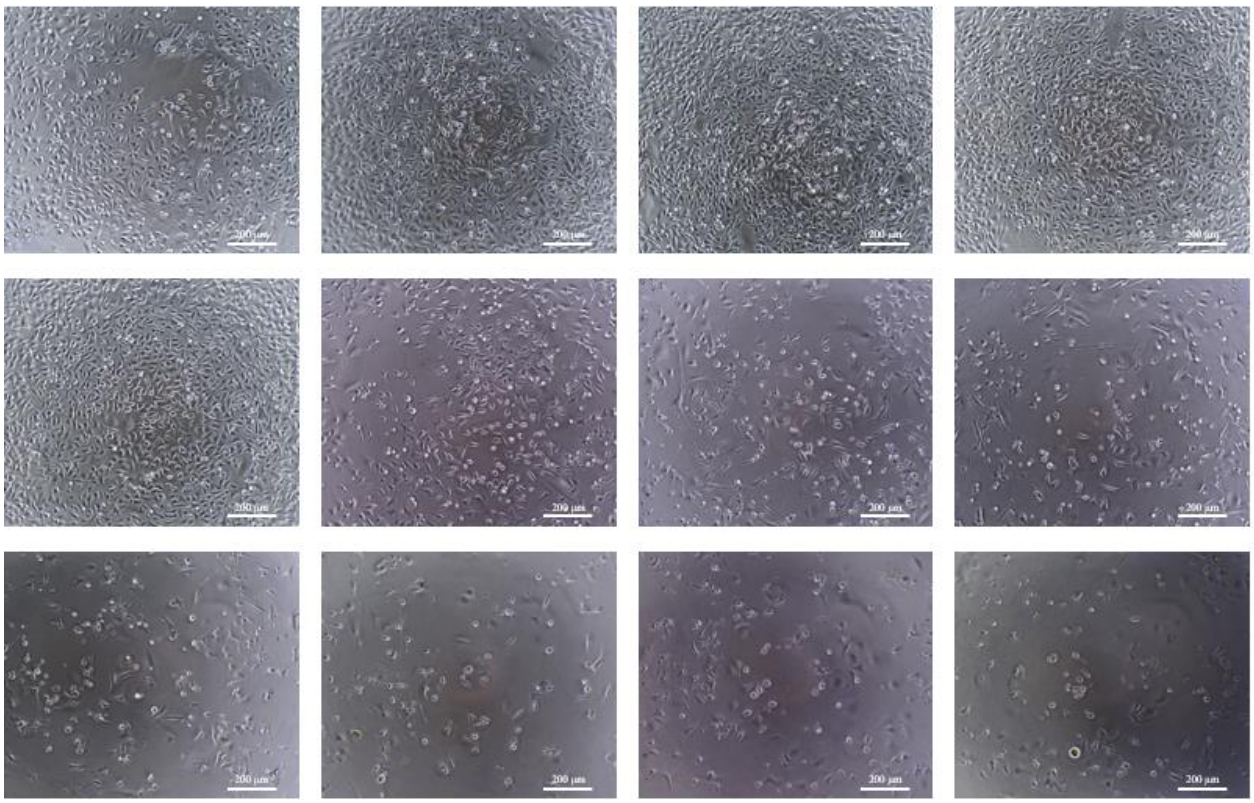

Figure 5.3: Cells exposed to varying concentrations of paclitaxel under 10x magnification. Concentrations: Top row, left to right: 0.00564 nM, 0.0169 nM, 0.0508 nM, 0.152 nM. Middle row, left to right: 0.45 nM, 1.37 nM, 4.11 nM, 12.34 nM. Bottom row, left to right: 37.03 nM, 111.11 nM, 333.33 nM, 1000 nM.

The cells exposed to the lowest concentrations of PTX had a similar appearance to the control cells (Figure 5.3). As the PTX concentration increased, the amount of metabolically active cells consistently decreased, and the appearance of these cells also changed. This change was first noticeable when cells were exposed to 0.45 nM PTX (Figure 5.3). Additionally, the number of cells in the images visibly decreased consistently until the concentration of 37 nM, where the images of increasing concentrations seem quite similar (Figure 5.3). Furthermore, the cells at the highest concentrations of PTX did not have the same tendrils associated with healthy cells, rather they were more oval-shaped (Figure 5.3). These images are supplemental to the resazurin assay results, and confirm the effectiveness of PTX treatment on breast cancer cells.

5.4 Conclusions

A breast cancer cell cytotoxicity model was developed with a range of PTX concentrations to kill MDA-MB-231 *in vitro*. The optimal PTX concentration for treatment was found to be 37 nM. This concentration results in the lowest viability of the cells (25%). As mentioned in Chapter 4.3.3, the plant cell culture (PCC) delivery system released PTX at concentrations of $8.5x10^{-4}$ mg/mL, or 995 nM. This concentration is above the minimum suggested PTX concentration, meaning the delivery system would be efficient in treating breast cancer cells. Additionally, the lowest PTX concentration for treatment was determined to be 0.45 nM, the concentration at which the percent viability of cells began to decrease. However, it is advisable to use higher concentrations, of at least 37 nM, which results in the lowest cell viability, to prevent surviving cells from developing PTX resistance due to non-lethal exposure.

These experiments suggest that the developed drug delivery system for PTX through PCC will release sufficient PTX concentrations to kill MDA-MB-231 breast cancer cells Follow up research should be performed to further understand the cytotoxic properties of PTX produced by PCC and released from alginate hydrogel microbeads. These tests should entail a comparison of pure PTX to PTX produced in PCC to confirm the hypothesized synergistic effects PTX has with other naturally produced metabolites, such as flavonoids and phenolics. Synergistic interactions between PTX and other specialized metabolites may cause PTX's cytotoxic properties to be enhanced; thus resulting in greater cell death at lower PTX concentrations. Additionally, to confirm that the drug delivery vehicle is not cytotoxic, cells should be introduced to calcium alginate. These experiments were going to be performed in D term; however, due to COVID-19 restrictions on lab access, additional experimentation was not possible.

Chapter 6: Pharmacokinetics of Paclitaxel Release System

Pharmacokinetics refer to the pathways a drug undergoes in the body and is described through the drug's administration/absorption, distribution, metabolism, and excretion (ADME) properties (Figure 6.1) [121].

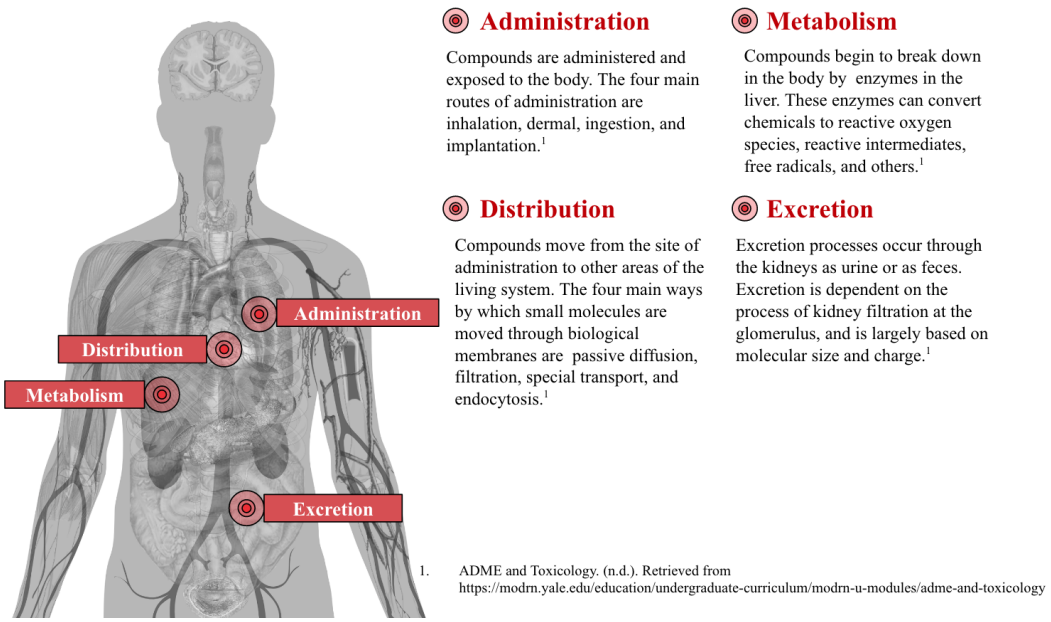

Figure 6.1. Overview of pharmacokinetics [122]. Image citation: Häggström, Mikael (2014). "Medical gallery of Mikael Häggström 2014". WikiJournal of Medicine 1 (2). DOI:10.15347/wjm/2014.008. ISSN 2002-4436. Public Domain.

For local administration of chemotherapy drugs, the compounds are applied directly to the tumor site through topical dosage forms. For instance, patients with basal cell carcinoma, a type of skin cancer, apply imiquimod cream (Aldara®) directly onto the skin [123]. Similarly, drug delivery vehicles can be implanted directly onto tumor sites inside of the body to target the release of anticancer drugs, such as the use of carmustine-loaded wafers to treat patients with brain tumors [14]. Once administered, cancerous tissues and cells absorb the drug for tumor cytotoxicity. Any drug compounds not absorbed into the tumor can diffuse into the circulatory system to be distributed to metabolism sites. Within the circulatory system, the drugs bind to plasma proteins [124]. For instance, weak acids and neutral drugs bind to albumin, whereas basic drugs bind to glycoproteins and red cell surface proteins [124]. The circulatory system distributes the drug compounds to either the liver or kidneys for metabolism [124]. The liver detoxifies and facilitates excretion of lipid-soluble drugs by enzymatically converting the lipid-soluble compounds to water-soluble compounds [124]. The most common form of conversion is Phase I metabolism, in which the drug is converted to a more polar compound by introducing polar functional groups [124]. Cytochromes P450 (CYP450s), hemoproteins that break down drug molecules into metabolic conjugates with reduced bioefficacy, catalyze this type of metabolism [124, 125]. If the body does not eliminate the metabolic conjugates rapidly, the drug may be further metabolized by Phase II metabolism, in which the newly

established polar group conjugates with endogenous compounds such as glucuronic acid, sulfuric acid, or amino acids [124]. Once converted into water-soluble compounds, the body may excrete the metabolized drug through feces, or it may undergo further metabolism in the kidneys [124]. Kidneys metabolize water-soluble drugs by filtering out compounds with less than 60,000 Da from blood and transporting the compounds into urine for excretion [126].

Ultimately, pharmacokinetic analyses allow researchers and practitioners to understand appropriate drug administration for patients. This chapter details the ADME properties of each component for the optimized release system consisting of paclitaxel (PTX), flavonoids, phenolics, alginate, and plant cell culture (PCC) material.

6.1 ADME of Release System Components

The hypothesized pharmacokinetics map for the optimized PTX release system is shown in Figure 6.2.

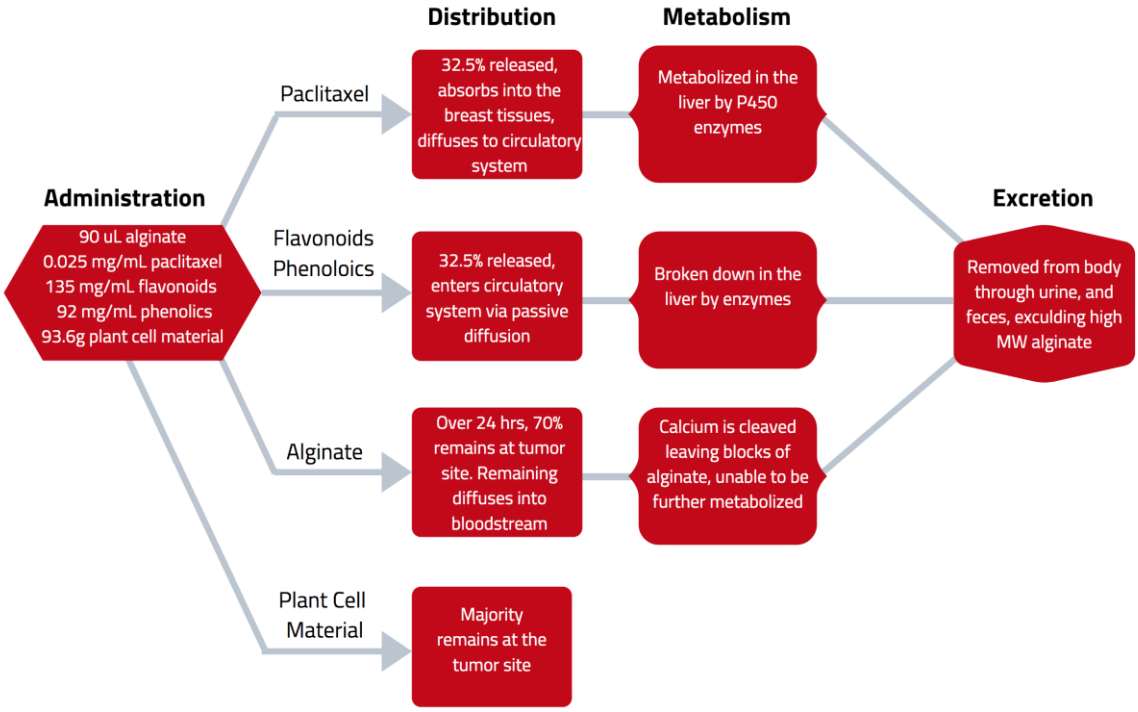

Figure 6.2. Pharmacokinetics of the paclitaxel release system [106, 127-129].

The specific ADME for each component of the system including PTX, flavonoids, phenolics, alginate, and PCC material are further detailed in the subsequent sections of this chapter.

6.1.1 Administration

For this system, 2.8 mm-diameter alginate microbeads loaded with *Taxus* PCC are surgically implanted onto a tumor site for a 24-hr targeted drug release to treat breast cancer patients. The alginate microbeads have a loading capacity of 77 mg PCC material/ mL alginate; therefore, the bead size is subject to change depending on PTX concentrations retained in the material through processing. For this implantation, the PCC under analysis contains 4.1 x 10^{-5} mg/mL PTX, 0.22 mg/mL flavonoids, and 0.15 mg/mL phenolics (as described in Chapter 3). Approximately 10.4 mg of lyophilized PCC is loaded into each alginate hydrogel microbead (methods detailed in Chapter 4), with each bead having respective PTX, flavonoid, and phenolic concentrations of 0.025 mg/mL, 135 mg/mL, and 92 mg/mL. In a nine bead system (4.68 mm^3 total volume), there is approximately 93.6 mg of plant cell material, and 90 µL of alginate. These loading amounts and concentrations are subject to alteration dependent on a patient's height, weight, age, and tumor characteristics.

6.1.2 Distribution

Paclitaxel

Over 24 hr, approximately 32.5% of the PTX (Chapter 4.3.3) is released from the microbeads to deliver a PTX concentration of 8.5 x 10^{-4} mg/mL to the tumor. PTX binds to tubulin in the tumor which activates apoptosis via phosphorylation pathways and subsequent cytotoxicity, thus, killing 75% of the tumor cells [127]. The remaining PTX that is released into the body travels via the circulatory system to its metabolism site.

The remaining PTX absorbs into the breast tissues and diffuses into the circulatory system through either the internal mammary vein or intercostal veins. Here, PTX may potentially bind to hydrophobic sites along the venous tissues and it can take up to 4 hr for the drug to diffuse through the venous wall [130]. Once the drug has entered the circulatory system, the compound binds to various plasma proteins including serum albumin, glycoproteins, and platelets [131]. PTX travels through the veins to the liver to be metabolized [127].

Flavonoids and Phenolics

Over 24 hr, approximately 32.5% of the flavonoids and phenolics are released from the microbeads to deliver a flavonoid concentration of 43.9 mg/mL and a phenolic concentration of 29.9 mg/mL to the tumor site. These metabolites may inhibit cell proliferation, induce apoptosis and cell arrest, or decrease the expression of pro-survival factors within the tumor cells; thus, enhancing the cytotoxic properties of PTX [48-50]. The remaining metabolite concentrations that are released into the body travel via the circulatory system metabolic sites.

The remaining metabolites absorb into the breast tissues and diffuse into the circulatory system through either the internal mammary vein or intercostal veins. Due to the hydrophilic properties of these metabolites, the compounds are able to directly enter the bloodstream via passive

diffusion. The compounds bind to glycoproteins in the plasma and travel through the circulatory system to the liver for metabolism [129, 132].

Alginate

Over 24 hr, a majority of the alginate degrades from natural calcium chelators, such as parathyroid hormones, that exist at the site of the tumor [106]. The degraded alginate either remains at the tumor site, or is carried away by blood. Studies suggest that up to 70% of the implanted alginate remains at the tumor site [133]. Additionally, *in vivo* studies show that there are no adverse side effects when 13,500 mg sodium alginate/kg body weight (BW) are administered per day, and no associated genotoxicity or carcinogenic effects when 37,500 mg sodium alginate/kg BW are administered per day [134]. These amounts of alginate are well beyond the amount of alginate that is used in the PTX DDS. For the alginate that is absorbed into the bloodstream, it is distributed through the body by the circulatory system to the kidney for metabolism [106].

Plant Cell Culture Material

The plant cell material primarily consists of cellulose; therefore, a majority of the encapsulated material remains at the tumor site because the human body does not have the necessary cellulase enzymes to break down the cellulose [135]. Considering plant cell material has not been used for drug delivery previously, it is unclear as to what adverse reactions that may result from the remaining biomass. However, it is hypothesized that some of the plant cell matrix may be broken down by macrophage phagocytosis, which can allow some of the particulates to be absorbed into the circulatory system for further metabolism [135].

6.1.3 Metabolism

Paclitaxel

In the liver, PTX is hydroxylated by hepatic CYPs (CYP2C8 and CYP3A4) to produce metabolites 6-α-hydroxy-paclitaxel and 3'-p-hydroxyphenyl-paclitaxel, which are upwards of thirty times less cytotoxic than PTX [127, 136]. These metabolite conjugates undergo biliary excretion to be eliminated from the body [136].

Flavonoids and Phenolics

Despite the natural benefactors of flavonoids and phenolics, the body continues to recognize these compounds as xenobiotics, or foreign substances, that must undergo Phase II metabolism in the liver to diminish each compound's bioefficacies [129]. These metabolite conjugates undergo biliary excretion to be eliminated from the body [129].

Alginate

The human body does not have the necessary enzyme, alginate lyase, to adequately breakdown and metabolize alginate. However, research has suggested that the degradation of alginate blocks can be aided by partial oxidation of the chains prior to implantation [106]. Alginate blocks that are not sufficiently degraded enter the bloodstream and are sent to the kidneys, where it undergoes glomerular filtration.

Plant Cell Culture Material

Macrophage phagocytosis can contribute to the breakdown of cellulose, which is a primary component of the plant cell matrix. However, further metabolism and breakdown of the plant cell culture material is unlikely due to its rigidity [135]. There is a need for more research in this area, as implantation and metabolism of plant cell material has not been extensively studied.

6.1.4 Excretion

Within 24 hr, a majority of the PTX, flavonoids, phenolics, and alginate is eliminated from the body through urine and feces [106, 127, 129]. However, there are several concerns that must be addressed with regards to the excretion of this system's components. Ten percent of the PTX is eliminated via renal excretion; therefore, it is recommended that patients with renal failure be administered lower doses of the drug [129]. With alginate, due to higher molecular weight blocks, the polymer may not get completely removed from the body, as it would be bigger than the renal clearance threshold of the kidneys [106]. Alginate blocks that have a molecular weight less than 60,000 Da are small enough to pass through the kidneys and get excreted in urine, while the larger polymer blocks continue to circulate in the body, not readily accumulating in any tissue [106]. For the remaining plant cell matrix, most of the material will remain at the site of the tumor after 24 hr, while some of the smaller molecules will pass through the kidneys to be excreted in urine.

6.2 Conclusions

Following the implantation of PTX-loaded alginate microbeads, absorption, distribution, metabolism, and excretion processes occur for the PTX, flavonoids, phenolics, alginate, and plant cell material of the delivery system. The manner of these pharmacokinetic processes depends on the material. While all of the materials are administered through the same method, the PTX, flavonoid, and phenolic compounds are metabolized and can be broken down by the body. Conversely, the remnants of the alginate microbeads and the additional plant cell material are unable to be metabolized and fully degraded due to a lack of necessary enzyme systems. Although the alginate and plant cell matrix cannot be degraded, these materials are still excreted with the plant metabolites, given that they are small enough to clear the renal clearance threshold of the kidneys. Molecules that are bigger than this threshold will continue to circulate in blood throughout the body, eventually

accumulating in tissues. However, it is expected that these materials will not cause further harm to the body.

There is a lack of research on the pharmacokinetics of materials in PCC drug delivery systems, as this is a novel delivery device. With the primary aspects of the pharmacokinetics for this system considered, a PCC drug delivery system is promising for future local drug delivery, as there does not appear to be an increase in risk or danger involved with such a treatment. A big concern regarding the pharmacokinetics of this system is the relatively unknown distribution, metabolism, and excretion of the plant cell material. This area would have to be researched and adequately tested before success of this system could be considered.

Chapter 7: Discussion and Future Research

This Major Qualifying Project (MQP) investigated the potential for local administration of paclitaxel (PTX) via targeted delivery of processed *Taxus* plant cell cultures (PCC). The studies analyzed sought to provide insight on the delivery of PTX through PCC by the following aims:

Aim 1: Develop a wash process that retains PTX, flavonoid, and phenolic compounds, and prepare PCC material for encapsulation.
Aim 2: Optimize delivery of PTX, flavonoid, and phenolic compounds by encapsulating PCC material in a biomaterial suitable for desired delivery.
Aim 3: Establish an in vitro model to optimize drug delivery design for maximum breast cancer cell culture cytotoxicity and predict release studies for PCC delivery.
Aim 4: Understand pharmacokinetics for components of the optimized drug delivery system to determine feasibility and administration parameters.

This chapter summarizes the key results of these aims as well as provides suggestions for future research opportunities to further understand targeted delivery of PTX through PCC.

7.1 Retention of Paclitaxel, Flavonoids, and Phenolics Through Wash Processing

While the washing process detailed in Chapter 3 can retain a significant amount of PTX, flavonoids, and phenolics through processing, there are several variables that can interfere with optimization of the process. For instance, the density of the initial PCC being washed impacted metabolite retention. If the initial sample density was relatively low, the pellet containing the cells after centrifugation was not sufficiently packed. This resulted in losing cells, and the cell-associated metabolites, in the removal of the supernatant. To maximize metabolite retention, cells should be transferred properly every 2 weeks (as detailed in Chapter 3.2.1), ensuring that there is a higher density of cells in the media. If a significant amount of cells are lost in transferring, it is recommended to allow the cells to grow for an extra day or two before elicitation to increase the density of cells before processing.

Additionally, researchers should perform further experiments using different solvents other than deionized water to wash the PCC. Due to the hydrophobic properties of PTX, polar protic solvents, such as alcohols or ammonia, can prevent significant losses of PTX because the drug compound cannot dissolve into these solvents [94]. Different solvents may also increase the retention of other metabolites in the PCC such as flavonoids and phenolics, the latter of which showed a statistical loss in our experiments. Researchers can test these different solvents individually, or as mixtures to optimize the retention of each metabolite of interest. However, while retention of PTX, flavonoids, and phenolics is important, the optimal solvent is one that retains the greatest concentration of PTX. By retaining greater amounts of PTX, less PCC material is needed for encapsulation to achieve cytotoxicity.

7.2 Optimization of Delivery

To optimize the local delivery of PTX through PCC, experiments were performed to determine the release of Nile Red (NR) and PTX from alginate hydrogel microbeads; however, future research is needed to further optimize the delivery vehicle and model system, and understand the release of PTX from encapsulated PCC.

The degradation profile of PTX at 37°C should first be understood to determine an appropriate material to minimize any potential degradation of PTX. Experiments aimed at determining the release of PTX from alginate hydrogels showed variability in the measured PTX concentrations. This variability may be due to PTX degrading through the incubation process, and a different temperature may have to be used for incubation. Due to this uncertainty, it is necessary to perform testing in order to understand the degradation of PTX at 37°C, and if this is determined to be an issue, a new temperature must be determined for the incubation process.

To optimize the delivery vehicle, other natural and synthetic polymers should be explored, and compared to the release kinetics collected from the alginate hydrogel studies. Utilizing materials such as gelatin, silk, dextran, collagen, and albumin, which have been successfully utilized as biomaterial options for drug delivery systems (DDSs), may improve the stability of the hydrogels [14]. Several of these polymers can also be used together to increase the stability of the polymers to sustain constant drug release rates, such as the addition of chitosan to alginate [137]. Additionally, synthetic polymers should be explored as a PCC DDS. At the onset of this project, polyvinyl alcohol hydrogel was utilized, but it proved to be too unstable for a sustained drug delivery. However, further research and testing should be carried out with synthetic polymers to properly explore their PCC drug delivery potential [138].

In addition to exploring different materials, altering the form factors of polymers may enhance their drug delivery kinetics. While hydrogel microbeads are a common and widely tested form factor for drug-loaded implants, others such as nanoparticles, polymeric films, rods, and wafers have been tested and have demonstrated promising results for delivery of PTX [14, 97]. Different form factors should be explored to achieve different release profiles of the drug. To shift the release profile of a drug to be faster, smaller form factors, such as nanoparticles, should be investigated, as a greater total surface area of the material will increase the early rate of drug release [14]. Conversely, larger geometries, like wafers, will have a longer duration, more delayed drug release [14]. For the use of a PCC DDS to treat breast cancer, nanoparticle formulations should be an immediate area for future research given their noted success in other studies involving PTX and breast cancer treatment [14, 139].

Because PTX is an expensive compound to be consistently used in release studies, further research on using NR as a model for PTX should be carried out to minimize PTX usage. A NR model was utilized due to its similar solubility and size to PTX. Additionally, the compound is pigmented, which allows for the use of a UV-Vis spectrometer to obtain release concentrations. A UV-Vis spectrometer is a simpler analyzing method when compared to UPLC, which can be time extensive. However, results from the release studies outlined in Chapter 4 demonstrate differences

in release profiles for the two compounds. More research should be conducted on using NR as a model for PTX, as well as research on other pigmented materials that could accurately simulate the release of PTX in a PCC DDS.

Lastly, future experimentation to determine the release of PTX through PCC from alginate hydrogel microbeads should be conducted. From initial experiments, it was determined that approximately 77 mg of PCC was the PCC volume threshold that could be encapsulated in 1 mL of alginate whilst maintaining uniform hydrogel microbeads. For future research, release of PCC from alginate hydrogels should be tested to confirm that a successful and concentrated drug delivery with PCC is possible.

7.3 Testing Optimized Drug Delivery System on Mammalian Cell Culture

Due to limitations from the COVID-19 pandemic and lack of access to the lab, not all the planned mammalian cell culture experiments were able to be conducted. While the effects of pure PTX on MDA-MB-231 breast cancer cells were determined, the optimized DDS was not able to be tested. This experiment would entail seeding a 96-well plate with 5,000 cells per well of MDA-MB-231 cells. In addition to a set of cells untreated as a control, these cells would be treated with 2 µL of either of the following solutions: release media from PCC encapsulated in alginate, alginate, or pure PTX. These cells would be treated with 2 µL to better replicate our testing we have performed. Treating cells with the release media would ensure that the DDS is able to release a high enough PTX concentration to kill the cells. Treating cells with alginate would ensure that the delivery vehicle is not cytotoxic to the cancer cells. Lastly, treating cells with pure PTX would serve as a comparison to the PTX released from the PCC. It is hypothesized that other naturally produced metabolites enhance the cytotoxic properties of PTX. The cells would be treated for periods of 12 and 24 hr to analyze the effects of drug exposure time on cell viability. Although 12 and 24 hour tests were performed in this MQP, it may be advisable to perform 48 hr tests, as previous studies show the doubling time of MDA-MB-231 cells to be about 30 hr and up to 40 hr [140]. Because PTX targets the microtubules of a cell, it is important to allow sufficient time for as many of the cells to double as possible. Cell viability data would be collected with the same methods detailed in Chapter 5.2. It is hypothesized that the designed DDS will successfully kill the cells considering the desired release concentration falls within the efficient range of treatment concentrations determined by the study detailed in Chapter 5. Effective PTX concentrations for breast cancer cell treatment ranges from 37 to 1000 nM, as this is the highest concentration tested. Higher concentrations may be usable, but testing may be necessary to determine how these higher concentrations will act, and if they introduce any new side effects as opposed to relatively low concentrations. However, the delivery system under analysis is expected to release 995 nM of PTX, which we calculated in section 4.3.3, which is within our tested and effective range.

7.4 Pharmacokinetics of the Paclitaxel Release System

This project hypothesized the pharmacokinetics of the proposed PTX release system based on literature review of current PTX treatment pharmacokinetics. The initial mapping of the system identified the administration, distribution, metabolism, and excretion (ADME) for each of the system's components—PTX, flavonoids, phenolics, alginate, and PCC material. Due to the lack of research regarding delivering drugs produced by PCC, researchers must conduct further experimental studies to fully understand the ADME for this release system; which, in turn, would allow practitioners to develop appropriate treatment plans for their patients with this system.

Prior to clinical studies, researchers should conduct experiments on mammalian disease models, such as mice bearing subcutaneous or orthotopic xenograft breast cancer tumors, to analyze the ADME of this system [141]. To analyze the administration and absorption of the system's compounds, researchers would have to implant the optimized drug delivery system onto the tumor site. At this time, researchers should collect data regarding changes in tissue concentrations for each of the system's components [142]. However, to evaluate this data for flavonoids and phenolics, researchers would need to identify particular metabolites of interest prior to testing. By collecting tissue samples at regular time intervals, researchers can construct concentration-versus-time plots to identify the release profile of each component. From these plots, researchers can extrapolate bioavailability, the rate at which each component accesses the tumor site, for each of the components by calculating the area under the curve (AUC) [143]. Similarly, distribution experiments should entail measuring drug concentrations in plasma. From these experiments, researchers should collect blood samples at regular time intervals and evaluate for absorption ratio and rate. Extrapolated from concentration-versus-time plots, absorption ratio (maximum concentration/AUC) can identify each component's absorption rate constant [144]. By identifying these constants, researchers can determine how long each component takes to penetrate into the circulatory system from its administration. Furthermore, to understand the metabolism and excretion of each of the system's components, researchers should assess concentrations of the components, as well as the suspected conjugate metabolites, in plasma, urine, bile, and feces. Throughout this process, researchers should collect samples at standard times and analyze the sample concentrations. Extrapolated information from model independent analytical models, such as minimum and maximum concentrations with associated times, mean residence time, half-life, and volume of distribution, can provide researchers with further insight into the system's ADME [142]. By identifying the system's minimum and maximum concentrations for PTX, researchers can determine if the system is releasing a drug concentration efficient for tumor cell cytotoxicity that does not cause further side effects to the patient. Additionally, mean residence time, the average time the component spends in the body, and half-life, the time for each component's administered concentration to decrease by 50%, allows researchers to understand the amount of time between administration and excretion for each component [145]. Lastly, volume of distribution is the theoretical volume of the administered drug needed to achieve the desired release concentration and is used to adjust loading concentrations into

the delivery vehicle [146]. Overall, these experimental studies would help researchers gain a better understanding of administering PTX through PCC and other plant-based drugs locally.

7.5 Reflections

A previous MQP group began the investigation for local administration of PTX via delivery of processed *Taxus* PCC by increasing cell-associated metabolite accumulation through processing procedures, removing DNA from the cells for biocompatibility, and comparing the release kinetics of free PTX to PTX encapsulated in alginate hydrogel microbeads [16]. Moving forward, this MQP sought to improve the processing procedure to increase cell-associated metabolite accumulation. Formerly, the PCC was washed from the plant media after lyophilization. By washing after lyophilization, along with using a Buchner funnel to dry the washed cell material, 85% of metabolites, such as PTX, were lost through processing [16]. However, by altering the processing procedure to lyophilize the cells after washing, 75% flavonoids, 40% phenolics, and 68.3% PTX were retained. Furthermore, this MQP sought to extend the knowledge of PTX release kinetics through various polymeric biomaterials. Previously, alginate, a natural polymer, was used to encapsulate PTX. The alginate hydrogel microbeads used in this study were unable to maintain integrity over 12 hr [16]. However, this MQP improved the durability of the alginate microbeads by altering the viscosity of the alginate so that the beads could withstand a 24 hr delivery period; thus, increasing the control over the system's release. Moreover, this MQP expanded the investigation for local administration of PTX by understanding the cytotoxic effects on *in vitro* breast cancer cell models, and the pharmacokinetics of the optimized delivery system. Overall, previous studies in conjunction with the extension in knowledge gained through this MQP expand the understanding of drug delivery using plant cell culture, and thus advances oncology treatments.

.

References

1. World Health Organization. *Cancer key facts*. 2018 [cited 2020 February 20].
2. Siegel, R.L., K.D. Miller, and A. Jemal, *Cancer statistics, 2020.* CA: A Cancer Journal for Clinicians, 2020. **70**(1): p. 7-30.
3. Sharpless, D.N.E. *FY 2020 budget boost for NCI increases research awards, improves paylines*. 2020 [cited 2020 February 20].
4. Modi, A., A. Grasso, and A. Simons. *Is understanding the molecular basis of cancer a prerequisite for its treatment?* [cited 2020 February 20].
5. American Cancer Society. *How chemotherapy drugs work*. 2019 [cited 2020 April 10].
6. American Cancer Society. *Chemotherapy side effects*. 2019 [cited 2020 April 10].
7. National Cancer Institute. *Taxol ®*. [cited 2019].
8. Reference, P.D. *Paclitaxel-drug summary*. 2019 [cited 2019 December 13].
9. Howat, S., et al., *Paclitaxel: biosynthesis, production and future prospects.* New biotechnology, 2014. **31**(3): p. 242-245.
10. Ketchum, R.E., J.V. Luong, and D.M. Gibson, *Efficient extraction of paclitaxel and related taxoids from leaf tissue of Taxus using a potable solvent system.* Journal of liquid chromatography & related technologies, 2007. **22**(11): p. 1715-1732.
11. Croteau, R., et al., *Taxol biosynthesis and molecular genetics.* Phytochemistry Reviews, 2006. **5**(1): p. 75-97.
12. Kabera, J.N., et al., *Plant secondary metabolites: biosynthesis, classification, function and pharmacological properties.* J Pharm Pharmacol, 2014. **2**: p. 377-392.
13. Ramirez-Estrada, K., et al., *Changes in gene transcription and taxane production in elicited cell cultures of Taxus× media and Taxus globosa.* Phytochemistry, 2015. **117**: p. 174-184.
14. Wolinsky, J.B., Y.L. Colson, and M.W. Grinstaff, *Local drug delivery strategies for cancer treatment: gels, nanoparticles, polymeric films, rods, and wafers.* Journal of controlled release, 2012. **159**(1): p. 14-26.
15. Wen, H., H. Jung, and X. Li, *Drug delivery approaches in addressing clinical pharmacology-related issues: opportunities and challenges.* The AAPS journal, 2015. **17**(6): p. 1327-1340.
16. Werner, A., D.A. Aldarondo, and D.P.R. Dione, *Taxus Cell Culture to Delivery System: A Novel Approach to Administer Paclitaxel.* 2019.
17. National Institute of Biomedical Imaging and Bioengineering. *Drug delivery systems*. 2016 [cited 2019].
18. Cancer Research UK. *Doxorubicin*. 2019 [cited 2020 April 19].
19. Cancer Research UK. *Capecitabine (Xeloda)*. 2018 [cited 2020 April 19].
20. Singh, N., et al., *Drug delivery: advancements and challenges*, in *Nanostructures for Drug Delivery*. 2017, Elsevier. p. 865-886.
21. Khanna, V., et al., *Perlecan-targeted nanoparticles for drug delivery to triple-negative breast cancer.* Future drug discovery, 2019. **1**(1): p. FDD8.
22. Rosenblum, D., et al., *Progress and challenges towards targeted delivery of cancer therapeutics.* Nature communications, 2018. **9**(1): p. 1-12.
23. Hoffman, A.S., *The origins and evolution of "controlled" drug delivery systems.* Journal of controlled release, 2008. **132**(3): p. 153-163.
24. Wang, Z., H. Sun, and J. Sebastian Yakisich, *Overcoming the blood-brain barrier for chemotherapy: limitations, challenges and rising problems.* Anti-Cancer Agents in

Medicinal Chemistry (Formerly Current Medicinal Chemistry-Anti-Cancer Agents), 2014. **14**(8): p. 1085-1093.
25. Langer, R., *Drug delivery and targeting.* Nature London-, 1998: p. 5-10.
26. O'Brien, M., et al., *Mortality within 30 days of chemotherapy: a clinical governance benchmarking issue for oncology patients.* British journal of cancer, 2006. **95**(12): p. 1632-1636.
27. Cunha, J.P. *Bleph*. 2020 [cited 2020 April 21].
28. Medline Plus. *Fluorouracil Topical*. 2016 [cited 2020 April 21].
29. Varma, M.V., et al., *Factors affecting mechanism and kinetics of drug release from matrix-based oral controlled drug delivery systems.* American Journal of drug delivery, 2004. **2**(1): p. 43-57.
30. Garg, T., et al., *Scaffold: a novel carrier for cell and drug delivery.* Critical Reviews™ in Therapeutic Drug Carrier Systems, 2012. **29**(1).
31. Ghasemiyeh, P. and S. Mohammadi-Samani, *Hydrogels as Drug Delivery Systems; Pros and Cons.* Trends in Pharmaceutical Sciences, 2019. **5**(1): p. 7-24.
32. Bhatia, S., *Natural polymer drug delivery systems*. 2016: Springer.
33. Kretlow, J.D., L. Klouda, and A.G. Mikos, *Injectable matrices and scaffolds for drug delivery in tissue engineering.* Advanced drug delivery reviews, 2007. **59**(4-5): p. 263-273.
34. Chen, T., et al., *Paclitaxel loaded phospholipid-based gel as a drug delivery system for local treatment of glioma.* International journal of pharmaceutics, 2017. **528**(1-2): p. 127-132.
35. National University of Singapore. *Cell-derived drug delivery systems*. 2017 [cited 2019.
36. Tyler, B., et al., *A thermal gel depot for local delivery of paclitaxel to treat experimental brain tumors in rats.* Journal of neurosurgery, 2010. **113**(2): p. 210-217.
37. Araújo, J., et al., *Effect of polymer viscosity on physicochemical properties and ocular tolerance of FB-loaded PLGA nanospheres.* Colloids and Surfaces B: Biointerfaces, 2009. **72**(1): p. 48-56.
38. Shojaee, S., et al., *An investigation on the effect of polyethylene oxide concentration and particle size in modulating theophylline release from tablet matrices.* AAPS PharmSciTech, 2015. **16**(6): p. 1281-1289.
39. Gillet, J.-P., S. Varma, and M.M. Gottesman, *The clinical relevance of cancer cell lines.* Journal of the National Cancer Institute, 2013. **105**(7): p. 452-458.
40. Raju, P., et al., *Effect of tablet surface area and surface area/volume on drug release from lamivudine extended release matrix tablets.* International Journal of Pharmaceutical Sciences and Nanotechnology, 2010. **3**(1): p. 872-76.
41. Veeresham, C., *Natural products derived from plants as a source of drugs*. 2012, Wolters Kluwer--Medknow Publications.
42. Taylor, L. *Plant based drugs and medicines*. 2000 [cited 2019].
43. Xu, J. and N. Zhang, *On the way to commercializing plant cell culture platform for biopharmaceuticals: present status and prospect.* Pharmaceutical bioprocessing, 2014. **2**(6): p. 499.
44. Elfawal, M.A., et al., *Dried whole plant Artemisia annua as an antimalarial therapy*. PLoS One, 2012. **7**(12): p. e52746.
45. Percário, S., et al., *Oxidative stress in malaria.* International journal of molecular sciences, 2012. **13**(12): p. 16346-16372.
46. Hussein, R.A. and A.A. El-Anssary, *Plants Secondary Metabolites: The Key Drivers of the Pharmacological Actions of Medicinal Plants*, in *Herbal Medicine*. 2018, IntechOpen.

47. Wang, D.S.Y. *Secondary metabolites from plants*. 52.
48. Erdogan, S., et al., *Naringin sensitizes human prostate cancer cells to paclitaxel therapy.* Prostate International, 2018. **6**(4): p. 126-135.
49. Xu, Y., et al., *Synergistic effects of apigenin and paclitaxel on apoptosis of cancer cells.* PloS one, 2011. **6**(12).
50. Ayyagari, V.N., et al., *Evaluation of the cytotoxicity of the Bithionol-paclitaxel combination in a panel of human ovarian cancer cell lines.* PloS one, 2017. **12**(9).
51. Pezzani, R., et al., *Synergistic effects of plant derivatives and conventional chemotherapeutic agents: An update on the cancer perspective.* Medicina, 2019. **55**(4): p. 110.
52. Wani, M.C. and S.B. Horwitz, *Nature as a remarkable chemist: A personal story of the discovery and development of Taxol.* Anti-cancer drugs, 2014. **25**(5): p. 482.
53. Kalechman, Y., et al., *Synergistic anti-tumoral effect of paclitaxel (taxol)+ AS101 in a murine model of B16 melanoma: Association with ras-dependent signal-transduction pathways.* Internation journal of cancer, 2000. **86**(2): p. 281-288.
54. Weaver, B.A., *How Taxol/paclitaxel kills cancer cells.* Molecular biology of the cell, 2014. **25**(18): p. 2677-2681.
55. Rowinsky, E., et al. *Clinical toxicities encountered with paclitaxel (Taxol)*. Seminars in oncology. 1993.
56. Lamb, H.M. and J.C. Adkins, *Letrozole.* Drugs, 1998. **56**(6): p. 1125-1140.
57. Ward, A. and P. Benfield, *Carboplatin: a preliminary review of its pharmacodynamic and pharmacokinetic properties and therapeutic efficacy in the treatment of cancer.* Drugs, 1989. **37**: p. 162-190.
58. Institute, N.C. *Letrozole with or without paclitaxel and carboplatin in treating patients with stage II-IV ovarian or primary peritoneal cancer*. [cited 2019].
59. National Cancer Institute. *Comparing proton therapy to photon radiation therapy for esophageal cancer*. 2019 [cited 2019].
60. Qian, J., et al., *Low density lipoprotein mimic nanoparticles composed of amphipathic hybrid peptides and lipids for tumor-targeted delivery of paclitaxel.* International journal of nanomedicine, 2019. **14**: p. 7431.
61. Institute, N.C. *Paclitaxel albumin-stabilized nanoparticle formulation*. 2019 [cited 2019].
62. Stinchcombe, T.E., *Nanoparticle albumin-bound paclitaxel: a novel Cremphor-EL®-free formulation of paclitaxel.* 2007.
63. Evans, W.C., *Trease and Evans Pharmacognosy, International Edition E-Book*. 2009: Elsevier Health Sciences.
64. Gagnon, K., *Measuring Electroneutral Chloride-dependent Ion Fluxes in Mammalian Cells and in Heterologous Expression Systems.* Physiology and Pathology of Chloride Transporters and Channels in the Nervous System: From Molecules to Diseases, 2009: p. 149.
65. Lambertz, C., et al., *Challenges and advances in the heterologous expression of cellulolytic enzymes: a review.* Biotechnology for biofuels, 2014. **7**(1): p. 135.
66. Singla, A.K., A. Garg, and D. Aggarwal, *Paclitaxel and its formulations.* International journal of pharmaceutics, 2002. **235**(1-2): p. 179-192.
67. Yassine, F., E. Salibi, and H. Gali-Muhtasib, *Overview of the formulations and analogs in the taxanes' story.* Current medicinal chemistry, 2016. **23**(40): p. 4540-4558.
68. Le Roux, M. and F. Gueritte, *Navelbine® and Taxotère®: Histories of Sciences*. 2016: Elsevier.

69. Dai, J. and R.J. Mumper, *Plant phenolics: extraction, analysis and their antioxidant and anticancer properties.* Molecules, 2010. **15**(10): p. 7313-7352.
70. Działo, M., et al., *The potential of plant phenolics in prevention and therapy of skin disorders.* International journal of molecular sciences, 2016. **17**(2): p. 160.
71. Kumar, S. and A.K. Pandey, *Chemistry and biological activities of flavonoids: an overview.* The Scientific World Journal, 2013.
72. Panche, A., A. Diwan, and S. Chandra, *Flavonoids: an overview.* Journal of nutritional science, 2016. **5**.
73. Kozlowska, A. and D. Szostak-Wegierek, *Flavonoids-food sources and health benefits.* Roczniki Państwowego Zakładu Higieny, 2014. **65**(2).
74. Kim, B.J., D.M. Gibson, and M.L. Shuler, *Effect of subculture and elicitation on instability of taxol production in Taxus sp. suspension cultures.* Biotechnology progress, 2004. **20**(6): p. 1666-1673.
75. Malik, S., et al., *Production of the anticancer drug taxol in Taxus baccata suspension cultures: a review.* Process Biochemistry, 2011. **46**(1): p. 23-34.
76. Naill, M.C., M.E. Kolewe, and S.C. Roberts, *Paclitaxel uptake and transport in Taxus cell suspension cultures.* Biochemical engineering journal, 2012. **63**: p. 50-56.
77. Bringi, V., et al., *Enhanced production of taxol and taxanes by cell cultures of Taxus species*. 1995, Google Patents.
78. Cusido, R.M., et al., *A rational approach to improving the biotechnological production of taxanes in plant cell cultures of Taxus spp.* Biotechnology advances, 2014. **32**(6): p. 1157-1167.
79. Choi, H.-K., et al., *Production of taxol from taxus plant cell culture adding silver nitrate*. 2001, Google Patents.
80. Mirjalili, N. and J.C. Linden, *Methyl jasmonate induced production of taxol in suspension cultures of Taxus cuspidata: ethylene interaction and induction models.* Biotechnology progress, 1996. **12**(1): p. 110-118.
81. Patil, R.A., et al., *Methyl jasmonate represses growth and affects cell cycle progression in cultured Taxus cells.* Plant cell reports, 2014. **33**(9): p. 1479-1492.
82. Atanasov, A.G., et al., *Discovery and resupply of pharmacologically active plant-derived natural products: A review.* Biotechnology advances, 2015. **33**(8): p. 1582-1614.
83. Liu, W., T. Gong, and P. Zhu, *Advances in exploring alternative Taxol sources.* RSC Advances, 2016. **6**(54): p. 48800-48809.
84. Son, S., et al., *Large-scale growth and taxane production in cell cultures of Taxus cuspidata (Japanese yew) using a novel bioreactor.* Plant Cell Reports, 2000. **19**(6): p. 628-633.
85. Zhong, J.-J., *Plant cell culture for production of paclitaxel and other taxanes.* Journal of Bioscience and Bioengineering, 2002. **94**(6): p. 591-599.
86. McPartland, T.J., et al., *Liquid–liquid extraction for recovery of paclitaxel from plant cell culture: solvent evaluation and use of extractants for partitioning and selectivity.* Biotechnology progress, 2012. **28**(4): p. 990-997.
87. Pyo, S.-H., et al., *A large-scale purification of paclitaxel from cell cultures of Taxus chinensis.* Process Biochemistry, 2004. **39**(12): p. 1985-1991.
88. Bui-Khac, T. and N. Dupuis, *Process for extraction and purification of paclitaxel from natural sources*. 2002, Google Patents.

89. Sautter, C., H.C. Bartscherer, and B. Hock, *Separation of plant cell organelles by zonal centrifugation in reorienting density gradients.* Analytical biochemistry, 1981. **113**(1): p. 179-184.
90. Alvi K. A., W., S., & Tous, G., *New and Rapid Ultra-Performance Liquid Chromatography Assay of Paclitaxel.* Journal of liquid chromatography & related technologies, 2008. **31**(7): p. 941-949.
91. Elansary, H.O., et al., *Phenolic Compounds of Catalpa speciosa, Taxus cuspidata, and Magnolia acuminata have antioxidant and anticancer activity.* Molecules, 2019. **24**(3): p. 412.
92. Khorasani Esmaeili, A., et al., *Antioxidant activity and total phenolic and flavonoid content of various solvent extracts from in vivo and in vitro grown Trifolium pratense L.(Red Clover).* BioMed Research International, 2015.
93. Sonmezdag, A.S., H. Kelebek, and S. Selli, *Characterization and comparative evaluation of volatile, phenolic and antioxidant properties of pistachio (Pistacia vera L.) hull.* Journal of Essential Oil Research, 2017. **29**(3): p. 262-270.
94. Chemistry Libretexts. *Polar protic and aprotic solvents*. 2019 [cited 2020 February 16].
95. Gelderblom, H., et al., *Cremophor EL: the drawbacks and advantages of vehicle selection for drug formulation.* European journal of cancer, 2001. **37**(13): p. 1590-1598.
96. Terwogt, J.M., et al., *Alternative formulations of paclitaxel.* Cancer treatment reviews, 1997. **23**(2): p. 87-95.
97. Avachat, A.M., R.R. Dash, and S.N. Shrotriya, *Recent investigations of plant based natural gums, mucilages, and resins in novel drug delivery systems.* Indian Journal of Pharmaceutical Education and Research, 2010. **45**(1): p. 86-99.
98. Li, J. and D.J. Mooney, *Designing hydrogels for controlled drug delivery.* Nature Reviews Materials, 2016. **1**(12): p. 16071.
99. Muppalaneni, S. and H. Omidian, *Polyvinyl alcohol in medicine and pharmacy: a perspective.* J. Dev. Drugs, 2013. **2**(3): p. 1-5.
100. Korsmeyer, R.W., et al., *Mechanisms of solute release from porous hydrophilic polymers.* International journal of pharmaceutics, 1983. **15**(1): p. 25-35.
101. Seib, F.P., E.M. Pritchard, and D.L. Kaplan, *Self-assembling doxorubicin silk hydrogels for the focal treatment of primary breast cancer.* Advanced functional materials, 2013. **23**(1): p. 58-65.
102. Tønnesen, H.H. and J. Karlsen, *Alginate in drug delivery systems.* Drug development and industrial pharmacy, 2002. **28**(6): p. 621-630.
103. Somo, S.I., O. Khanna, and E.M. Brey, *Alginate microbeads for cell and protein delivery*, in *Cell Microencapsulation*. 2017, Springer. p. 217-224.
104. Aguilar, Z., *Nanomaterials for medical applications*. 2012: Newnes.
105. Flora, S.J. and V. Pachauri, *Chelation in metal intoxication.* International journal of environmental research and public health, 2010. **7**(7): p. 2745-2788.
106. Lee, K.Y. and D.J. Mooney, *Alginate: properties and biomedical applications.* Progress in polymer science, 2012. **37**(1): p. 106-126.
107. Campbell, N.A., et al., *Biology: concepts & connections*. 2000: Benjamin/Cummings.
108. Martinez, V. and M. Henary, *Nile red and Nile blue: applications and syntheses of structural analogues.* Chemistry–A European Journal, 2016. **22**(39): p. 13764-13782.
109. LeRoux, M.A., F. Guilak, and L.A. Setton, *Compressive and shear properties of alginate gel: effects of sodium ions and alginate concentration.* Journal of Biomedical Materials

Research: An Official Journal of The Society for Biomaterials, The Japanese Society for Biomaterials, and The Australian Society for Biomaterials and the Korean Society for Biomaterials, 1999. **47**(1): p. 46-53.
110. Amini-Fazl, M.S., H. Mobedi, and J. Barzin, *Investigation of aqueous stability of taxol in different release media.* Drug development and industrial pharmacy, 2014. **40**(4): p. 519-526.
111. Li, J., et al., *Pharmacokinetic profile of paclitaxel in the plasma, lung, and diaphragm following intravenous or intrapleural administration in rats.* Thoracic cancer, 2015. **6**(1): p. 43-48.
112. Wikanta, T., et al., *Synthesis of polyvinyl alcohol-chitosan hydrogel and study of its swelling and antibacterial properties.* Squalen Bulletin of Marine and Fisheries Postharvest and Biotechnology, 2013. **7**(1): p. 1-10.
113. World Health Organization. *Cancer*. 2018 [cited 2019].
114. Sparano, J.A., et al., *Weekly paclitaxel in the adjuvant treatment of breast cancer.* New England Journal of Medicine, 2008. **358**(16): p. 1663-1671.
115. Villanueva-Flores, F., et al., *Poly (vinyl alcohol co-vinyl acetate) as a novel scaffold for mammalian cell culture and controlled drug release.* Journal of materials science, 2019. **54**(10): p. 7867-7882.
116. Yan, C., et al., *Biotin and arginine modified hydroxypropyl-β-cyclodextrin nanoparticles as novel drug delivery systems for paclitaxel.* Carbohydrate polymers, 2019. **216**: p. 129-139.
117. Kuete, V., O. Karaosmanoğlu, and H. Sivas, *Anticancer activities of African medicinal spices and vegetables*, in *Medicinal Spices and Vegetables from Africa*. 2017, Elsevier. p. 271-297.
118. Liebmann, J., et al., *Cytotoxic studies of paclitaxel (Taxol®) in human tumour cell lines.* British journal of cancer, 1993. **68**(6): p. 1104-1109.
119. Xu, F., et al., *Differential drug resistance acquisition to doxorubicin and paclitaxel in breast cancer cells.* Cancer cell international, 2014. **14**(1): p. 538.
120. Jeong, Y.J., et al., *Breast cancer cells evade paclitaxel-induced cell death by developing resistance to dasatinib.* Oncology letters, 2016. **12**(3): p. 2153-2158.
121. Turfus, S., et al., *Pharmacokinetics pharmacognosy*. 2017, Academic, Boston.
122. Anastas, P.P.H.I., H. John. *ADME and toxicology*. [cited 2020 May 9].
123. *Topical medication (topical chemotherapy) for skin cancer*. 2020 [cited 2020 May 5].
124. AE, R. *Drug absorption, distribution and elimination; pharmacokinetics*. 2019 [cited 2020 May 5].
125. Mcdonnell, A.M. and C.H. Dang, *Basic review of the cytochrome p450 system.* Journal of the advanced practitioner in oncology, 2013. **4**(4): p. 263.
126. U.S. National Library of Medicine. *Urinary excretion*. [cited 2020 May 5].
127. Vaishampayan, U., et al., *Taxanes: an overview of the pharmacokinetics and pharmacodynamics.* Urology, 1999. **54**(6): p. 22-29.
128. Stender, E.G., et al., *Structural and functional aspects of mannuronic acid–specific PL6 alginate lyase from the human gut microbe Bacteroides cellulosilyticus.* Journal of Biological Chemistry, 2019. **294**(47): p. 17915-17930.
129. Velderrain-Rodríguez, G., et al., *Phenolic compounds: their journey after intake.* Food & function, 2014. **5**(2): p. 189-197.
130. Creel, C.J., M.A. Lovich, and E.R. Edelman, *Arterial paclitaxel distribution and deposition.* Circulation research, 2000. **86**(8): p. 879-884.

131. Scripture, C.D., W.D. Figg, and A. Sparreboom, *Paclitaxel chemotherapy: from empiricism to a mechanism-based formulation strategy.* Therapeutics and clinical risk management, 2005. **1**(2): p. 107.
132. Hussain, M.B., et al., *Bioavailability and Metabolic Pathway of Phenolic Compounds*, in *Plant Physiological Aspects of Phenolic Compounds*. 2019, IntechOpen.
133. Al-Shamkhani, A. and R. Duncan, *Radioiodination of alginate via covalently-bound tyrosinamide allows monitoring of its fate in vivo.* Journal of bioactive and compatible polymers, 1995. **10**(1): p. 4-13.
134. European Food Safety Authority Panel on Additives and Products or Substances used in Animal Feed, et al., *Safety and efficacy of sodium and potassium alginate for pets, other non food-producing animals and fish.* EFSA Journal, 2017. **15**(7): p. e04945.
135. Yutin, N., et al., *The origins of phagocytosis and eukaryogenesis.* Biology direct, 2009. **4**(1): p. 9.
136. Spratlin, J. and M.B. Sawyer, *Pharmacogenetics of paclitaxel metabolism.* Critical reviews in oncology/hematology, 2007. **61**(3): p. 222-229.
137. Segale, L., et al., *Calcium alginate and calcium alginate-chitosan beads containing celecoxib solubilized in a self-emulsifying phase.* Scientifica, 2016.
138. Rahman, C.V., et al., *PLGA/PEG-hydrogel composite scaffolds with controllable mechanical properties.* Journal of Biomedical Materials Research Part B: Applied Biomaterials, 2013. **101**(4): p. 648-655.
139. Surapaneni, M.S., S.K. Das, and N.G. Das, *Designing Paclitaxel drug delivery systems aimed at improved patient outcomes: current status and challenges.* ISRN pharmacology, 2012.
140. Risinger, A.L., N.F. Dybdal-Hargreaves, and S.L. Mooberry, *Breast cancer cell lines exhibit differential sensitivities to microtubule-targeting drugs independent of doubling time.* Anticancer research, 2015. **35**(11): p. 5845-5850.
141. Wang, W., S. Nag, and R. Zhang, *Pharmacokinetics and pharmacodynamics in breast cancer animal models*, in *Breast Cancer*. 2016, Springer. p. 271-287.
142. National Institute of Health Services. *Clinical pharmacokinetic studies of pharmaceuticals*. 2001 [cited 2020 April 10].
143. Le, J., *Drug Bioavailability.* Merck Manuals, 2019.
144. Endrenyi, L., S. Fritsch, and W. Yan, *Cmax/AUC is a clearer measure than Cmax for absorption rates in investigations of bioequivalence.* Int J Clin Pharmacol Ther Toxicol, 1991. **29**(10): p. 394-399.
145. Sobol, E. and M. Bialer, *The relationships between half-life (t1/2) and mean residence time (MRT) in the two-compartment open body model.* Biopharmaceutics & drug disposition, 2004. **25**(4): p. 157-162.
146. Petty, R.E., et al., *Textbook of pediatric rheumatology e-book.* 2015: Elsevier Health Sciences.

Appendix A. Raw Data

A.1 Chapter 3 Data

A.1.1 Phase 1

Table A1: UPLC standard curve data

Standard Curve: Area = 35162*Concentration R^2: 0.9991 y-intercept: 0

Standard Run Number	Standard Concentration (mg/L)	Retention Time (min)	Area (µV*sec)
1	0	0	0
1	3.125	2.712	95649
1	6.25	2.712	211418
1	12.5	2.712	421461
1	25	2.716	851965
1	50	2.729	1776391
2	0	0	0
2	3.125	2.720	95421
2	6.25	2.722	211405
2	12.5	2.716	421105
2	25	2.715	849731
2	50	2.713	1781005

Table A2: Paclitaxel retention through processing for various initial culture samples

Sample	Retention Time (min)	Area (µV*sec)	Sample Concentration PTX (mg/L)
Initial Culture (IC) 1	2.714	261168	7.427564
IC2	2.708	225267	6.406547
IC3	2.708	225118	6.402309
1.1	2.707	29638	0.842899

(Tube No. Wash No.)			
2.1	2.709	24992	0.710767
3.1	2.710	25515	0.725641
4.1	2.712	12025	0.341989
5.1	2.716	11934	0.339400
6.1	2.715	12787	0.363660
1.2	2.714	36007	1.024032
2.2	2.713	16724	0.475627
3.2	2.713	25227	0.717451
4.2	2.716	5262	0.149650
5.2	2.717	8156	0.231955
6.2	2.718	8307	0.236249
1.3	2.719	21371	0.607787
2.3	2.721	19279	0.548291
3.3	2.721	12959	0.368551
4.3	2.723	4872	0.138559
5.3	2.724	4903	0.139440
6.3	2.722	6718	0.191059
Final Culture (FC) 1	2.722	139095	3.955833
FC2	2.721	160758	4.571924
FC3	2.718	186166	5.294522
FC4	2.716	122298	3.478130
FC5	2.711	89890	2.556453
FC6	2.712	130705	3.717223

A.1.2 Experiment 2

Flavonoid Assay Data

Table A3: Flavonoid assay standard curve data

Standard Curve: Absorbance = 2.4043*Concentration R^2: 0.9975
y-intercept: 0 Blank Subtraction: 0.042

Standard Concentration (mg/mL)	0.000	0.100	0.200	0.400	0.600	0.800	1.000
Absorbance	0.000	0.184	0.542	1.070	1.569	2.083	2.441

Table A4: Flavonoid retention through processing and lyophilization

Sample	Absorbance	Sample Concentration (mg/mL)
IC 1	0.196	0.326082
IC2	0.144	0.239571
IC3	0.176	0.292809
1.1	0.013	0.005407
2.1	0.021	0.008734
3.1	0.022	0.009150
4.1	0.013	0.005407
5.1	0.013	0.005407
6.1	0.013	0.005407
1.2	0.008	0.003327
2.2	0.016	0.006655
3.2	0.018	0.007487
4.2	0.024	0.009982
5.2	0.025	0.010398
6.2	0.020	0.008318
1.3	0.033	0.013725
2.3	0.034	0.014141
3.3	0.033	0.137250
4.3	0.030	0.012478

5.3	0.031	0.012894
6.3	0.028	0.011646
Cells	0.037	0.015389
Cells	0.074	0.030778
Media	0.437	0.727031
Media	0.301	0.500769
FC1	0.106	0.176351
FC2	0.118	0.196315
FC3	0.118	0.196315
FC4	0.113	0.187997
FC5	0.182	0.302791
FC6	0.126	0.209624
FC1L	0.123	0.204633
FC2L	0.157	0.261199
FC3L	0.107	0.178014
FC4L	0.138	0.229589
FC5L	0.148	0.246226
FC6L	0.133	0.221270

Phenolic Assay Data

Table A5: Phenolic assay standard curve data

Standard Curve: Absorbance = 9.6261*Concentration R^2: 0.9960
y-intercept: 0 Blank Subtraction: 0.039

Standard Concentration (mg/mL)	0.000	0.025	0.050	0.075	0.100	0.150	0.200
Absorbance	0.000	0.277	0.494	0.662	0.977	1.454	1.530

Table A6: Phenolic retention through processing and lyophilization

Sample	Absorbance	Sample Concentration (mg/mL)
IC 1	0.856	0.355700
IC2	0.644	0.267606
IC3	0.907	0.376892
1.1	0.146	0.015167
2.1	0.130	0.013505
3.1	0.053	0.005506
4.1	0.081	0.008415
5.1	0.122	0.012674
6.1	0.062	0.006856
1.2	0.042	0.004363
2.2	0.066	0.006856
3.2	0.062	0.006441
4.2	0.071	0.007376
5.2	0.047	0.004883
6.2	0.062	0.006441
1.3	0.044	0.004571
2.3	0.043	0.004467
3.3	0.051	0.005298
4.3	0.041	0.004259
5.3	0.033	0.003428
6.3	0.033	0.003428
Cells	1.549	0.643667
Cells	1.082	0.449611
Media	0.249	0.025867
Media	0.319	0.033139
FC1	0.344	0.0142945
FC2	0.321	0.133387
FC3	0.294	0.122168

FC4	0.243	0.100975
FC5	0.262	0.108871
FC6	0.158	0.065655
FC1L	0.331	0.137543
FC2L	0.376	0.156242
FC3L	0.368	0.152918
FC4L	0.299	0.124246
FC5L	0.307	0.127570
FC6L	0.421	0.174941

UPLC Data

Table A7: UPLC standard curve

Standard Curve: Area = 25825*Concentration R^2: 0.9977 y-intercept: 0

Standard Run Number	Standard Concentration (mg/L)	Retention Time (min)	Area (µV*sec)
1	0	0	0
1	3.125	2.912	51087
1	6.25	2.914	141016
1	12.5	2.915	287253
1	25	2.915	639419
1	50	2.913	1298257
2	0	0	0
2	3.125	2.989	51526
2	6.25	2.999	141721
2	12.5	3.016	287507
2	25	3.008	643980
2	50	3.000	1314609

Table A8: Paclitaxel retention through processing and lyophilization

Sample	Retention Time (min)	Area (μV*sec)	Sample Concentration (mg/L)
IC1	2.912	10989	0.425517909
IC2	2.903	10812	0.418664085
IC3	2.904	13809	0.534714424
Cells	3.005	7547	0.292236205
Cells	3.009	10848	0.420058083
Media	3.014	40	0.001548887
Media	3.012	78	0.003020329
FC1	3.005	1254	0.048557599
FC2	3.005	1419	0.054956757
FC3	3.004	1511	0.058509197
FC4	3.004	1760	0.068151016
FC5	3.000	1533	0.059361084
FC6	3.000	1620	0.062729913
FC1L	3.000	1375	0.053242982
FC2L	3.001	782	0.030280736
FC3L	2.997	1165	0.045111326
FC4L	2.999	778	0.030125847
FC5L	2.996	1145	0.044336883
FC6L	2.992	1169	0.045266215

A.2 Chapter 4 Data

A.2.1 Nile Red Dye Encapsulated in Alginate Hydrogel Release Profile

Nile Red Standard Curve Data

Table A9: Nile red standard curve at t = 0 hr data

Standard Curve: Absorbance = 27.697*Concentration R^2: 0.9976
y-intercept: 0 Blank: 0.046

Standard concentration (mg/mL)	Absorbance (nm)
$1.25x10^{-2}$	0.339
$6.25x10^{-3}$	0.183
$3.125x10^{-3}$	0.091
$1.563x10^{-3}$	0.051
$7.81x10^{-4}$	0.023
$3.91x10^{-4}$	0.012
$1.95x10^{-4}$	0.008
$9.77x10^{-5}$	0.006
$4.88x10^{-5}$	0

Table A10: Nile red standard curve at t = 2 hr data

Standard Curve: Absorbance = 27.949*Concentration R^2: 0.9918
y-intercept: 0 Blank: 0.037

Standard concentration (mg/mL)	Absorbance (nm)
$1.25x10^{-2}$	0.340
$6.25x10^{-3}$	0.184
$3.125x10^{-3}$	0.095
$1.563x10^{-3}$	0.058
$7.81x10^{-4}$	0.029
$3.91x10^{-4}$	0.020
$1.95x10^{-4}$	0.018
$9.77x10^{-5}$	0.012
$4.88x10^{-5}$	0

Table A11: Nile red standard curve at t = 7 hr data

Standard Curve: Absorbance = 27.131*Concentration R^2: 0.9985
y-intercept: 0 Blank: 0.045

Standard concentration (mg/mL)	Absorbance (nm)
$1.25x10^{-2}$	0.334
$6.25x10^{-3}$	0.177
$3.125x10^{-3}$	0.087
$1.563x10^{-3}$	0.048
$7.81x10^{-4}$	0.022
$3.91x10^{-4}$	0.012
$1.95x10^{-4}$	0.008
$9.77x10^{-5}$	0.007
$4.88x10^{-5}$	0

Table A12: Nile red standard curve at t = 10 hr data

Standard Curve: Absorbance = 26.899*Concentration R^2: 0.9988
y-intercept: 0 Blank: 0.045

Standard concentration (mg/mL)	Absorbance (nm)
$1.25x10^{-2}$	0.332
$6.25x10^{-3}$	0.174
$3.125x10^{-3}$	0.086
$1.563x10^{-3}$	0.047
$7.81x10^{-4}$	0.022
$3.91x10^{-4}$	0.012
$1.95x10^{-4}$	0.009
$9.77x10^{-5}$	0.007
$4.88x10^{-5}$	0

Table A13: Nile red standard curve at t = 23 hr data

Standard Curve: Absorbance = 26.123*Concentration R^2: 0.9986
y-intercept: 0 Blank: 0.046 t= 23 hr

Standard concentration (mg/mL)	Absorbance (nm)
$1.25x10^{-2}$	0.322
$6.25x10^{-3}$	0.170
$3.125x10^{-3}$	0.083
$1.563x10^{-3}$	0.046
$7.81x10^{-4}$	0.021
$3.91x10^{-4}$	0.012
$1.95x10^{-4}$	0.009
$9.77x10^{-5}$	0.006
$4.88x10^{-5}$	0

Nile Red Release Data

Table A14: Three beads containing 3% low viscosity sodium alginate release data

Time (hr)	Sample 1		Sample 2		Sample 3	
	Absorbance (nm)	Sample Concentration NR (mg/mL)	Absorbance (nm)	Sample Concentration NR (mg/mL)	Absorbance (nm)	Sample Concentration NR (mg/mL)
0	0	0	0	0	0	0
0.5	0.0003	0.00011	0.003	0.00011	0.004	0.00014
1	0.013	0.00047	0.013	0.00047	0.014	0.00050
1.5	0.015	0.00054	0.013	0.00047	0.017	0.00061
2	0.011	0.00039	0.010	0.00036	0.024	0.00086
3	0.019	0.00068	0.016	0.00057	0.016	0.00057
4	0.026	0.00093	0.023	0.00082	0.028	0.00100
5	0.019	0.00070	0.017	0.00063	0.014	0.00052
6	0.036	0.00133	0.030	0.00111	0.028	0.00103
7	0.044	0.00162	0.042	0.00155	0.031	0.00114
8	0.049	0.00181	0.045	0.00166	0.044	0.00162

9	0.06	0.00223	0.048	0.00178	0.052	0.00193
10	0.068	0.00253	0.075	0.00279	0.081	0.00301
11	0.066	0.00245	0.068	0.00253	0.073	0.00271
12	0.067	0.00249	0.072	0.00268	0.070	0.00260
23	0.072	0.00276	0.07	0.00268	0.067	0.00256

Table A15: Nine beads containing 3% low viscosity sodium alginate release data

Time (hr)	**Sample 1**		**Sample 2**		**Sample 3**	
	Absorbance (nm)	**Sample Concentration NR (mg/mL)**	**Absorbance (nm)**	**Sample Concentration NR (mg/mL)**	**Absorbance (nm)**	**Sample Concentration NR (mg/mL)**
0	0	0	0	0	0	0
0.5	0.004	0.00014	0.004	0.00014	0.004	0.00014
1	0.014	0.00050	0.013	0.00047	0.013	0.00047
1.5	0.031	0.00111	0.014	0.00050	0.019	0.00068
2	0.024	0.00086	0.015	0.00054	0.018	0.00064
3	0.019	0.00068	0.030	0.00107	0.039	0.00140
4	0.042	0.00150	0.033	0.00118	0.044	0.00157
5	0.038	0.00140	0.036	0.00133	0.045	0.00166
6	0.044	0.00162	0.052	0.00192	0.061	0.00225
7	0.054	0.00199	0.059	0.00218	0.068	0.00251
8	0.069	0.00254	0.063	0.00232	0.078	0.00288
9	0.088	0.00327	0.067	0.00249	0.082	0.00305
10	0.134	0.00498	0.091	0.00338	0.093	0.00346
11	0.080	0.00297	0.086	0.00320	0.107	0.00398
12	0..085	0.00316	0.094	0.00350	0.114	0.00424
23	0.130	0.00498	0.112	0.00429	0.130	0.00498

Table A16: Three beads containing 5% low viscosity sodium alginate release data

Time (hr)	Sample 1		Sample 2		Sample 3	
	Absorbance (nm)	**Sample Concentration NR (mg/mL)**	**Absorbance (nm)**	**Sample Concentration NR (mg/mL)**	**Absorbance (nm)**	**Sample Concentration NR (mg/mL)**
0	0	0	0	0	0	0
0.5	0.005	0.00018	0.004	0.00014	0.002	0.00007
1	0.015	0.00054	0.013	0.00047	0.014	0.00050
1.5	0.014	0.00050	0.014	0.00050	0.013	0.00047
2	0.022	0.00079	0.018	0.00064	0.019	0.00068
3	0.034	0.00122	0.024	0.00086	0.024	0.00086
4	0.036	0.00129	0.033	0.00118	0.029	0.00104
5	0.040	0.00147	0.030	0.00111	0.028	0.00103
6	0.048	0.00177	0.042	0.00155	0.035	0.00129
7	0.057	0.00210	0.043	0.00159	0.050	0.00184
8	0.069	0.00254	0.057	0.00210	0.077	0.00284
9	0.071	0.00264	0.064	0.00238	0.075	0.00279
10	0.085	0.00316	0.073	0.00271	0.069	0.00257
11	0.097	0.00361	0.088	0.00327	0.081	0.00301
12	0.092	0.00342	0.093	0.00346	0.078	0.00290
23	0.092	0.00352	0.090	0.00345	0.092	0.00352

Table A17: Nine beads containing 5% low viscosity sodium alginate release data

Time (hr)	Sample 1		Sample 2		Sample 3	
	Absorbance (nm)	**Sample Concentration NR (mg/mL)**	**Absorbance (nm)**	**Sample Concentration NR (mg/mL)**	**Absorbance (nm)**	**Sample Concentration NR (mg/mL)**
0	0	0	0	0	0	0
0.5	0.007	0.00025	0.002	0.00008	0.013	0.00049
1	0.023	0.00082	0.014	0.00050	0.029	0.00104
1.5	0.29	0.00104	0.019	0.00068	0.035	0.00125
2	0.037	0.00132	0.026	0.00093	0.043	0.00154
3	0.049	0.00175	0.043	0.00154	0.064	0.00229
4	0.057	0.00204	0.051	0.00182	0.071	0.00254
5	0.054	0.00199	0.056	0.00206	0.063	0.00232
6	0.063	0.00232	0.065	0.00240	0.078	0.00287
7	0.082	0.00302	0.084	0.00310	0.086	0.00317
8	0.093	0.00343	0.093	0.00343	0.102	0.00376
9	0.101	0.00375	0.102	0.00379	0.108	0.00402
10	0.103	0.00383	0.106	0.00394	0.126	0.00468
11	0.115	0.00428	0.098	0.00364	0.111	0.00413
12	0.110	0.00409	0.130	0.00483	0.129	0.00480
23	0.196	0.00750	0.174	0.00666	0.163	0.00624

Chelation of Alginate Beads in EDTA Data

Table A18: EDTA standard curve data

Standard Curve: Absorbance = 25.397*Concentration R^2: 0.99992
y-intercept: 0 Blank: 0.042

Standard concentration (mg/mL)	Absorbance (nm)
$2.50x10^{-2}$	0.635
$1.25x10^{-2}$	0.315
$6.25x10^{-3}$	0.161
$3.125x10^{-3}$	0.083
$1.563x10^{-3}$	0.041
$7.81x10^{-4}$	0.021
$3.91x10^{-4}$	0.010
$1.95x10^{-4}$	0.007
$9.77x10^{-5}$	0.003
$4.88x10^{-5}$	0

Table A19: Chelation of 3% sodium alginate beads release data

	3 Beads, Sample 1	3 Beads, Sample 2	3 Beads, Sample 3	9 Beads, Sample 1	9 Beads, Sample 2	9 Beads, Sample 3
Absorbance (nm)	0.014	0.013	0.013	0.014	0.009	0.014
Sample Concentration NR (mg/mL)	0.00055	0.00051	0.00051	0.00055	0.00035	0.00035

Table A20: Chelation of 5% sodium alginate beads release data

	3 Beads, Sample 1	3 Beads, Sample 2	3 Beads, Sample 3	9 Beads, Sample 1	9 Beads, Sample 2	9 Beads, Sample 3
Absorbance (nm)	0.005	0.008	0.002	0.046	0.041	0.034
Sample Concentration NR (mg/mL)	0.00020	0.00032	0.00008	0.00181	0.00161	0.00134

A.2.2 Paclitaxel Encapsulated in Alginate Hydrogel Release Profile

Table A21: Mass release PTX from calcium alginate hydrogel microbeads after 12 hr

Bead Concentration (mg/mL)	Sample 1 Concentration (mg/mL)	Sample 2 Concentration (mg/mL)	Sample 3 Concentration (mg/mL)
0.1	0.000920	0.00473	0.00304
0.05	0.00191	0.00184	0.00175
0.01	0.000324	0.000636	0.000839
0.005	0.000346	0.000243	0.000231
0.001	0.0000127	0.00000828	0.0000523

Table A22: Mass release PTX from calcium alginate hydrogel microbeads after 24 hr

Bead Concentration (mg/mL)	Sample 1 Concentration (mg/mL)	Sample 2 Concentration (mg/mL)	Sample 3 Concentration (mg/mL)
0.1	0.00196	0.00355	0.00336
0.05	0.00182	0.000929	0.00128
0.01	0.000468	0.000404	0.000776
0.005	0.000286	0.000268	0.000314
0.001	0.000141	0.0000834	0.000138

A.3 Chapter 5 Data

A.3.1 Determining Optimal Paclitaxel Concentration for Breast Cancer Treatment

Resazurin Assay

Table A23: Raw resazurin assay data

PTX Concentration (nM)	Sample 1	Sample 2	Sample 3	Sample 4	Sample 5	Sample 6
1000	139076	137661	140584	136555	N/A	N/A
333.33	143894	152717	148222	141078	N/A	N/A
111.11	152628	160830	151455	144338	N/A	N/A
37.03	163401	151153	166770	133789	N/A	N/A
12.34	254560	211292	219469	216599	N/A	N/A
4.11	26639	248287	262220	270820	N/A	N/A
1.37	357744	364835	333936	367403	N/A	N/A
0.45	455111	415126	455700	493272	N/A	N/A
0.152	559789	502711	514604	545391	N/A	N/A
0.0508	558300	525431	500233	522172	N/A	N/A
0.0169	553800	546179	530164	537358	N/A	N/A
0.00564	562725	540312	548663	509918	N/A	N/A
0	563545	601563	528135	542249	559981	545449
Resazurin (Background)	1772	1413	1444	N/A	N/A	N/A

Table A24: Raw cell vitality data

PTX Concentration (nM)	Sample 1	Sample 2	Sample 3	Sample 4	Sample 5	Sample 6
1000	0.246673133	0.244135251	0.249377815	0.242151578	N/A	N/A
333.33	0.255314486	0.27113903	0.263076996	0.250263832	N/A	N/A
111.11	0.270979404	0.28569015	0.268875562	0.256110825	N/A	N/A
37.03	0.290301382	0.268333908	0.296343872	0.237190603	N/A	N/A
12.34	0.453800151	0.376196571	0.390862478	0.385714972	N/A	N/A
4.11	0.475464513	0.442549174	0.467538789	0.482963371	N/A	N/A
1.37	0.63886643	0.651584535	0.596165449	0.656190387	N/A	N/A
0.45	0.813499594	0.741784258	0.814555998	0.881943483	N/A	N/A
0.152	1.001245445	0.898872858	0.920203619	0.975421826	N/A	N/A
0.0508	0.99857484	0.939622449	0.894428426	0.93377725	N/A	N/A
0.0169	0.990503839	0.976835149	0.94811135	0.961014191	N/A	N/A
0.00564	1.006511326	0.966312356	0.981290342	0.911799016	N/A	N/A
0	1.007982041	1.076169452	0.944472225	0.969786474	1.001589808	0.975525853

Appendix B. Product Information

B.1 Cell Lines

Taxus cuspidata: 48.82A.11
Breast cancer cell line: MDA-MB-231

B.2 Chemicals and Reagents

1-napthalenacetic acid: Sigma-Aldrich, St. Louis, MO
Aluminum chloride: Sigma-Aldrich, St Louis, MO, 7784-13-6
Ascorbic acid: Fisher Scientific, Hampton, NH
Benzyl adenine: Sigma-Aldrich, St. Louis, MO
BSA-PBS: sigma-Aldrich, St. Louis, MO
Calcium chloride: C1016, Sigma-Aldrich, St. Louis, MO
Catechin: Cayman Chemical, Ann Arbor, MI, 70940
Citric Acid: PhytoTechnology Laboratories, Lenexa, KS
Dimethylsulfoxide: Fisher Scientific, Fair Lawn, NJ
DPBS (-): Cat # 21-031-CV, Corning
EDTA disodium salt: Fisher Scientific, Fair Lawn, NJ
Fetal bovine serum: Fisher Scientific, Hampton, NH
Gallic acid: Acros Organics, Hampton, NH
Gamborg-B5: PhytoTechnology Laboratories, Lenexa, KS
L-glutamine: Caisson Laboratories, Smithfield, UT
L-glutamine: Fisher Scientific, Hampton, NH
Low viscosity sodium alginate: Alfa Aesar, Haverhill, MA
Methyl jasmonate: Sigma-Aldrich, St Louis MO, 392707
Nile red dye: Sigma-Aldrich, St. Louis, MO
Paclitaxel: Alfa aesar, Ward Hill, MA
Penicillin: Fisher Scientific, Hampton, NH
Polyvinyl alcohol: 363170, Sigma-Aldrich, St. Louis, MO
Sodium carbonate: Fisher Scientific, Hampton, NH, S263-500
Sodium hydroxide: Sigma-Aldrich, St Louis, MO, 1310-73-2
Sodium nitrite: Acros, NJ, 42435-5000
Streptomycin: Fisher Scientific, Hampton, NH
Sucrose: Caisson Laboratories, Smithfield, UT
Trypsin: Cat # 25-053-Cl, Corning

B.3 Instruments and Products

0.15 mL low-volume insert: VWR, Radnor, PA
1.0 mL syringe: PrecisionGlide®, Becton Dickinson, Franklin Lakes, NJ
22-gauge needle: PrecisionGlide, Becton Dickinson, Franklin Lakes, NJ
2 mL UPLC vial: VWR, Radnor, PA
50 mL conical tubes: Eppendorf, Hamburg, Germany
-80 °C freezer: SU80XLE, Global Cooling Inc., Athens, OH
Centrifuge: 5808F, Eppendorf, Hamburg, Germany
Colorimetric absorbance reader: Accuskan GO, Fisher Scientific, Hampton, NH
Evaporative centrifuge: Vacufuge plus, Eppendorf, Hamburg, Germany
Fixed-angle rotor: FA-45-6-30, Eppendorf, Hamburg, Germany
Fluorescence plate reader: Victor 3 – PerkinElmer 1420 Multilabel, Counter
Gyratory shaker: New Brunswick Scientific Co. Inc, Edison, NJ, Model 44
Inverted microscope: Nikon Eclipse TS100, Tokyo, Japan
Microcentrifuge: 5242, Eppendorf, Hamburg, Germany
Multiskan™ GO Microplate Spectrophotometer: Accuskan GO, Fisher Scientific, Hampton, NH
Shaker: MaxQ 4000, Thermo Fisher Scientific, Waltham, MA
Shaker: New Brunswick Scientific Co. Inc, Edison, NJ, Model 44
Shelf lyophilizer: VirTis BenchTop Pro with Omnitronics, SP Scientific, Stone Ridge, NY
Sonicator: Aquasonic 75HT, VWR, Radnor, PA
UPLC: Waters, Milford, MA, Acquity UPLC H-Class
Vortex: Scientific Mini Vortexer, VWR, Radnor, PA